Placental Transfer, Pharmacokinetics and Cardiovascular Effects of Dexmedetomidine in Pregnant Ewe and Fetus

A Dissertation Presented to the

Faculty of the Department of Pharmacological and Pharmaceutical Sciences

College of Pharmacy, University of Houston

In Partial Fulfillment of

the Requirements for the Degree of

Doctor of Philosophy

By

Zhiyi Cui

January, 2015

Placental Transfer, Pharmacokinetics and Cardiovascular Effects of Dexmedetomidine in Pregnant Ewe and Fetus

By

Zhiyi Cui

Approved By:

Diana S-L Chow, Ph.D. (Advisor)

Ming Hu, Ph.D.

Douglas Eikenburg, Ph.D.

Erik Rytting, Ph.D.

Dong Liang, Ph.D.

F. Lamar Pritchard, Ph.D.
Dean, College of Pharmacy

January, 2015

Acknowledgements

I would like to take this opportunity to acknowledge many people who have made my stay at the College of Pharmacy memorable.

First and foremost, I would like to express my deepest gratitude and appreciation to my primary advisor, Dr. Diana Chow for her guidance, patience and encouragement throughout my graduate study. I have enjoyed each and every moment I spent in her lab which I will cherish for my entire life. I know I will continue to lean on her for supports wherever my career takes me to. Thank you for taking me as your student.

I also would like to sincerely thank my advisory committee members, Dr. Ming Hu, Dr. Douglas Eikenburg, Dr. Erik Rytting and Dr. Dong Liang for their invaluable suggestions and comments on my project that improve the content of this dissertation.

I also want to extend my gratitude to our collaborator, Dr. Olutoyin A. Olutoye from Texas Children's hospital, Baylor College of Medicine for conducting the animal surgery and providing preclinical samples. Additionally, I would like to thank Dr. Song Gao and Yulan Qi for their helps and advices on my project.

My appreciation also goes to Dong Dong, Yang Teng, Tanay Samant and my fellow graduate students, especially Stanley Hsiao, Lei Wu, Lili Cui, Daping Zhang, Sumit Basu, Yu He and Qiying Fan in the Department of Pharmacological and Pharmaceutical Sciences. It was their friendship, beneficial discussion and timely help that made my graduate life both enjoyable and productive.

Last, but not the least, special thanks to Jing Xu and my parents who are always being there, encouraging and inspiring me in all my pursuit. Thank you for all your unconditional love and support.

Abstract

Purpose and Specific Aims: Anesthetic agents used for pregnant mothers have been evaluated in an attempt to improve the safety of maternal-fetal anesthesia. Dexmedetomidine (DEX; Precedex®), a potent and highly selective α_2-adrenoceptor agonist approved by FDA in 1999 as a sedative, has been suggested to be suitable for maternal-fetal anesthesia. It offers significant sedative, analgesic and anxiolytic effects without causing respiratory depression. The mechanism of DEX action mediated by signaling pathways other than the α_2-adrenoceptor has been reported to play a role in neuroprotection. Animal studies have indicated that DEX could provide neuroprotective effects on anesthetic-induced neurotoxicity in neonatal rats. However, the impact of maternal use of DEX that may be associated with hypotension and bradycardia on fetal development during pregnancy is not fully understood; this greatly limits its usage in pregnant women.

Our proposed research has focused on the investigation of fetal exposure and response to the maternal use of DEX during pregnancy. In this study, pregnant ewe was selected as an experimental model due to the ethical issues in performing experiments on human fetuses. Pregnant ewe has been an extensively used model for human pregnancy due to its main advantage that the relatively large size of the fetus enables catheters implantation in both maternal and fetal blood vessels for repeated sampling.

Towards our goal, three major specific aims were proposed to: (1) determine the DEX exposure and cardiovascular response in pregnant ewe and fetus, as well as the extent of placental transfer; (2) investigate the degree of plasma protein binding and UDP-glucuronosyltransferase (UGT) metabolism in pregnant ewe and fetus; and (3) establish

pharmacokinetic (PK) model and pharmacodynamic (PD) model of cardiovascular effects in pregnant ewe and fetus.

Methods: Surgeries and catheterizations were carried out on eight pregnant Western Cross ewes at the Texas Children's Hospital, Baylor College of Medicine. Pregnant ewes received an initial 1 µg/kg loading infusion over 10 min followed by an intravenous (IV) infusion of 1 µg/kg/h for 1 h. Arterial and venous blood samples were collected at 10 min up to 250 min from both pregnant ewe and fetus. Free and total DEX plasma concentrations were quantified by our developed and validated LC-MS/MS assay. Non-compartmental PK analysis was performed to determine the partition coefficient from pregnant ewe to fetus (K_{FM}), followed by the PK analysis using non-linear mixed effect (NLME) approach to describe the free and total DEX concentrations in the pregnant ewe and fetus. Maternal and fetal heart rates (HR) and arterial blood pressure (BP) were monitored. *In vitro* UGT metabolism studies with liver and placental microsomes were also conducted.

Results: DEX concentrations in maternal artery and fetal vein were 815.1±497.2 and 104.4±40.3 pg/mL at 10 min. K_{FM} were 0.13 ± 0.10 and 0.23 ± 0.14 at 10 min and 250 min, respectively. A two-compartment model with first-order elimination best described the maternal data. An effect compartment linked to maternal circulation by first-order processes adequately characterized fetal concentrations. The relationship between free and total concentrations was satisfactorily described by linear protein binding model. For cardiovascular effects, pregnant ewes demonstrated a 30-40% decrease in BP and significant bradycardia with a 42-49% decrease in HR. In contrast, hypotension was not observed and only a modest decrease in heart rate was noted in fetuses. *In vitro* metabolism studies found negligible DEX glucuronide metabolites after incubation for up to 24 h with hepatic and placental microsomes prepared from the pregnant ewe and

fetus. Differential UGT enzyme activity in hepatic microsomes between pregnant ewe and fetus was determined using genistein as a typical known UGT substrate. It was demonstrated that pregnant ewe has 17 times higher UGT enzyme capacity than that in the fetus.

Conclusion and Significance: The contribution of our study is a better understanding of fetal exposure and cardiovascular response to maternal administration of DEX in pregnant ewes. We have demonstrated that 1) DEX can rapidly cross pregnant ewe placenta with K_{FM} of 23% to fetuses; (2) administration of DEX to pregnant ewe does not result in fetal hypotension or significant bradycardia; (3) in pregnant ewe DEX undergoes rapid distribution and a relatively slow elimination after administration; (4) fetus has lower plasma protein binding than that in pregnant ewe based on results from PK modeling and *in vitro* assessments; (5) there is a differential UGT enzyme capacity between pregnant ewe and fetus; and (6) direct N-glucuronidation is a negligible metabolic pathway for DEX in pregnant ewe which differs from that in humans. Therefore, our findings in combination with other related publications support conducting additional DEX studies for its clinical utility during pregnancy, but pregnant ewe may not be a representative model for DEX phase II metabolism study in humans. Future physiological-based pharmacokinetic modeling for the prediction of human fetal exposure and response should be investigated.

List of Tables

Table 1 Maternal physiology changes during pregnancy (Ke AB et al., 2014)..... 8

Table 2 Pharmacokinetics of DEX *vs.* other commonly used sedatives (Short J, 2010). 18

Table 3 Clinical effects of DEX *vs.* other commonly used sedatives (Short J, 2010). 19

Table 4 United States FDA pharmaceutical pregnancy categories (Wikipedia Pregnancy category http://en.wikipedia.org/) 22

Table 5 Linearity of calibration curves for DEX (n=6)..... 70

Table 6 Accuracy and precision of DEX at three levels of QC samples..... 72

Table 7 Recovery and matrix effect of DEX in pregnant ewes and fetuses (n=6)..... 74

Table 8 Stability of DEX under various conditions (n=3)..... 76

Table 9 Pharmacokinetic parameters by non-compartmental analysis of arterial concentration in pregnant ewes (n=8) and fetuses (n=12) 81

Table 10 K_{FM} from pregnant ewe (n=8) to fetus (n=12) at different time points 83

Table 11 Arterial blood gas at baseline and 120 min (n=4)..... 88

Table 12 Nonspecific binding with the Centrifree® device (n=3) 90

Table 13 Plasma protein binding assay of fraction unbound DEX 92

Table 14 Kinetic analysis of genistein glucuronidation with different models (n=3) ... 113

Table 15 Parameter estimates from the PK model (model d in Fig. 38) 124

Table 16 Pharmacokinetic parameter by bootstrap and comparison with model parameters 132

Table 17 Pharmacodynamic parameter estimates in pregnant ewe 135

List of Figures

Figure 1 Chemical structures of dexmedetomidine and FDA-approved Precedex® ... 10

Figure 2 Responses mediated by α_2-adrenoceptors (Kamibayashi T et al., 2000) 12

Figure 3 Physiology of α_2-adrenoceptor agonists receptor (Gertler R et al., 2001) 13

Figure 4 Placentation classifications by (A) appearance and (B) layers (Rurak DW, 2001)…….. 24

Figure 5 Drug disposition in mother and fetus after drug administration (Syme MR et al., 2004)… 29

Figure 6 Schematic representation of pregnant ewe model (Barry JS et al., 2008) 31

Figure 7 MRM product ions mass spectra for (a) DEX and (b) internal standard..... 46

Figure 8 Centrifree® ultrafiltration devices for plasma protein binding study (Millipore Centrifree® Ultrafiltration Devices Instructions)..... 55

Figure 9 Chromatograms of DEX with LLOQ (25 pg/mL) in maternal plasma 66

Figure 10 Chromatograms of DEX with LLOQ (25 pg/mL) in fetal plasma 67

Figure 11 Calibration curves of DEX in maternal plasma (R^2 = 0.9985) and fetal plasma (R^2 = 0.9993) 69

Figure 12 Mean (± SD) DEX concentration-time profiles for pregnant ewes (n=8) and fetuses (n=12). Line a: end of loading dose and Line b: end of infusion... 79

Figure 13 Mean (±SD) blood pressure profiles of pregnant ewe and fetus (n=4) 85

Figure 14 Mean (±SD) heart rate profiles of pregnant ewe and fetus (n=4) 86

Figure 15 Mean (±SD) profiles of cardiovascular effects (percentage change) 87

Figure 16 Calibration curve of DEX in PBS (R^2 = 0.9997) for nonspecific binding 91

Figure 17 Fractions unbound (%) in DEX-spiked (a) maternal plasma, and (b) fetal plasma over selected ranges 93

Figure 18 Fractions unbound (%) DEX at concentrations of 50 and 100 pg/ml in pregnant ewe and fetus. 94
Figure 19 Fractions unbound (%) DEX in PK samples.. 95
Figure 20 UV spectra of (a) DEX and (b) IS 97
Figure 21 Chromatograms of DEX and IS (a) with and (b) without pregnant ewe liver microsomes after 12 h-incubation 98
Figure 22 Calibration curve of DEX in KPI buffer (R^2 = 0.9974) 99
Figure 23 LC-MS/MS chromatograms of (a) DEX and IS, (b) extracted ion chromatograms (XIC) of DEX glucuronide (m/z: 377→201) in liver microsomes prepared from pregnant ewe. 100
Figure 24 LC-MS/MS chromatograms of (a) DEX and IS, (b) XIC of DEX glucuronide (m/z: 377→201) in liver microsomes prepared from fetus. 101
Figure 25 LC-MS/MS chromatograms of (a) DEX and IS, (b) XIC of DEX glucuronide (m/z: 377→201) in placental microsomes. 102
Figure 26 LC-MS/MS chromatograms of (a) DEX and IS, (b) XIC of DEX glucuronide (m/z: 377→201) in pHLM 104
Figure 27 UV spectra of (a) genistein, (b) genistein glucuronides and (c) IS 106
Figure 28 Chromatograms of genistein, genistein glucuronide and IS (a) with and (b) without maternal liver microsomes after 30 min-incubation. 107
Figure 29 Chromatograms of genistein, genistein glucuronide and IS (a) with and (b) without fetal liver microsomes after 40 min-incubation. 108
Figure 30 Calibration curve of genistein in KPI buffer (R^2 = 0.9989) 109
Figure 31 LC-MS/MS chromatograms of (a) genistein, genistein glucuronide and IS, (b) XIC of genistein glucuronide (m/z: 445.0→268.9) in liver microsomes prepared from pregnant ewe. 110

Figure 32 LC-MS/MS chromatograms of (a) genistein, genistein glucuronide and IS, (b) XIC of genistein glucuronide (m/z: 445.0→268.9) in liver microsomes prepared from fetus. 111
Figure 33 (a) Kinetics of genistein glucuronidation by maternal liver microsomes and (b) corresponding Eadie-Hofstee plot (n=3) 114
Figure 34 (a) Kinetics of genistein glucuronidation by fetal liver microsomes and (b) corresponding Eadie-Hofstee plot (n=3) 115
Figure 35 (a) Kinetics of genistein glucuronidation by pooled human liver microsomes and (b) corresponding Eadie-Hofstee plot (n=3). 118
Figure 36 PK model for total DEX concentration prediction in pregnant ewes. 118
Figure 37 Observed (DV) *vs.* predicted concentrations from the (a) population (PRED) and (b) individual (IPRED) fits 119
Figure 38 Population weighted residuals (CWRES) *vs*. (a) time and (b) predicted concentrations (PRED) 120
Figure 39 Schematic representations of pharmacokinetic models for the distribution of DEX to maternal central compartment, peripheral compartment and fetus after intravenous infusion administration to pregnant ewes. 123
Figure 40 Observed *vs.* population predicted free DEX concentrations in (a) pregnant ewe and (b) fetus 126
Figure 41 Observed *vs.* population predicted total DEX concentrations in (a) pregnant ewe and (b) fetus 127
Figure 42 Observed *vs.* individual predicted free DEX concentrations in (a) pregnant ewe and (b) fetus 128
Figure 43 Observed *vs.* individual predicted total DEX concentrations in (a) pregnant ewe and (b) fetus 129

Figure 44 Population weighted residuals *vs.* time for (a) maternal free, (b) fetal free, (c) maternal total and (d) fetal total DEX 130

Figure 45 Population weighted residuals *vs.* predicted concentrations for (a) maternal free, (b) fetal free, (c) maternal total and (d) fetal total DEX. 131

Figure 46 Cardiovascular changes (%) *vs.* predicted free DEX concentrations in (a) pregnant ewe and (b) fetus 134

List of Abbreviations

ACN	Acetonitrile
AIC	Akaike's Information Criterion
ANOVA	Analysis of Variance
AUC	Area under the Curve
BP	Blood Pressure
CNS	Central Nervous System
CYPs	Cytochrome P450
DBP	Diastolic Blood Pressure
DEX	Dexmedetomidine
FDA	Food and Drug Administration
fu	Fraction Unbound
G-DEX	DEX Glucuronidate
HED	Human Equivalent Dose
HPLC	Higher Performance Liquid Chromatography
ICU	Intensive Care Unit
IS	Internal Standard
IV	Intravenous
K_m	Michaelis Constant
KPI	Potassium Phosphate Buffer
LLOQ	Low Limit of Quantification
MAP	Mean Arterial Pressure
MRM	Multiple Reaction Monitoring
MS	Mass Spectroscopy
NLME	Nonlinear Mixed Effect

PBS	Phosphate Buffered Saline
PD	Pharmacodynamics
pHLM	Pooled Human Liver Microsomes
PK	Pharmacokinetics
SBP	Systolic Blood Pressure
UDPGA	Uridine Diphosphoglucuronic Acid
UGT	UDP-glucuronosyltransferase
UPLC	Ultra Performance Liquid Chromatography
V_{max}	Maximum Velocity
XIC	Extracted Ion Chromatograms

Contents

Acknowledgements i

Abstract ii

List of Tables v

List of Figures vi

List of Abbreviations x

Contents xii

Chapter 1 Literature Review 1

1.1. Anesthesia for non-obstetric surgery 1

1.2. Physiological changes in pregnancy 2

1.2.1. Respiratory system changes 2

1.2.2. Changes in cardiovascular and hematologic systems 3

1.2.3. Gastrointestinal system changes 4

1.2.4. Renal system changes 5

1.2.5. Changes in central and peripheral nervous systems 5

1.2.6. Physiologically related PK changes 6

1.3. Dexmedetomidine 9

1.3.1. Physicochemical properties 9

1.3.2. Pharmacology 11

1.3.3. Clinical pharmacokinetics and pharmacodynamics 16

1.3.4. Toxicity/Adverse effects 20

1.3.5. Usage during pregnancy 20

1.4. Placental transfer and metabolism 23

1.4.1. Placentation 23

1.4.2. Placental transfer 25
1.4.3. Placental metabolism 27
1.5. Pregnant ewe 30
1.6. Placental drug transfer in pregnant ewe 32
Summary 34
Chapter 2 Objective and Specific Aims 35
2.1. Hypotheses 35
2.2. Objective 35
2.3. Specific Aims 36
2.3.1. To determine the DEX exposure and cardiovascular response in pregnant ewe and fetus, as well as the extent of placental transfer 36
2.3.2. To characterize the differential plasma protein binding and drug metabolism in pregnant ewe and fetus 36
2.3.3. To establish the models of PK and PD in pregnant ewe and fetus 37
Chapter 3 Materials and Methods 38
3.1. Materials 38
3.1.1. Chemicals and Materials 38
3.1.2. Supplies 40
3.1.3. Animals 41
3.1.4. Equipment, Apparatuses and Software 41
3.2. Methods 43
3.2.1. LC-MS/MS assay development for quantifications of DEX in pregnant ewe and fetus plasma samples 43
3.2.2. Pharmacokinetic and pharmacodynamic studies in pregnant ewe and fetus 50
3.2.3. Plasma protein binding 54
3.2.4. *In vitro* UGT metabolism 58

3.2.5. Pharmacokinetic/pharmacodynamic modeling 61
Chapter 4 Results 65
4.1. LC-MS/MS assay for quantification of DEX in plasma 65
4.1.1. LC Chromatographs 65
4.1.2. Linearity of calibration curves 68
4.1.3. Accuracy and precision 71
4.1.4. Recovery and matrix effect 73
4.1.5. Stability 75
4.2. Pharmacokinetics of DEX in pregnant ewe and fetus 77
4.2.1. Plasma concentration-time profiles 77
4.2.2. Non-compartmental pharmacokinetic analysis 80
4.2.3. Placental transfer of DEX 82
4.3. Pharmacodynamics of DEX in pregnant ewe and fetus 84
4.4. Plasma protein binding assay 89
4.5. UGT metabolism of DEX in pregnant ewe and fetus 96
4.5.1. Negligible N-glucuronidation of DEX in pregnant ewe model 96
4.5.2. DEX glucuronidation by human liver microsomes 103
4.5.3. Differential UGT activities in hepatic microsomes between pregnant ewe and fetus 105
4.6. PK and PD models of DEX in pregnant ewe model 117
4.6.1. PK with nonlinear mixed effect (NLME) 117
4.6.2. PD modeling 133
Chapter 5 Discussion 136
5.1. LC-MS/MS assay for quantification of DEX in plasma 136
5.2. Pharmacokinetics of DEX in pregnant ewe and fetus 138
5.3. Pharmacodynamics of DEX in pregnant ewe and fetus 140

5.4. Plasma protein binding assay 143
5.5. UGT metabolism of DEX in pregnant ewe and fetus 146
5.6. PK and PD modeling of DEX in pregnant ewe and fetus 146
5.7. Data extrapolation from pregnant ewe to pregnant women 149
Chapter 6 Summary 151
Appendix 153
References 154

Chapter 1 Literature Review

1.1. Anesthesia for non-obstetric surgery

Surgery unrelated to delivery during pregnancy is defined as non-obstetric surgery. Because of additional risk to the mother and children, this type of surgery should be avoided during pregnancy. Nevertheless, non-obstetric surgery may be performed during any stage of pregnancy depending on the urgent indications. Generally 0.75-2% of pregnant women require non-obstetric surgery during their pregnancy (Reitman E et al., 2011). Approximately 42%, 35% and 23% of non-obstetric surgeries were performed in the first, second and third trimesters of pregnancy, respectively (Mazze RI et al., 1989). Each year more than 80,000 pregnant women undergo non-obstetric surgery in the U.S. (Goodman S et al., 2002). This number is growing continuously because of the advances in fetal and obstetric procedures.

Safe anesthesia must be provided for both pregnant women and children during non-obstetric surgery. During pregnancy, the women undergo profound physiological changes. These changes have been extensively reviewed in many textbooks and numerous reports in the literature (Cohen SE et al., 1999; Goodman S et al., 2002; Ní Mhuireachtaigh R et al., 2006; Cheek TG et al., 2009, Pacheco L et al., 2013; Costantine MM et al., 2014). On the other hand, the maternal use of anesthetic agents, that may have direct or indirect effects on the fetuses, is less understood. The potential risk of drug teratogenic effects to the fetus that is associated with the intrinsic toxicity, as well as the dosage and duration of exposure should be avoided. Therefore, considerations

for the safety on both mother and fetuses are extremely necessary when we select the anesthetic drugs to ensure successful maternal and fetal outcomes.

1.2. Physiological changes in pregnancy

The physiological changes during pregnancy affect almost every organ system and influence the anesthetic and perioperative management of the pregnant women. Some of these changes, including in the respiratory, cardiovascular, gastrointestinal, and renal as well as nervous systems, might directly influence the pharmacokinetics (absorption, distribution, metabolism and elimination) of drugs. These changes are primarily caused by the profound increases in hormone concentrations. Apart from increased concentration of hormones, other factors such as increased metabolic demand, mechanical effects of an enlarged uterus and presence of the low resistance placental circulation play important roles in physiological changes in pregnancy.

1.2.1. Respiratory system changes

Anesthesiologists are concerned regarding the clinically relevant changes in respiratory physiology due to the use of anesthesia in pregnancy. Several physiological alterations in the respiratory system make pregnant women susceptible to develop hypoxemia (Mahli A et al., 2000).

During pregnancy, observed reduction in Pa_{O2} in pregnant women is due to increased oxygen consumption and decreased pulmonary functional residual capacity (Hegewald MJ et al., 2011). Maternal obesity and/or preeclampsia could accentuate the risk of hypoxemia related to the induction of general anesthesia. Progesterone enhances

brainstem activity to Pa_{CO2} leading to maternal hyperventilation, which is hindered by greater CNS sensitivity to general anesthetics in the anaesthetized patient.

Pregnancy could also result in anatomic changes in the airway, including swelling and friability of oropharyngeal tissues which ultimately lead to the significant reduction of the glottic opening near the end term of pregnancy. These changes have been observed since the mid-second trimester and become most pronounced before delivery. Physiological changes in the maternal airway can also make endotracheal intubation more difficult, which increases the risk of failed intubation. Failed intubation is the primary cause of death related to anesthesia (Kuczkowski KM et al., 2003).

1.2.2. Changes in cardiovascular and hematologic systems

Early in the first trimester during pregnancy, cardiac output starts to increase and is elevated approximately by 50% of non-pregnant values by the end of the second trimester (Capeless EL et al., 1989). This results from both an increase in heart rate (by about 25%) and stroke volume (by about 30%) (Clark SL et al., 1989). This increase in cardiac output is necessary because of the high metabolic demands of fetuses.

Minor changes occur in blood pressure during pregnancy. It falls down slightly in the first trimester, increases during the second trimester, and returns to approximately its pre-pregnancy level in the third trimester. Usually, blood volume expands in the first trimester by 35-50% (Cohen SE et al., 1999). The increased blood volume associated with red cell mass results in physiologic anemia and hemodilution. This particular physiologic function might provide protection to women during pregnancy as well as lead to increased red cell mass coupled with increased uterine blood flow, optimizing oxygen

transport to the fetus (Pacheco L et al., 2013). The reduction in blood viscosity is also another reason for improvement of flow through the utero-placental circulation.

During pregnancy, some significant changes in the coagulation and fibrinolytic pathway, such as elevated plasma circulating levels of clotting factors (VII, VIII, IX, X, and XII), fibrinogen and platelet turnover are observed. Though fibrinolysis produces the hypercoagulable state which places pregnant women at high risks of experiencing thromboembolic events, it also provides a survival advantage by minimizing blood loss in the postoperative period or after delivery (Hellgren M et al., 1996).

1.2.3. Gastrointestinal system changes

Pregnant women have been considered to experience delayed gastric emptying, prolonged intestinal transit time, decreased lower esophageal sphincter tone and slightly increased gastric acidity. They were thought to be caused by both the endocrinologic factor of progesterone and the mechanical factor of an enlarging uterus. More recent data have suggested that pregnancy itself does not delay gastric emptying. Evidence has shown that except for laboring women, no significant delay in gastric emptying was demonstrated in the three trimesters of pregnancy compared to non-pregnant women (Macfie AG et al., 1991; Whitehead EM et al., 1993). In contrast, gastric motility decreases during active labor.

During pregnancy increased gastric pressure along with the reduced resting muscle tone of the lower esophageal sphincter leads to an increased incidence of reflux esophagitis and heartburn which places pregnant women at increased risk for gastric acid aspiration in sedated/anesthetized conditions (after about 16 weeks' gestation) (Wong CA et al., 2002).

1.2.4. Renal system changes

In pregnancy, renal plasma flow and glomerular filtration rate (GFR) are both increased. As early as the first trimester, renal plasma flow and GFR increase by 50-80% and 40-65%, respectively (Jeyabalan A et al., 2007). As a result, the renal clearance has increased by approximately 50% which leads to the increased renal excretion rate and consequentially decreased serum concentrations of creatinine, urea, and uric acid. Therefore, adjustment of dosages and administration schedules for anesthesia is necessary in order to compensate for these changes. During pregnancy, the renal glucose threshold decreases which can produce glucosuria. However, sodium excretion remains normal (Davison JM et al., 1980).

1.2.5. Changes in central and peripheral nervous systems

It is well known that pregnancy can change pharmacokinetic and pharmacodynamic of many drugs, lowering the required anesthetic dose. Pregnant women have demonstrated an approximately 30% reduction in the minimum alveolar concentrations for inhalation anesthetics (Gin T et al., 1994). Similarly, intravenous drugs that induce general anesthesia also are given in lower doses to pregnant women (Gin T et al., 1997). Several studies have also demonstrated neural tissues are more sensitive to the effects of local anesthetic drugs in pregnant women compared to non-pregnant women, which results in reduced anesthetic doses and lower plasma concentrations during pregnancy (Sanson BJ et al., 1999).

Several mechanisms including mechanical, biochemical and hormonal mechanisms, have been suggested to explain the phenomenon. Changes in inferior vena cava compression and epidural venous plexus cause the reduction of total volume of the

epidural and subarachnoid spaces, which may explain the decreased anesthetic requirement and extensive distribution of local anesthetic agents administered during central neuraxial blockade.

In adult, the autonomic nervous system shows a biphasic response to the hemodynamic changes (e.g. blood pressure and heart rate). A published study has indicated that the autonomic nervous activity shifted towards a higher vagal tone and lower sympathetic activity along with elevated blood volume in the first trimester, and was altered towards a lower vagal tone and increased sympathetic activity in the third trimester. (Kuo CD et al., 2000).

1.2.6. Physiologically related PK changes

Based on a comprehensive meta-analysis of data with healthy adult women, maternal physiology changes at each trimester during pregnancy that have direct influence on ADME/PK have been summarized in **Table 1** (Ke AB et al., 2014).

In short, these changes include previously discussed changes in (1) cardiovascular systems (cardiac output, stroke volume and heart rate); (2) hematologic systems (plasma volume, red blood cell volume and hematocrit as well as blood flow); (3) GI systems (gastric emptying and GI transit time); (4) renal systems (GFR, creatinine clearance) and (5) others, including body weight and body fat composition as well as albumin and α1-acid glycoprotein levels.

Changes in liver enzyme activity during pregnancy also have significant effects on PK alterations in pregnant women comparing to the non-pregnant counterparts. These changes involve both phase I and phase II metabolic pathways. For example, enzyme

activity of CYP3A4 (Little BB et al., 1999) and UGT1A4 (de Haan GJ et al., 2004) both increased during pregnancy.

Table 1 Maternal physiology changes during pregnancy (Ke AB et al., 2014)

Parameters	1st Trimester	2nd Trimester	3rd Trimester
Total body weight (kg)	6% ↑	16% ↑	23% ↑
Total fat mass (kg)	11% ↑	16% ↑	32% ↑
Total body water (L)	11% ↑	27% ↑	41% ↑
Cardiac output (L)	18% ↑	28% ↑	33% ↑
Plasma volume (L)	7% ↑	42% ↑	50% ↑
Red blood cell volume (L)	4% ↑	20% ↑	28% ↑
Hematocrit (%)	3% ↓	8% ↓	14% ↓
Albumin	5% ↓	16% ↓	31% ↓
α1-acid glycoprotein	1% ↓	22% ↓	19% ↓
Glomerular filtration rate (mL/min)	19% ↑	37% ↑	40% ↑
Effective renal plasma flow (L/h)	38% ↑	48% ↑	31% ↑
Creatinine clearance (mL/min)	28% ↑	58% ↑	26% ↑
Uterine blood flow (L/h)	923% ↑	1567% ↑	2771% ↑
Hepatic blood flow (L/h)	↔	↔	↔

1.3. Dexmedetomidine

Dexmedetomidine (DEX; Precedex®), approved by Food and Drug Administration (FDA) in 1999 for the use as a sedative in intensive care unit (ICU), is a potent and highly selective α_2-adrenoceptor agonist. Its affinity for binding to the α_2: α_1 receptor is 1600:1 compared with 200:1 for clonidine (most commonly used α_2 agonist by anesthesiologists). DEX has significant sedative, analgesic and anxiolytic effects without causing respiratory depression. In comparison to most of the clinically used anesthetic agents, DEX offers a sedative-hypnotic as well as analgesic effect (Farag E et al., 2012). Its major side effects include hypotension and bradycardia. In recent years, DEX has become one of the effective therapeutic drugs with substantial merits in the perioperative use for a wide range of anesthetic management (Arcangeli A et al., 2009). It can be used either as the sole sedative or as an adjunct to general anesthesia. Its favorable pharmacodynamics and clinical effects are due to its distinguished mechanism of actions (Gertler R et al., 2001).

1.3.1. Physicochemical properties

The molecular weight of Precedex (DEX hydrochloride) is 236.7 Da and the structural formula is shown in **Figure 1.** Its logP at pH 7.4 is 2.89 and the pKa = 7.1. It is a white powder and is soluble in water (Precedex injection label). Each vial contains 236 µg of DEX hydrochloride equivalent to 200 µg of DEX in 2 mL to make the concentration equal to 100 µg/mL (**Figure 1**).

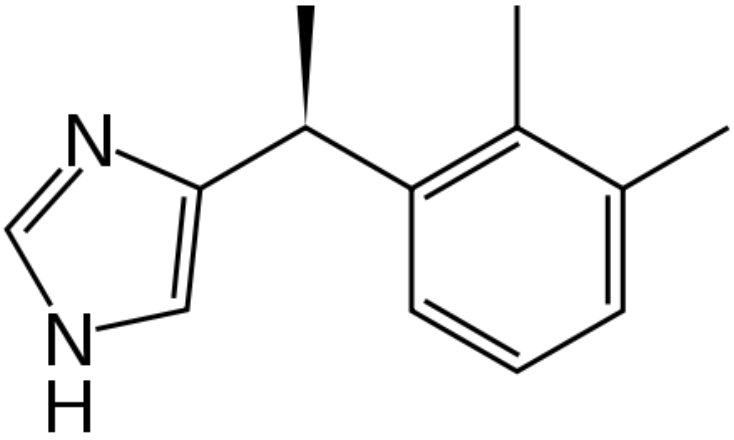

Dexmedetomidine **Precedex®** (DEX hydrochloride injection)

Figure 1 Chemical structures of dexmedetomidine and FDA-approved Precedex®

1.3.2. Pharmacology

1.3.2.1 Mechanism of action

The mechanism of action of DEX is different from those of currently used sedatives, including clonidine. Physiologic responses mediated by the stimulation of the receptors vary by locations (**Figure 2**) (Kamibayashi T et al., 2000; Gertler R et al., 2001). The pharmacological effects of α_2-adrenoceptor agonists that act on pre- and post-synaptic adrenoceptors are quite complex. Normally, norepinephrine release that terminates propagation of pain signals is hindered by the activation of presynaptic α_2-adrenoceptors (**Figure 3**), while the inhibition of sympathetic activity by postsynaptic activation in the CNS leads to hypotension and bradycardia (Gertler R et al., 2001). Therefore, DEX combines these actions and produces the effects of sedation, analgesia and anxiolysis.

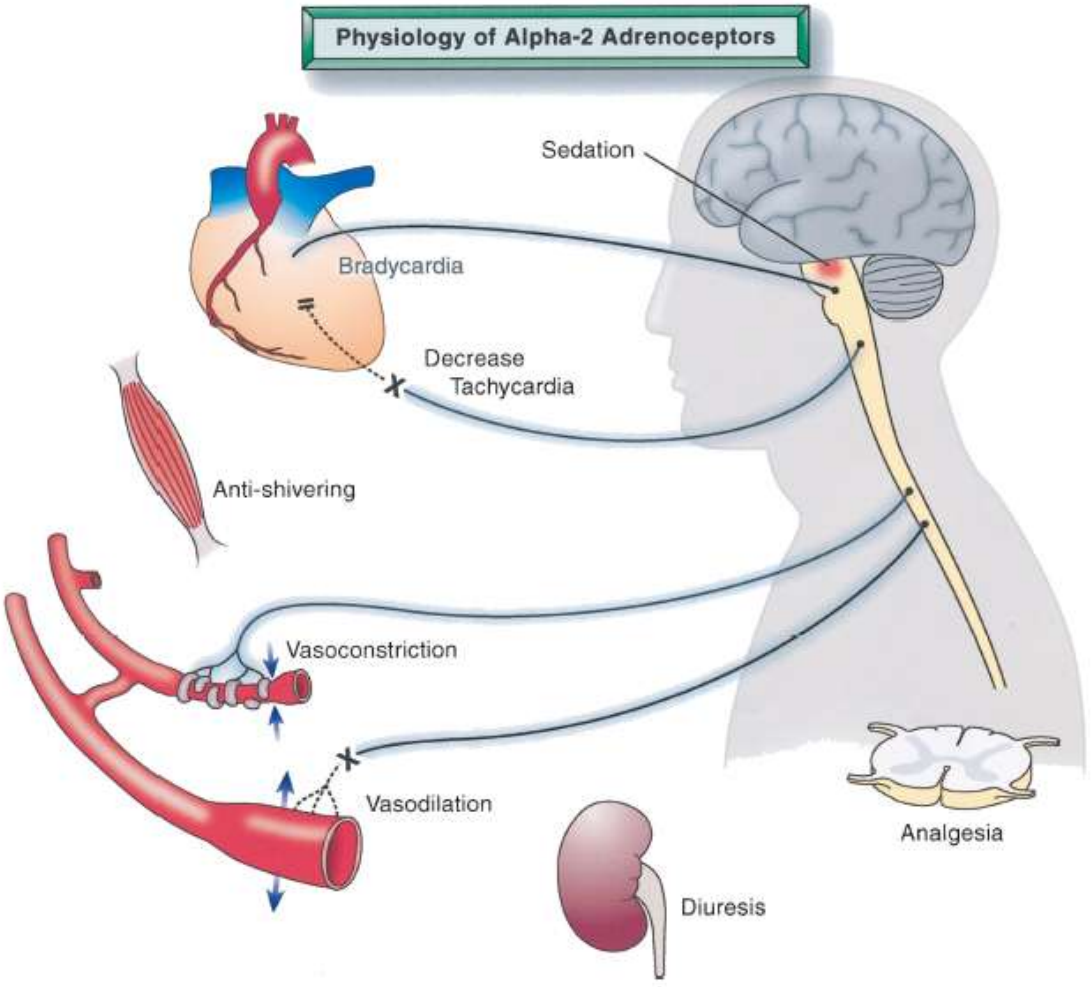

Figure 2 Responses mediated by α_2-adrenoceptors (Kamibayashi T et al., 2000)

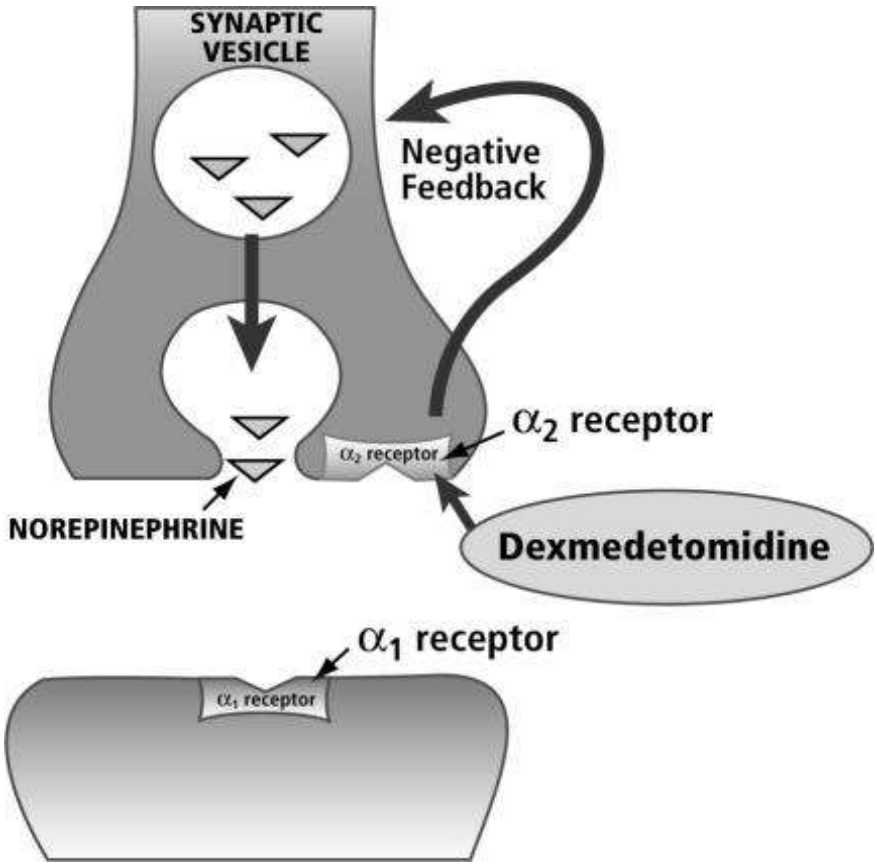

Figure 3 Physiology of α_2-adrenoceptor agonists receptor (Gertler R et al., 2001)

1.3.2.2 CNS effects

DEX has activity at various locations in the CNS. The sedative effects produced by DEX primarily depend on the activation of G-protein binding receptors in the locus coeruleus of the brain stem, rather than the activation of the γ-aminobutyric acid (GABA) receptor that is caused by traditional sedatives like propofol and benzodiazepines (midazolam). Sedation and analgesia as well as hypotension and bradycardia that are caused by the inhibition of neuronal firing are associated with the stimulation of α_2-adrenoceptors in the brain and spinal cord.

The neuroprotective properties of DEX have been demonstrated in neonatal rats to attenuate anesthetic-induced neurotoxicity (Sanders RD et al., 2009; Sanders RD et al., 2010). Experimental data have suggested that the neuroprotective effect of DEX might involve other signaling pathways in the brain in addition to α_2-adrenoceptor agonism. Observations have also revealed the clinical benefits of these brain protective effects as DEX shortens the period of coma or delirium in patients in the ICU. Therefore, DEX may be a desirable anesthetic agent for pregnant mothers by providing adequate sedation with the added benefit of neuroprotection on fetuses (Afonso J et al., 2012).

1.3.2.3 Cardiovascular effects

A biphasic, dose-dependent cardiovascular response has been described after DEX administration (Dyck JB et al., 1993; Hall JE et al., 2000; Gertler R et al., 2001). At low doses, through the activation in both peripheral and central systems, DEX exerts several pharmacological actions such as modest decrease in heart rate and a slight reduction in blood pressure (Khan ZP et al., 1999). Stable hemodynamic response is expected when DEX is administered as a continuous infusion. Severe hypotension usually occurs in

patients with hypovolemia. High doses of DEX could cause hypertension mainly due to its activation of α_{2B}-adrenoceptors located in vascular smooth muscles.

1.3.2.4 Respiratory effects

In general, α_2-adrenoceptor agonists have minimal effects on ventilation. DEX could provide sedative, analgesic, and anxiolytic effects, as well as respiratory stability without causing ventilator depression. The lack of respiratory depression with DEX makes it attractive for use in the pregnant woman as avoiding respiratory depression prevents the development of apnea which may easily occur in the sedated pregnant woman (Bucklin A et al., 2012). In *in vivo* studies, α_2 stimulation is also indicated to cause airway smooth muscle relaxation, thereby preventing bronchoconstriction.

1.3.2.5 Renal system effects

The diuresis and natriuresis owing to the reduced efferent sympathetic outflow of the renal nerve are caused by the activation of α_2-adrenoreceptors in kidney. A study has demonstrated that low DEX doses could inhibit the vasopressin secretion, causing aqueous diuresis in anesthetized dogs. By these actions it is suggested that DEX plays a potential role in protecting kidneys against ischemic events (Villela NR et al., 2005).

1.3.2.6 Endocrine effects

Generally, α_2-adrenoreceptor agonists affect the endocrine system through their effects on sympathetic outflow and the decrease of catecholamines. This can inhibit the secretions of cortisol and adrenocorticotropic hormone attenuating the responses to stress (Venn RM et al., 2001). Stimulation of α_2-adrenoreceptors by agonists could also

temporarily result in direct inhibition of insulin release in Langerhans cells along with detectable clinical hyperglycemia (Angel I et al., 1988).

1.3.3. Clinical pharmacokinetics and pharmacodynamics

1.3.3.1 Dosage

The dosage for adult ICU sedation is usually started with a loading infusion of 1 μg/kg for 10 min, then a maintenance infusion (< 24 h), at 0.2-0.7 μg/kg/h. The usual dosage for non-ICU adult procedural sedation is started with an initial infusion of 1 μg/kg over 10 min, followed by a maintenance infusion initiated at 0.6 μg/kg/h and titrated with doses in the range of 0.2-1 μg/kg/h to achieve the desired clinical effect (Precedex injection label).

1.3.3.2 Pharmacokinetics

Following IV administration of DEX at the clinical dose range of 0.2-0.7 μg/kg/h up to 24 h, linear PK has been observed. It has been reported that DEX could be rapidly distributed to the body with a distributional half-life ($t_{1/2}$) of 6 min. The terminal elimination half-life ($t_{1/2}$) is approximately 2 h. Volume of distribution (V_{ss}) and clearance (CL) are approximately 118 L and 39 L/h, respectively (for a body weight of 72 kg). **Table 2** provides a comparison of DEX pharmacokinetics with those of other commonly used sedatives (Short J, 2010). Therefore, DEX has been suggested to have a very rapid onset of action and be suitable for short-term sedation due to both its relatively rapid distribution and short elimination. Moreover, the dosage of DEX can be easily adjustable by titration to achieve the desired clinical effect.

The plasma protein binding of DEX in males and females is similar (93.7%) and consistent over the different plasma concentrations tested. There is no significant

difference in protein binding between groups with normal and impaired renal function. In contrast, plasma protein bound DEX is significantly decreased in hepatic impaired subjects compared to healthy subjects.

DEX undergoes both direct glucuronidation (major metabolic pathway) and cytochrome P450 (CYP) mediated oxidation, largely mediated by CYP2A6. In a mass balance study, 95% and 4% of DEX radioactive metabolites were recovered in urine and feces, respectively, following IV administration of radiolabeled DEX. In contrast, only a small amount of unchanged DEX was excreted through the urine and feces. The result indicated that the N-glucuronide metabolite of DEX accounts for 34% of DEX excreted in the urine. (Precedex injection label).

1.3.3.3 Pharmacodynamics

Clinical effects of DEX compared with other commonly used sedatives are summarized in **Table 3** (Short J, 2010). Unlike the other commonly used sedatives, DEX offers a variety of favorable pharmacodynamic properties, such as arousability promotion during sedation, stress response control, shivering reduction, etc. Therefore, combining all these effects, DEX can be used as a single agent to produce adequate and cooperative sedation avoiding the side effects of multi-agent treatments.

Table 2 Pharmacokinetics of DEX *vs.* other commonly used sedatives (Short J, 2010)

Agent	Elimination Half-life, h	Systemic Clearance, mL/kg/min	Potential Effects for Accumulation
Dexmedetomidine	2	0.005-0.011	Hepatic insufficiency
Clonidine	6-23	1.9-4.3	Renal insufficiency
Diazepam	21-120	0.4-0.9	Hepatic/renal insufficiency
Midazolam	3.4-11	4.3-6.6	Hepatic/renal insufficiency
Lorazepam	10-15	1.2-4.1	Hepatic insufficiency
Propofol	6.3-32	17-31	None
Morphine	2.0-5.5	8.6-23	Hepatic/renal insufficiency
Fentanyl	6.9-36.0	8.6-15	Hepatic impairment
Haloperidol	28-38	10-13	Hepatic insufficiency

Table 3 Clinical effects of DEX *vs.* other commonly used sedatives (Short J, 2010)

Effects	Dexmedetomdine	Benzodiazepines	Propofol	Opioids	Haloperidol
Sedation	X	X	X	X	X
Alleviation of anxiety	X	X			
Analgesic properties	X			X	
Promotion of arousability during sedation	X				
Facilitation of ventilation during weaning	X				
No respiratory depression	X				X
Control of delirium	X				X
Organ protection	X		X		
Control of stress response	X				
Reduction of shivering	X				
Cooperative sedation	X				
Mimicking of natural sleep	X				

1.3.4. Toxicity/Adverse effects

DEX exerts several adverse effects such as hypotension, bradycardia, hypertension, nausea, atrial fibrillation and hypoxia. A short period of rapidly increased blood pressure and heart rate fall occur following DEX administration due to the initial loading dose of 1 μg/kg. Slow infusion of DEX can attenuate the initial hypertension that results from the stimulation of α_{2B}-adrenoceptor in vascular smooth muscle. The change in elevated mean arterial pressure for the first 10 min is within the range of 7%, and the heart rate is reduced by 16-18% (Hall JE et al., 2000). After the first 10 min, slight hypotension is usually observed due to the inhibition of the central sympathetic outflow. Additionally, stimulation of the presynaptic α_2-adrenoceptors decreases the release of norepinephrine causing hypotension and bradycardia. In the postoperative period, these similar effects might also be seen. But for patients with hypovolemia, those effects could be very harmful (Precedex injection label). The instances of respiratory depression caused by DEX have been less compared to other sedatives.

1.3.5. Usage during pregnancy

Research on the use of DEX during pregnancy is still limited and its impact on the developing fetus associated with the adverse effects is yet unclear. Several studies have indicated that DEX crosses the placenta, but its safety has not been established in pregnancy. In an *in vitro* human placenta study, approximately 23.9% of DEX transferred from the maternal to the fetal side of the placenta (Ala-Kokko TI et al., 1997). In an *in vivo* pregnant rat study, transfer of DEX from mother to fetus is observed when radiolabeled DEX is administered subcutaneously. To date there are no reports of teratogenic effects in rats after subcutaneous administration and in rabbits after IV administration during fetal development. However, lower rat offspring weights were

observed in another reproductive toxicity study (Precedex injection label). In a case report on the use of DEX during pregnancy close to term, human placental transfer of DEX has been demonstrated by measuring the drug concentrations in the neonate, but no information is available on its PK or PD during pregnancy (Neumann MM et al., 2009). There have been no adequate and well-controlled studies of DEX use in pregnant women. The FDA has classified DEX as a Pregnancy Category C drug which indicates that this drug is recommended for use during pregnancy only if the potential benefits justify the potential risk to the fetus (**Table 4**).

Table 4 United States FDA pharmaceutical pregnancy categories (Wikipedia Pregnancy category http://en.wikipedia.org/)

Class	Description
Pregnancy Category A	Adequate and well-controlled human studies have failed to demonstrate a risk to the fetus in the first trimester of pregnancy (and there is no evidence of risk in later trimesters).
Pregnancy Category B	Animal reproduction studies have failed to demonstrate a risk to the fetus and there are no adequate and well-controlled studies in pregnant women OR Animal studies have shown an adverse effect, but adequate and well-controlled studies in pregnant women have failed to demonstrate a risk to the fetus in any trimester.
Pregnancy Category C	Animal reproduction studies have shown an adverse effect on the fetus and there are no adequate and well-controlled studies in humans, but potential benefits may warrant use of the drug in pregnant women despite potential risks.
Pregnancy Category D	There is positive evidence of human fetal risk based on adverse reaction data from investigational or marketing experience or studies in humans, but potential benefits may warrant use of the drug in pregnant women despite potential risks.
Pregnancy Category X	Studies in animals or humans have demonstrated fetal abnormalities and/or there is positive evidence of human fetal risk based on adverse reaction data from investigational or marketing experience, and the risks involved in use of the drug in pregnant women clearly outweigh potential benefits.
Pregnancy Category N	FDA has not yet classified the drug into a specified pregnancy category.

1.4. Placental transfer and metabolism

1.4.1. Placentation

Mammalian placentas can be classified by their macroscopic appearance, as being diffuse, cotyledonary, zonary, and discoid (**Figure 4A**). Another conventional way of classification is according to the Grosser classification based on the number of layers between maternal and fetal blood: (1) hemochorial (human and rat); (2) endotheliochorial (cat and dog); and (3) epitheliochorial (sheep, pig and horse), as shown in **Figure 4B**. The structural differences in placentas among different species affect their functions, as summarized below (Rurak DW, 2001; Syme MR et al., 2004; Włoch S et al., 2009; Furukawa S et al., 2014).

Hemochorial placenta: Maternal blood in the hemochorial placenta is in direct contact with trophoblast layers. According to the number of trophoblast layers between maternal blood and fetal endothelium, hemochorial placentas are further divided into three subgroups. The hemochorial placenta exhibits the greatest destruction, with the uterine epithelium underlying basement membrane and maternal endothelium all being lost.

Endotheliochorial placenta: The endotheliochorial placenta lacks the uterine epithelium, which is destroyed during placentation; thus, on both sides of the placenta the capillary endothelium is in contact with the trophoblast.

Epitheliochorial placenta: Placentas with endometrial epithelium and uterine endothelium are classified as epitheliochorial. In epitheliochorial placenta, no uterine cell layers are destroyed. Thus there are six layers that separate maternal from fetal blood and the uterine epithelium is in contact with the trophoblast layer of the conceptus.

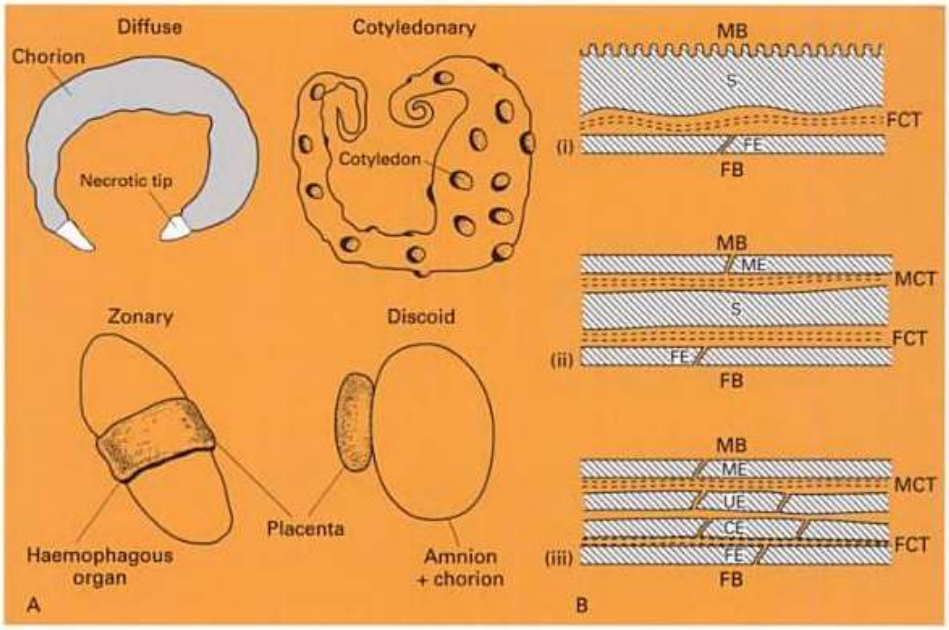

Figure 4 Placentation classifications by (A) appearance and (B) layers (Rurak DW, 2001)

(i) hemochorial, (ii) endotheliochorial, and (iii) epitheliochorial.

MB: maternal blood, ME: maternal endothelium, MCT: maternal connective tissue, S: syncytiotrophoblast, UE: uterine epithelium, CE: chorionic epithelium, FCT: fetal connective tissue, FE: fetal endothelium, and FB: fetal blood.

1.4.2. Placental transfer

The role of placenta involves supplying the fetus with oxygen, nutrients, cytokines, growth factors, and hormones, as well as eliminating toxic metabolites, but also acting as a protective barrier for xenobiotics. There are several ways of placental exchange including passive diffusion, facilitated diffusion, active transport, phagocytosis and pinocytosis (Reynolds F et al., 1989; Syme MR et al., 2004; Włoch S et al., 2009).

1.4.2.1 Passive diffusion

Passive transport appears to be the primary way of substrate exchange in the placenta, using the differences in the concentration gradient between the maternal and fetal blood to drive the flux. During pregnancy, most of the drugs that are administered to the maternal circulation will enter the fetal circulation via passive diffusion to varying extents. This process does not involve energy consumption, nor is it subject to saturation or competitive inhibition.

Passive diffusion can be described by Fick's Law:

$$V_{diff} = \frac{D \times S \times (C_M - C_F)}{a}$$

Where V_{diff} is diffusion rate, D is the coefficient of diffusion, S is the exchange surface area, C_M is the maternal concentration, C_F is the fetal concentration and a represents the thickness of placenta.

According to the above equation, the amount of substrates that can cross a membrane depends on the concentration difference between two sides of the membrane, and

surface area and thickness of membrane. With the advancement of gestational age, the placental surface area increased and placental thickness decreased, and that leads to the increased amount of nutrition and energy across the placenta for fetal development. The trend is the same for the drugs across the placenta by passive diffusion.

The physicochemical properties of drugs that determine the placental transfer through passive diffusion are molecular weight, pKa, lipid solubility and protein binding. Highly lipid-soluble drugs with low-molecular weight (< 500 Da) that are predominantly non-ionized are easily transferred across placenta, and only the free fraction of drugs can cross the placenta.

1.4.2.2 Facilitated diffusion

Facilitated diffusion is a process of spontaneous passive transport across placenta via specific transmembrane proteins. This is process can become saturated at high concentrations, but does not require energy input. Unlike the passive diffusion which does not undergo saturation, the rate of the facilitated diffusion is saturable with respect to the concentration difference between maternal and fetal circulations. It is a suitable mechanism for nutrients such as glucose, which is in plentiful supply in the maternal circulation. To date, only a few drugs have been suggested as being transported across the placenta by the facilitated diffusion mechanism.

1.4.2.3 Active transport

Unlike passive and facilitated diffusion, active transport across the placenta requires energy consumption that is usually provided by ATP hydrolysis or energy stored in the transmembrane electrochemical gradients. Active transporters are located in the apical membrane facing the maternal blood space or basal membrane facing the fetal

capillaries, where they transfer compounds in and out of synctiotrophoblasts. In addition, some transporter proteins are expressed on the capillary endothelium. All active transporters can transport drugs against concentration gradients and undergo saturation with time. The transport systems are involved with nutrients and drugs whose structure are similar to those of endogenous substrates. These active transporters include P-glycoprotein (P-gp), multidrug resistance proteins (MRPs), breast cancer resistant protein (BCRP), monoamine transporters (SERT, NET, OCT3), and organic cation transporters (Eshkoli T et al., 2011).

1.4.2.4 Phagocytosis and pinocytosis

Drugs can also cross placenta via phagocytosis and pinocytosis. But these processes of transfer mechanisms are considered too time-consuming to have any notable impact on fetal exposure.

1.4.3. Placental metabolism

The placenta acts as a metabolic barrier to foreign substances; however, it plays a relatively minor role in drug metabolism compared to hepatic metabolism. Therefore, placental metabolism is not considered as a limiting step in the transfer of xenobiotics across the placenta. Moreover, in some cases, xenobiotics can become toxic to the fetus upon activation by placental enzymes. The expression and activity of phase I enzymes (including cytochrome P450s (CYPs)) and phase II enzymes (including UDP-glucuronosyltransferases (UGTs)) in the human placenta have been well reviewed (Syme MR et al., 2004).

Figure 5 demonstrates the drug disposition in mother and fetus after maternal drug administration (Syme MR et al., 2004). Several PK variables including hepatic

metabolism, free drug fraction, as well as transplacental transport and metabolism affect drug transfer across the placenta and drug exposure to the fetus. Moreover, these PK variables are drug-dependent and vary with fetal and placental development during pregnancy.

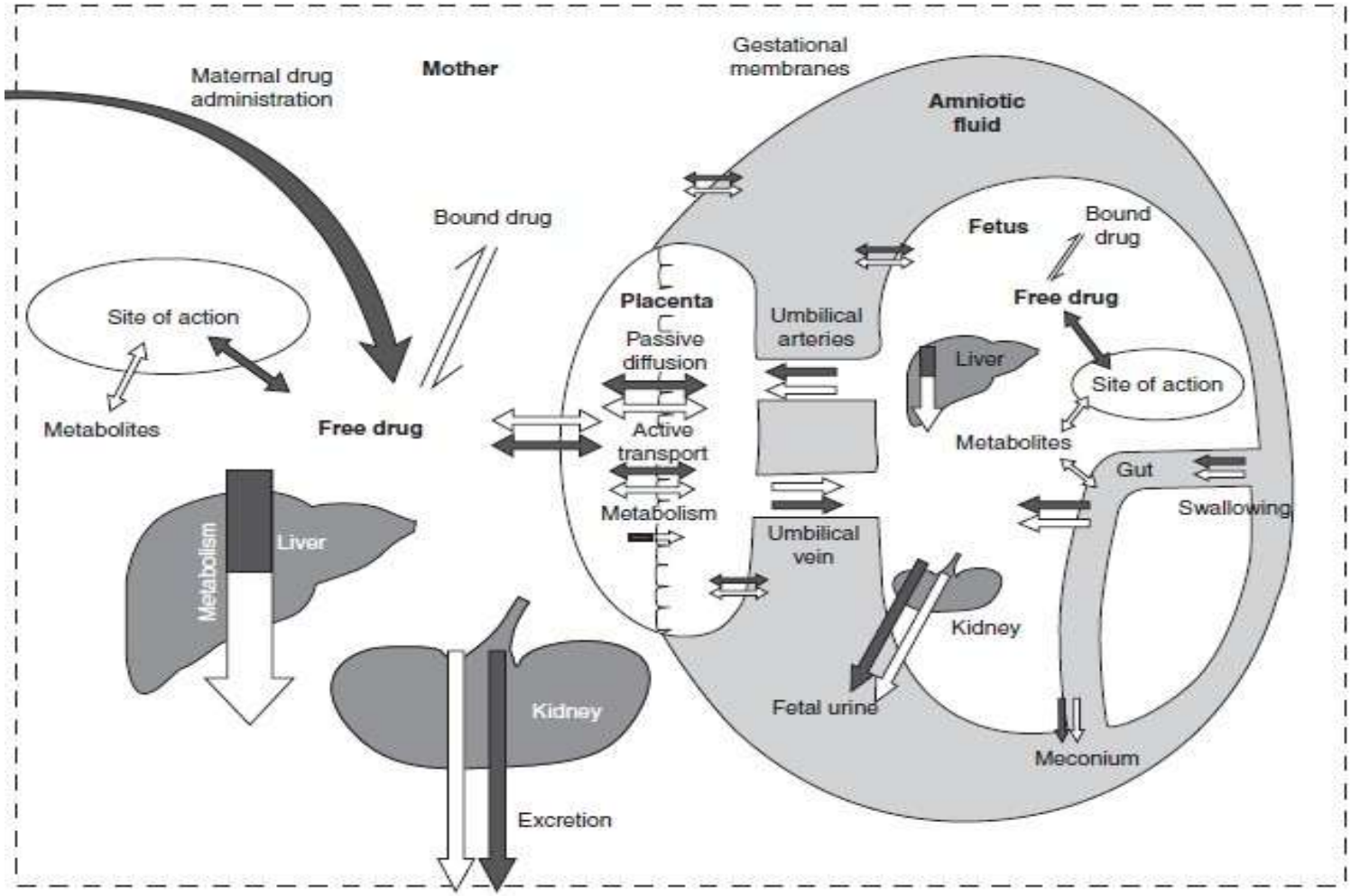

Figure 5 Drug disposition in mother and fetus after drug administration. Black and white arrows indicate parent compounds and metabolites, respectively (Syme MR et al., 2004).

1.5. Pregnant ewe

During the past decades our knowledge of human fetal growth and development has increased significantly with advanced prenatal diagnosis and care. However, there are still many unknowns in complicated cases of human pregnancies. Until today, many aspects of human pregnancy cannot be adequately studied, primarily due to both ethical and practical challenges and constraints. Alternatively, a variety of animal models have been developed and have contributed to our current state of knowledge in both normal and complicated pregnancies (Pardi G et al., 2006; Carter AM, 2007).

While there is no ideal animal model that can truly represent human pregnancy, the pregnant ewe has been extensively used to delineate maternal-fetal interactions. This is in part due to the distinguished merit of the relatively large size of the fetus that permits the implantation of catheters in both maternal and fetal blood vessels for repeated sampling from both maternal and fetal sides of the placenta. **Figure 6** shows the schematic representation of a pregnant ewe model (modified from Barry JS et al., 2008). Drug administration/Infusate can be given into either the maternal or the fetal side, and blood samples can be collected from maternal and fetal circulations simultaneously. At term, fetal lamb is almost the same weight as a human fetus.

In addition, the relatively large size of the fetal lamb makes fetal surgery easy to handle, and the fetus is considered to be more tolerable to the invasive procedures. (Carter AM, 2003). Therefore, our knowledge of physiology of fetal lamb is more advanced compared to that of fetuses of other species.

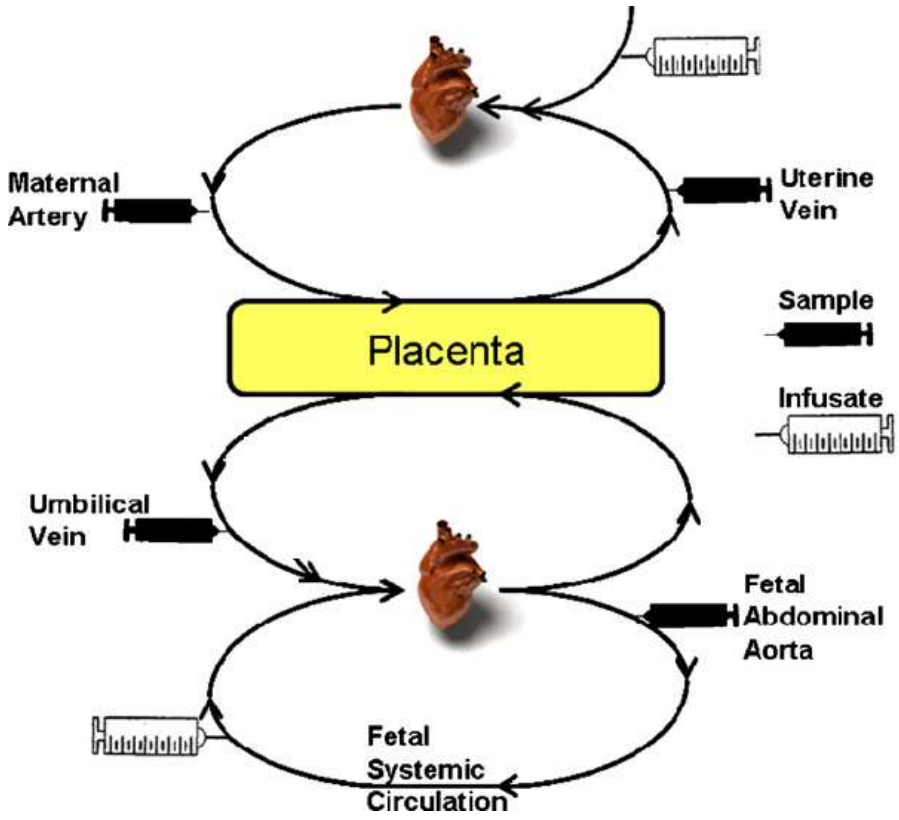

Figure 6 **Schematic representation of pregnant ewe model (modified from Barry JS et al., 2008)**

1.6. Placental drug transfer in pregnant ewe

To date, a variety of drugs have been evaluated using pregnant ewe to understand the placental transfer and data extrapolation to humans. These drugs include sedatives (Vree TB et al., 1984; Fresno L et al., 2008; Musk GC et al.,2012), opioids (Craft et al., 1983; Vertommen et al., 1995; Coonen JB et al., 2010), propofol (Andaluz A et al., 2003), metoclopramide (Riggs KW et al., 1990), ritodrine (Fujimoto S et al., 1984), diphenhydramine (Kumar S et al., 1999), and valproic acid (Kumar S et al., 2000). Most of the experiments were carried out in chronically instrumented pregnant ewe at 120 days to near term of gestation after intravenous administration for maternal-fetal PK studies with or without the evaluation of drug effects in the fetus. Generally, the extent of placental transfer is described by fetal/maternal ratio of AUC or fetal/maternal concentration ratio at steady state. A compartmental PK model is helpful to describe the inter-compartmental relationship between fetus and mother, and to evaluate factors that potentially affect the fetal drug exposure. However, non-compartmental PK analysis of total drug concentrations was primarily performed for the studies in pregnant ewe.

Musk GC et al. have demonstrated that medetomidine and ketamine can rapidly cross the pregnant ewe placenta. Although blood samples were obtained only at three time points, comparable maternal and fetal concentrations were observed (Musk GC et al., 2012). Fresno L et al. have reported that etomidate, an anesthetic agent, also has the ability to transfer across the placenta of pregnant ewe. The fetal/maternal AUC ratio is 0.4, and maternal and fetal elimination rates are similar (Fresno L et al., 2008). Diphenhydramine has also exhibited similar elimination rates in pregnant ewe and fetus, but the fetal/maternal AUC ratio is very high (0.85) (Yoo SD et al., 1986). In another

study of propofol in pregnant ewe, it has been demonstrated that the fetal exposure was approximately 19% of maternal exposure. The elimination rate in fetus was comparatively slower than that in pregnant ewe (Andaluz A et al., 2003). These differences are due to drug specific variations in physicochemical and pharmacokinetic characteristics.

Other authors have suggested that although plasma drug concentrations were detected in fetus, maternal administration of remifentanil (Coonen JB et al., 2010) did not result in significant fetal hemodynamic changes, nor ritodrine (Fujimoto S et al., 1984) for cardiovascular changes. Similarly, high amount of tritiated digoxin in fetus and amniotic fluid did not have significant adverse effects (Hernandez A et al., 1975).

A few placental transfer studies using a two-compartmental PK model were reported. Kumar et al. have found that the maternal plasma concentration of diphenhydramine was affected by maternal plasma protein binding and non-placental clearance; whereas the concentration in the fetus was determined by the first-pass hepatic drug uptake. The unbound fraction of diphenhydramine in pregnant ewe (12%) at steady state was less than that in the fetus (30%) (Kumar S et al., 1999). The placental transfer of metoclopramide was also investigated to derive the non-placental clearance, and lower plasma protein binding in fetus was also observed (Riggs KW et al., 1990). Another study has systematically examined the disposition of valproic acid in pregnant ewe, and determined the mechanism of valproic acid placental transfer and nonlinear plasma protein binding in both pregnant ewe and fetus (Kumar S et al., 2000).

Recently, Uemura et al. have monitored the cardiovascular effects of DEX using pregnant ewe at 92 days of gestation, where significant fetal response was not detected. However, the drug concentrations were not reported (Uemura K et al., 2012).

Summary

This survey of the literature reveals that DEX has been suggested to be suitable for maternal-fetal anesthesia due to its distinguished clinical merits with the added benefit of neuroprotection on fetuses. However, the impact of the use of DEX during pregnancy on fetal development that may be associated with hypotension and bradycardia is not fully understood. The physiological changes during pregnancy have the potential to alter both the pharmacokinetics and pharmacodynamics of DEX. Therefore, investigation of fetal exposure and response to the maternal use of DEX during pregnancy will contribute to our understanding for the recommendation of DEX usage in pregnancy. Due to the ethical issues in performing experiments on fetuses, maternal-fetal PK research in humans is limited. Despite the lower permeability of pregnant ewe placenta compared to that of humans, the effect should be less pronounced for DEX. The pregnant ewes may be a desirable experimental model to study the placental transfer, pharmacokinetic, and cardiovascular effects of DEX in both pregnant ewe and fetus.

Chapter 2 Objective and Specific Aims

2.1. Hypotheses

Our first hypothesis is that the “maternal use of DEX will have no significant or manageable adverse effects on fetuses if the fetal exposure to DEX is limited or predictable”.

Our second hypothesis is that “understanding of the fetal exposure and response to DEX after drug administration to maternal circulation will provide a more rational recommendation of DEX use during pregnancy based on pharmacokinetic (PK) and pharmacodynamic (PD) studies”.

2.2. Objective

Our proposed research is focused on the investigation of fetal exposure (pharmacokinetics) and response (safety) to the maternal use of DEX during pregnancy. In this study, pregnant ewe was selected as an experimental model due to the ethical constraints to the acquisition of maternal-fetal information in humans. The overall objective of the study is to characterize the maternal-fetal PK and placental transfer of DEX, as well as to evaluate the PD (cardiovascular response) in the pregnant ewe and fetus. The rationale is that the severity of adverse effects is associated with the extent of fetal drug exposure. Factors such as the degree of protein binding and drug metabolism in fetuses can play critical roles in drug disposition in pregnant ewe and fetus, and thus have a significant impact on the extent of fetal drug exposure.

2.3. Specific Aims

Towards our goal, three major specific aims were proposed: (1) to determine the DEX exposure and cardiovascular response in pregnant ewe and fetus, as well as the extent of placental transfer, (2) to characterize the differential plasma protein binding and drug metabolism in pregnant ewe and fetus, and (3) to establish the models of PK and PD in pregnant ewe and fetus.

2.3.1. To determine the DEX exposure and cardiovascular response in pregnant ewe and fetus, as well as the extent of placental transfer

- To establish a validated LC-MS/MS assay that can be used for the quantification of DEX in both pregnant ewes and fetuses
- To establish plasma concentration-time profiles of DEX in pregnant ewe and fetus
- To evaluate the areas under concentration-time curves in pregnant ewe and fetus using non-compartmental PK analysis
- To evaluate the extent of placental transfer from pregnant ewe to fetus by the ratio between fetal and maternal systemic exposures
- To evaluate the adverse effects (hypotension and bradycardia) on pregnant ewe and fetus after maternal administration of DEX

2.3.2. To characterize the differential plasma protein binding and drug metabolism in pregnant ewe and fetus

- To comparatively evaluate plasma protein binding of DEX between pregnant ewe and fetus in blank plasma, and in PK plasma samples from DEX-treated ewes.

- To identify the UGT microsomal metabolism of DEX in placenta, as well as in maternal and fetal livers
- To determine the differential UGT activities in hepatic microsomes between pregnant ewe and fetus.

2.3.3. To establish the models of PK and PD in pregnant ewe and fetus

- To develop a PK model that can best describe the maternal and fetal DEX data in pregnant ewe and fetus
- To develop a PD model that can best describe the maternal and fetal cardiovascular response to DEX in pregnant ewe and fetus
- To evaluate the PK/PD relationship in pregnant ewe

Chapter 3 Materials and Methods

3.1. Materials

3.1.1. Chemicals and Materials

- Dexmedetomidine (DEX) hydrochloride powder purchased from Fisher Scientific (Pittsburgh, PA, USA) was used for LC-MS/MS assay development and validation.
- Testosterone purchased from Indofine Chemical Co., Inc (Hillsborough, NJ, USA) was used as internal standard (IS) for LC-MS/MS analysis of DEX.
- Acetonitrile (ACN) HPLC-grade (EMD, Gibbstown, NJ, USA) was used for preparing mobile phase for LC-MS/MS analysis.
- Methanol HPLC-grade (EMD, Gibbstown, NJ, USA) was used to prepare washing solution for LC-MS/MS assays and as a solvent of DEX stock solution.
- Ethyl acetate (EMD, Gibbstown, NJ, USA) was used as the organic solvent in the liquid-liquid extraction of DEX from samples of different biomatrices for LC-MS/MS analysis.
- Formic acid (~ 98%) (Sigma-Aldrich Co., St. Louis, MO, USA) was used as an acidic solution to adjust the pH value of mobile phase.
- Double distilled water was produced by a MiliporeMilli-Q system (Billerica, MA, USA).
- Phosphate-buffered saline (PBS), containing 140 mM NaCl (Sigma Chemical Co., St. Louis, MO, USA), 0.4 mM KH_2PO_4 (Sigma Chemicals Co., St. Louis, MO, USA), and 2 mM K_2HPO_4 (Fisher Scientific Co., Fair Lawn, NJ, USA), was used for plasma protein binding assessments.

- Drug-free blank plasma samples of pregnant ewe and fetus provided by the Texas Children's Hospital Baylor College of Medicine, Houston, TX, USA, were used to prepare the calibration curves for LC-MS/MS assay development, for *in vitro* plasma protein binding assessment, and analysis of pharmacokinetic samples of *in vivo* studies.
- Drug-free blank placenta and liver samples from pregnant ewe and fetus were provided as cubes, approximately 2 cm * 2 cm, by Texas Children's Hospital Baylor College of Medicine, Houston, TX, USA, for *in vitro* metabolism studies.
- Homogenization buffer containing 50 mM potassium phosphate buffer (pH 7.4), 250 mM sucrose (Sigma Chemicals Co., St. Louis, MO, USA), 1 mM EDTA (Sigma Chemicals Co., St. Louis, MO, USA), was used in the preparation of liver and placenta microsomes.
- Sodium chloride (Sigma Chemical Co., St. Louis, MO, USA) was dissolved in double distilled water to prepare normal saline solution.
- Genistein was purchased from Indofine Chemicals (Somerville, NJ, USA), and used as a typical UGT substrate for *in vitro* metabolism studies.
- Pooled human liver microsomes were purchased from BD Biosciences (Woburn, MA, USA) for *in vitro* metabolism studies.
- BCA protein assay kit (Thermo Scientific Pierce, Rockford, IL, USA) with bovine serum albumin as the standard for protein concentration determination.
- Magnesium chloride (Sigma Chemical Co., St. Louis, MO, USA) for UGT microsomal metabolism.
- Uridine diphosphoglucuronic acid (UDPGA) (Sigma Chemical Co., St. Louis, MO, USA) was used for UGT microsomal metabolism.
- Alamethicin (Sigma Chemical Co., St. Louis, MO, USA) was used as a surfactant

in microsomal metabolism incubation

- Saccharolactone was purchased from Sigma-Aldrich Chemical Co. (St. Louis, MO, USA) to drive the UGT metabolism reaction forward to completion.

3.1.2. Supplies

- Pipette tips (disposable, white: 1-10 µL, yellow: 10-100 µL and blue: 100-1000 µL, VWR, West Chester, PA, USA) were used along with appropriate pipettes (VWR, West Chester, PA, USA) for measuring and delivering liquid samples for all experiments.
- Glass pipettes (10 and 20 mL, Drummond Scientific Co., Broomall, PA, USA) were used for transferring solutions
- Polyethylene microcentrifuge tubes (1.5 ml, Axygen Scientific Inc., Union City, CA, USA) were used for storing samples from different experiments.
- Disposable vials (250 µL) were used for preparation of samples for LC-MS/MS injections.
- Flat bottom, clear glass bottles (500, 1000 and 2000 ml; VWR, West Chester, PA, USA) were used to store mobile phase and buffers.
- YM-30 Centrifree® ultrafiltration devices (Millipore Ireland Ltd., Tullagreen, Carrigtwohill, Co. Cork, Ireland) were used to separate free from bound DEX in plasma protein binding studies.
- Alcohol wipes (Webcol® Alcohol Preps, Kendall Healthcare Products Co., Mansfield, MA, USA) were used to disinfect tissue dissection equipment for microsome studies.
- Cylindrical homogenization glass tubes (Wheaton, Millville, NJ, USA) for microsomal preparation.

- Polycarbonate centrifuge tubes (Beckman Coulter, Palo Alto, CA, USA) for microsomal preparation.
- 96-well plates (BD Biosciences, Woburn, MA, USA) for protein assay
- Membrane filters (47mm, 0.45 µm, hydrophilic polypropylene; Pall Corp., Ann Arbor, MI, USA) were used to filter the mobile phase prior to LC-MS/MS assays.
- Gloves (lightly powdered, Latex) were used in handling chemicals and samples for all experiments.

3.1.3. Animals

Following approval by the Institutional Animal Care and Use Committee of Baylor College of Medicine, eight third-trimester pregnant Western Cross ewes (Edmiston Farms, West Texas, TX, USA) at 132-134 days of gestation (term approximately 147 days) were studied. Ewes were allowed to acclimatize to the environment for one week prior to initiating the studies. Four of the eight ewes had twin pregnancies.

3.1.4. Equipment, Apparatuses and Software

- Electronic balance, sensitivity of 0.0001 g (Mettler AE100, Mettler Instrument Corp., Hightstown, NJ, USA) was used for all weighing purposes.
- Centrifuge (Marathon 13K/M, B Hermle AG, Germany) was used for sample preparations.
- Vortex mixer (Vortex-2 Genie, Scientific Industries, Bohemia, NY, USA) was used for sample mixing.
- Columns: Agilent ZORBAX SB-CN column (5.0 µm, 150 *2.1 mm I.D.) was used for all HPLC analysis. Waters BEH C18 (1.7 µm, 2.1×50 mm I.D.) was used for all UPLC analysis.

- HPLC-MS/MS system consisted of:
    - LC system: Agilent Technologies 1200 series HPLC system (Agilent Technologies, Inc., Foster City, CA, USA)
    - MS system: 3200 QTRAP triple quadruple mass spectrometer equipped with a TurboIonSpray ion source (Applied Biosystems/MDS SCIEX, Foster City, CA, USA). The MS/MS was used to develop and validate the method for quantification of DEX in both pregnant ewe and fetus plasma samples. 5500 QTRAP mass spectrometer equipped with a TurboIonSpray ion source (Applied Biosystems/MDS SCIEX, Foster City, CA, USA) was also used to achieve a lower LLOQ.
    - The Analyst Software version 1.5 was used to analyze the data.
- Waters ACQUITY UPLC system with photodiode array detector and Empower software was employed to analyze the parent compounds and the corresponding glucuronides.
- pH-meter (Corning Scholar 425, Corning, NY, USA) was routinely used to measure the pH of the mobile phase and to confirm the pH of buffer solutions.
- Dissection equipment set (Miltex ®, Thomas Scientific, Swedesboro, NJ, USA) was used for dissection of liver and placenta tissues.
- Shaking water bath (model YB-521, American Scientific Products, Japan) was used for *in vitro* metabolism studies.
- Biotek plate reader (Biotek, Winooski, VT, USA) was used to measure protein concentrations.
- Pipettes (1-10 µL, 10-100 µL, 20-200 µL and 100-1000 µL, Eppendorf, Brinkmann Instrument, Inc., Westbury, NY, USA) were used with different sizes

of pipette tips to measure and transfer liquid samples.

- Pipette-aid (Drummond Scientific, Broomall, PA, USA) was attached to glass pipettes (10 and 20 mL) and used to transfer liquids.
- PKSolver, an add-in program in Microsoft Excel was used for non-compartmental pharmacokinetic data analysis.
- Phoenix WinNonlin version 1.3 (Pharsight Corp., Mountainview, CA, USA) was used for pharmacokinetic data analysis and pharmacokinetic model development. The Phoenix NLME (non-linear mixed effect) package is capable of analyzing data with sparse samples, deviated sampling time and/or missing samples.
- Graphpad Prism version 5.02 (GraphPad Software, San Diego, CA) was used for Student's t test, and one-way ANOVA with Tukey's post hoc test.
- SigmaPlot 13.0 (Systat Software, San Jose, CA) was used for kinetic analysis in the microsome study

3.2. Methods

3.2.1. LC-MS/MS assay development for quantifications of DEX in pregnant ewe and fetus plasma samples

3.2.1.1 Rationale

In order to investigate the DEX usage during pregnancy and maternal-fetal pharmacokinetic of DEX in the pregnant ewe model, we have developed a sufficiently sensitive, specific, accurate and reliable assay for the determination of DEX in both pregnant ewe and fetus plasma samples, as a prerequisite for pharmacokinetic characterization of DEX in the pregnant ewe model. This assay could also be employed in quantifying DEX in urine and amniotic fluid samples for the pregnant ewe model with the same assay protocol. To our knowledge, there are no published HPLC or LC-MS/MS

assay readily available to quantify DEX in these biometric samples for pregnant ewe and fetus. Methods for the quantification of DEX in rats and humans have been reported. However, these methods may not be suitable for the determination of DEX in the ewe as the performance of LC-MS/MS methods can vary significantly among species due to the matrix effects of different biometrics (Taylor PJ, 2005; Van Eeckhaut A et al., 2009; Trufelli H et al., 2011). Analytical bias between species due to different phospholipid profiles among human, rodent and non-rodent species has been reported (Gray NP et al., 2012). Matrix components present in biological samples can suppress or enhance the response of the analyte of interest, which may affect the assay sensitivity and/or accuracy. Therefore, we have developed and validated a new HPLC-MS/MS assay which enables quantification of DEX concentrations in plasma, urine and amniotic fluid for the pregnant ewe model with a single assay protocol. This assay can be easily modified to quantify DEX in liver and placental microsomal samples.

3.2.1.2 Chromatographic conditions

An Agilent 1200 series HPLC system (Foster City, CA, USA) was used for chromatographic analysis. DEX and testosterone (IS) were resolved on an Agilent ZORBAX SB-CN column (5.0 µm, 150 mm*2.1 mm I.D.). The mobile phases consisted of water (mobile phase A) and 0.5% formic acid in acetonitrile (mobile phase B). A gradient elution was started with 5% of mobile phase B, maintaining for 1 min and with a linear increment to 100% of mobile phase B from 1 to 3.5 min. The elution was kept constant at 100% of mobile phase B for 1.5 min, and then decreased to 5% of mobile phase B in 0.5 min. This composition was maintained at 5% of mobile phase B for 2.5 min. The total running time was 8.0 min. The flow rate was delivered at 0.5 mL/min, and the injection volume was 50 µL.

3.2.1.3 Mass spectrometry conditions

The column effluent was monitored using an HPLC-MS/MS of 3200 QTRAP® with a TurboIonSpray ion source. The IonSpray heater was set at 500°C. Curtain gas, nebulizer gas and heater gas were at 10, 20 and 60 psi, respectively. IonSpray needle voltage was set at 5,500 V, and the collision activated dissociation gas was set to medium.

Transition ions from a specific precursor ion to product ion $[M+H]^+$ were detected by using optimal multiple reaction monitoring (MRM): m/z 201.5 → 95.4 for DEX and m/z 289.2 → 109.1 for the IS, respectively. The collision energy was set at 22 and 34 eV for DEX and IS, respectively. Other compound parameters were determined using the QTRAP instrument and Analyst® Software. Finally, the positive ion electrospray MS/MS product ion spectra of DEX and IS were established in **Figure 7**. Formic acid of 0.1, 0.3 and 0.5% in mobile phase B were tested, and 0.5% was selected as it resulted in the sharpest and symmetrical peak shape, with no significant suppression issue in positive ion mode.

(a) DEX

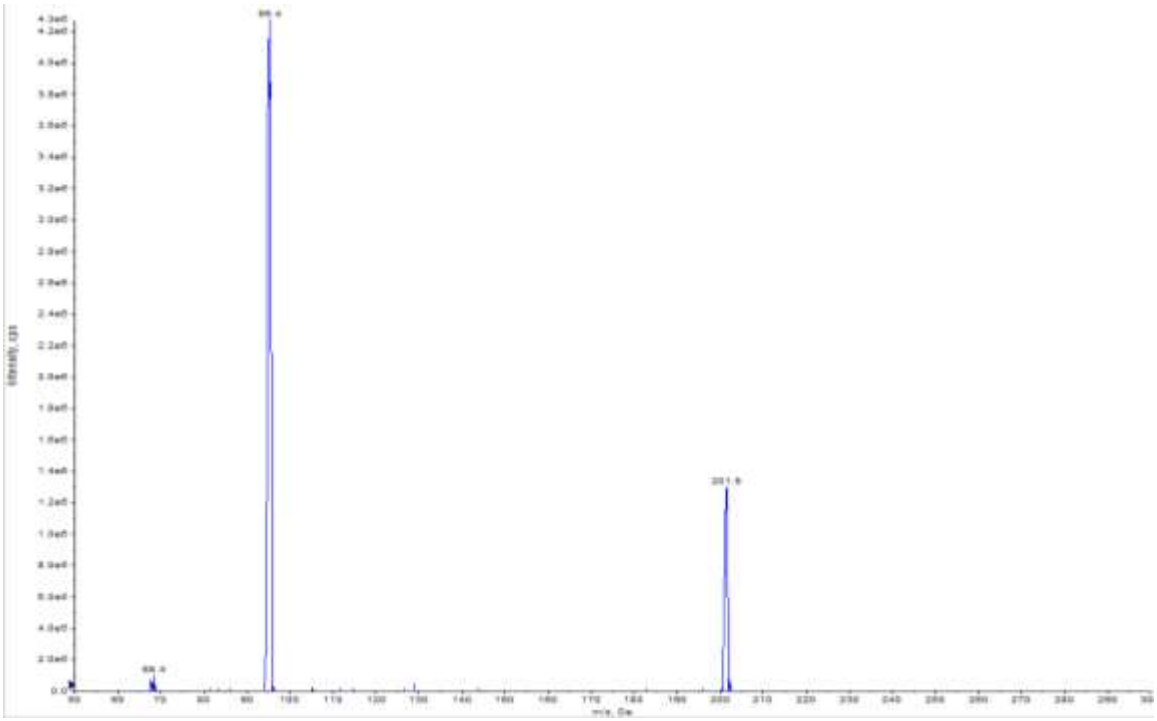

(b) IS

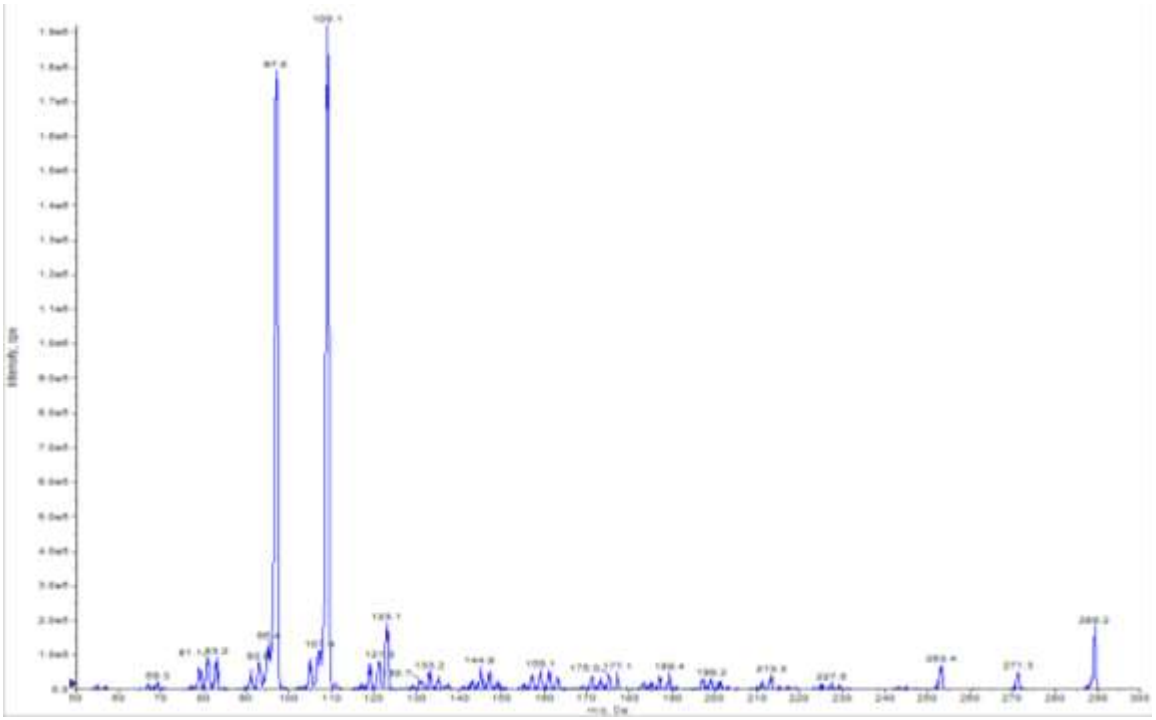

Figure 7 MRM product ions mass spectra for (a) DEX and (b) internal standard.

3.2.1.4 Preparation of calibration standards and quality control (QC) samples

Stock solutions of DEX and IS were prepared at concentrations of 1.0 mg/mL in methanol and 100 µM in acetonitrile, respectively. Stock solutions were stored at - 20°C until use for the preparation of working solutions. A series of DEX standard working solutions were freshly prepared by adding appropriate volumes of DEX stock solution (1.0 mg/mL) with 30% aqueous acetonitrile to obtain the DEX concentrations of 0.25, 0.50, 1, 2.5, 5, 10, 25 and 50 ng/mL, respectively. These standard working solutions of DEX (20 µL) were spiked to blank ewe samples (180 µL) to yield calibration standards of 25, 50, 100, 250, 500, 1000, 2500 and 5000 pg/mL in plasma. Three levels of QC samples of 50, 500 and 2500 pg/mL were prepared in the same manner.

3.2.1.5 Preparation of plasma samples

Standards and QC samples were extracted by liquid-liquid extraction. An aliquot (200 µL) of plasma samples was extracted with 1 mL of ethyl acetate after the addition of 20 µL of freshly prepared IS stock dilution (0.5 µM testosterone in 30% acetonitrile). The mixture was then vortexed for 1.5 min. After centrifugation of the mixture at 14,800 rpm for 20 min, the upper organic layer was transferred to eppendorf vials and evaporated to dryness by air. The residue was reconstituted with 200 µl of 30% acetonitrile in water followed by centrifugation at 14,800 rpm for 20 min. A volume of 50 µL of the supernatant was injected into HPLC-MS/MS for the DEX quantification.

3.2.1.6 Method validation

Method validation was performed for sensitivity, specificity, accuracy, precision, recovery, and stability, according to the “Guidance for Industry -Bioanalytical Method Validation" document from the United States Food and Drug Administration (FDA) (FDA Guidance

for Industry, 2001). Each analytical run included samples of a double blank (without IS), a blank (with IS) and calibration standards, as well as replicate sets of QC samples.

3.2.1.6.1 Linearity, sensitivity and specificity

Linear calibration curves in ewe samples were constructed by plotting the peak area ratio of DEX/IS versus DEX concentrations over the range of 25-5000 pg/ml. The linearity expressed as y = a + bx was established by using linear regression analysis. The LLOQ was determined as the concentration producing a peak with a signal-to-noise ratio of 10:1. The noise level was the peak area resulting from the blank sample. Each nominal concentration should meet the FDA criteria that deviations should not exceed 20% at LLOQ and be less than 15% at other calibration standard concentrations. The specificity of the HPLC-MS/MS method towards endogenous components in plasma was determined by analyzing six different sources of non-pooled and analyte-free matrices over the selected concentration range.

3.2.1.6.2 Accuracy and precision

QC samples containing low, medium and high DEX concentrations were used to evaluate accuracy and precision of the developed assay method. The intra-day assay accuracy and precision were determined by analyzing replicates (n=6) of the QC samples prepared on the same day, while inter-day assay accuracy and precision were determined using replicates of the QC samples conducted on 3 different days. The assay accuracy was expressed as a percentage of the nominal concentration, (observed concentration/nominal concentration) ×100%, and the precision was expressed by the coefficient of variance (CV).

3.2.1.6.3 Recovery and matrix effect

To determine extraction recoveries, three level concentrations of DEX (50, 500, 2500 pg/ml) were prepared in blank ewe samples and reconstitution solution (30% acetonitrile in water), respectively. The extraction recoveries (expressed as a percentage) were calculated by comparing the peak area of samples spiked before extraction with those spiked after extraction into blank ewe extracts at three different DEX concentration levels.

Matrix effect from endogenous substances present in extracted biological samples may cause ion suppression or enhancement of the signal. Matrix effects were assessed by comparing the peak areas of DEX after the addition of low, medium and high concentrations into reconstitution solution (30% acetonitrile) (A) with those of DEX spiked after extraction into blank extracts (B). The studies were performed with six different lots of matrices. The peak area ratio of B/A as a percentage was used as a quantitative measure of the matrix effect.

3.2.1.6.4 Stability

Replicates (n=6) of three levels of QC samples of maternal and fetal plasma, respectively, were used to assess the stability of DEX during sample storage and preparation procedures. The freeze and thaw stability was assessed after three freeze and thaw cycles. The short-term stability was tested after the QC samples were kept at room temperature for 3 h. The post-preparative stability was measured by determining QC samples prior to and 24 h after storage in the autosampler condition (20°C). Mean (± SD) percentage of nominal concentrations was calculated for the above stability tests using observed concentration from the stability testing samples in reference to that from freshly prepared samples.

3.2.2. Pharmacokinetic and pharmacodynamic studies in pregnant ewe and fetus

3.2.2.1 Animal study protocol

Surgeries and catheterization of the ewes and fetuses were carried out by our collaborators at Texas Children's Hospital, Baylor College of Medicine (Houston, TX, USA), using a technique described previously (Olutoye OA et al., 2011). Briefly, the third-trimester pregnant ewes received anesthesia with 5% isoflurane in oxygen and surgical anesthesia maintained with 2% isoflurane in oxygen following endotracheal intubation. The ewes had a peripheral vein and internal jugular vein catheter inserted for intravenous fluid and study drug administration, respectively. Ewes received a maintenance infusion as well as fluid replacement of 10 mL/kg/h of lactated Ringer's solution for the duration of abdominal exposure. A carotid arterial catheter was inserted for invasive blood pressure monitoring and ewes were positioned supine with a left lateral tilt to avoid aortocaval compression. A laparotomy was performed with a hysterotomy in each gravid uterine horn. The hind limb of each fetus was exposed and femoral arterial and venous catheters placed for invasive arterial blood pressure monitoring and blood sampling.

Administration of DEX to the ewe was initiated following instrumentation of the fetuses as the hysterotomy incision was being closed. A loading dose of DEX at 1 μg/kg over 10 min followed by an infusion of 1 μg/kg/h for 1 h was administered as in prior studies. Maternal and fetal arterial and venous blood samples were obtained at baseline (0 min), after the loading dose (10 min), and at 20, 40, 70 (end of 1 h infusion), 130, 190 and 250 min (3 h after initiation of the loading dose) for DEX quantification. Maternal (1 ml) and fetal (0.5 ml) samples were drawn simultaneously by two investigators. Blood samples

were centrifuged, plasma separated aliquotted and stored at -80°C for subsequent LC-MS/MS analysis. Blank plasma samples collected before drug administration from pregnant ewe and fetus were used as the respective baseline for quantifications.

Maternal and fetal heart rates as well as systolic and diastolic blood pressures were monitored continuously (Spacelabs Monitor Ultraview SL, Garnerville, NY, USA). Arterial blood gas values were obtained at baseline and 60 min following completion of DEX infusion. At the conclusion of this acute, non-survival experimental protocol, all the animals were euthanized with intravenous pentobarbital and potassium chloride.

3.2.2.2 LC-MS/MS assay of plasma samples from pharmacokinetic studies

Maternal and fetal plasma samples from the pharmacokinetic studies were assayed using the LC-MS/MS method in Section 3.2.1

3.2.2.3 Non-compartmental pharmacokinetic analysis

Pharmacokinetic analysis of data was performed using non-compartmental method with PKSolver, an add-in program in Microsoft Excel (Zhang Y et al., 2010). The maximum plasma DEX concentration (C_{max}) and the time to reach C_{max} (T_{max}) were derived from the individual plasma concentration profiles. The area under the curve from the time of administration to the last quantifiable sample time point (AUC_t) was calculated with the linear-up/log down trapezoidal rule (Equations 1 and 2) (Gabrielsson J et al., 2012). The systemic exposure was calculated from the time of administration to infinity (AUC_∞) and represents the sum of AUC_t plus the area under the extrapolated curve (Equation 3). The AUC extrapolated from the last quantifiable time point was calculated as C_{last}/λ (Equation 4). The terminal elimination rate constant (λ) was estimated from the terminal three datum points of the plasma concentrations (natural logarithmic transformed

concentrations) versus time profile, using linear regression. The terminal elimination half-life ($t_{1/2}$) was calculated by ln(2)/λ (Equation 5). The maternal systemic clearance (CL) was derived by the ratio of the total dose to AUC_∞ (Dose/ AUC_∞) (Equation 6). The volume of distribution (V) was derived by the ratio of CL/λ (Equation 7).

The two main trapezoidal rules for AUC calculations are linear and log-linear rules.

Linear rules:

$$AUC_{t_1-t_2} = \frac{C_1 + C_2}{2} \times (t_2 - t_1) \quad (1)$$

Log-linear rule:

$$AUC_{t_1-t_2} = \sqrt[2]{C_1 \times C_2} \times (t_2 - t_1) \quad (2)$$

$$AUC_t = \int_0^t C_p \times dt \quad (3)$$

$$AUC\_extrapolated = \frac{C_{last}}{\lambda} \quad (4)$$

$$t_{1/2} = \frac{0.693}{\lambda} \quad (5)$$

$$CL = \frac{Dose}{AUC_\infty} \quad (6)$$

$$V = \frac{CL}{\lambda} \quad (7)$$

3.2.2.4 Placental transfer of DEX from pregnant ewe to fetus

The ratio between fetal and maternal systemic exposures was calculated to evaluate the degree of placental transfer. Maternal and fetal DEX areas under the concentration-time curve (AUCs) from 0 to 250 min were derived individually, and the partition coefficient from mother to fetus (K_{FM}) was established by the ratio of AUC_{fetus}/AUC_{mother}. The lower the K_{FM}, the lower the degree of drug transfer from ewe to fetus.

$$K_{FM} = \frac{AUC(t)_{fetus}}{AUC(t)_{mother}} = \frac{\int_0^t C_{fetus}(t)dt}{\int_0^t C_{mother}(t)dt}$$

3.2.2.5 Pharmacodynamic analysis

Blood pressure is measured in millimeters of mercury (mmHg). Systolic pressure is the greatest blood pressure on the wall of the arteries when blood is pumping through the arteries, whereas diastolic pressure is the resting phase of the blood pumping cycle. In practice, mean arterial pressure (MAP) was determined by measurements of the systolic blood pressure (SBP) and diastolic blood pressure (DBP) as follows:

$$MAP = \frac{1}{3}SBP + \frac{2}{3}DBP$$

3.2.2.6 Statistical analysis

DEX concentration data, non-compartmental PK parameters and K_{FM} among different time points were reported as mean and standard deviation (SD). The statistical difference in K_{FM} was examined using one-way ANOVA followed by Tukey's post hoc test at $p < 0.05$ (Graphpad Prism version 5.02). Blood pressure and heart rate were

analyzed using ANOVA for repeated measures and the student's t-test was used where appropriate.

3.2.3. Plasma protein binding

3.2.3.1 Determination of fraction unbound of DEX in pharmacokinetic samples

Maternal and fetal plasma samples from pharmacokinetic studies in Section 3.2.3 were thawed and incubated at 37 °C for 30 min. YM-30 Centrifree® ultrafiltration devices (**Figure 8**) were used to determine the unbound fraction (fu) of DEX for each sample. Two hundred µL aliquots of the plasma samples were added into the sample reservoir of the ultrafiltration units, and then the units were centrifuged with a swinging-bucket rotor at 1,000 g (37 °C) for 30 min. Fifty µL ultrafiltrate from the filtrate cup was transferred for sample preparation and analysis.

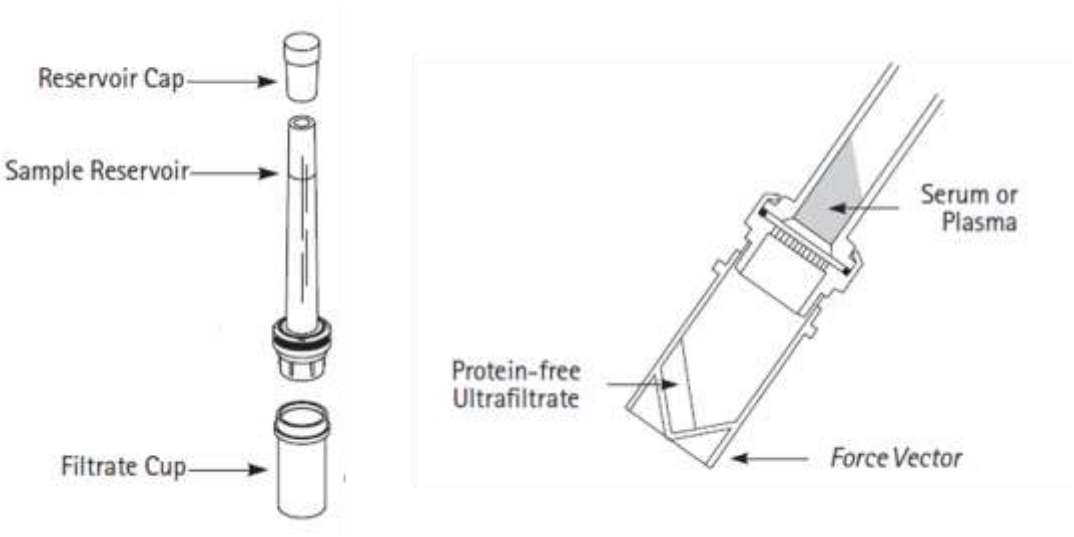

Figure 8 **Centrifree® ultrafiltration devices for plasma protein binding study (Millipore Centrifree® Ultrafiltration Devices Instructions)**

3.2.3.2 Determination of fraction unbound in DEX-spiked blank samples

Stock solutions of DEX (1 mg/mL) in methanol were added to blank pregnant ewe and fetus plasma, respectively, to provide maternal and fetal plasma samples at different concentrations over the respective concentration ranges relevant to those in pregnant ewe and fetus samples of pharmacokinetic studies in Section 3.2.2. Aliquots of plasma were placed in a rolling incubator at 37 °C for 30 min to ensure that equilibrium was established. Following incubation, two hundred µL aliquots of the spiked plasma samples were added into the sample reservoir of ultrafiltration unit. The plasma samples were then centrifuged with fixed angle rotor at 1,000 g (37 °C) for 30 min. Fifty µL of ultrafiltrate from the filtrate cup was transferred for sample preparation and analysis.

3.2.3.3 Determination of the extent of nonspecific binding

Nonspecific binding (NSB) of DEX onto the YM-30 Centrifree® ultrafiltration filter membrane and plastic devices was determined by using PBS samples at three DEX concentrations of 100, 500 and 2500 pg/ml. The PBS samples were prepared by the same procedure described in Section 3.2.3.2.

3.2.3.4 Sample preparation and analysis

The sample extraction and reconstitution procedures previously described in Section 3.2.1.5 were followed. After sample preparation, aliquots of samples (10-20 µL) were analyzed using the modified LC-MS/MS assay with an advanced mass spectrometer of AB Sciex 5500 QTRAP® that can achieve a LLOQ of 10 pg/mL.

All experimental procedures were performed with more than three replicates, and NSB and fu were reported as mean with standard deviation (SD) unless otherwise noted.

Statistical analysis was performed using two-tailed Student's t test between two mean values or one-way ANOVA with post-hoc Tukey's test among mean values more than two groups. A probability of less than 0.05 ($p < 0.05$) was considered to be statistically significant.

3.2.3.5 Plasma protein binding (%) calculation

NSB of ultrafiltration units was determined from the measured concentrations of filtrate and PBS samples using the following equation:

$$\% \text{ NSB} = (1 - \frac{Cpbs_{uf}}{Cpbs}) \times 100\%$$

Where C_{pbs} is the (total) drug concentration in the initial PBS solution before centrifugation and $Cpbs_{uf}$ is the drug concentration in the PBS ultrafiltrate after centrifugation. When $Cpbs_{uf} = C_{pbs}$, NSB is 0, and there is no need of NSB correction for the protein binding calculation. When $Cpbs_{uf} < C_{pbs}$, it can be assumed that a fraction of drug disappeared in UF. The NSB correction of plasma protein binding was calculated as follows:

$$\% \text{ fu} = \frac{Cp\_uf}{(1 - NSB) \cdot Cp} \times 100\%$$

$$\% \text{ PPB} = (1 - \text{fu}) \times 100\%$$

Where fu is the free fraction, Cp_uf is the drug concentration in the plasma filtrate, and Cp is the nominal plasma concentration.

3.2.4. *In vitro* UGT metabolism

3.2.4.1 Preparation of liver and placental microsomes

Blank placenta and liver samples from pregnant ewes and fetuses were supplied by Texas Children's Hospital, Baylor College of Medicine (Houston, TX, USA). Microsomes were prepared using a procedure adopted from the literature with minor modifications as described below (Chen J et al., 2003). Briefly, organ samples were thawed and then minced on a glass plate placed on ice with a sharp and clean blade to make the samples ready for homogenization. The minced organ samples were then transferred into 10 ml cylindrical homogenization glass tubes placed on ice. The livers were then homogenized using a motorized homogenization gun fitted with a Teflon pestle in ice-cold homogenization buffer comprised of 10 mM potassium phosphate solution (pH 7.4), 250 mM sucrose and 1 mM EDTA.

The mixture was then transferred into clean polycarbonate centrifuge tubes and centrifuged at 10,500 rpm at 4°C for 15 min. The pellet which contained cell debris and unwanted waste was discarded and the supernatant was collected into clean polycarbonate ultracentrifuge tubes and centrifuged again at 35,000 rpm at 4°C for 60 min. The fat layer on the top was carefully aspirated using rubber droppers to yield the microsomal pellets. The microsomal pellets were then washed three times with 250 mM sucrose and resuspended in 250 mM sucrose by manually homogenizing and grinding the microsomal pellets with a Teflon pestle. The final liver or placental microsomes were stored frozen at -80 °C until the use for study of DEX metabolism. Protein concentration was determined using a BCA protein assay kit with bovine serum albumin (BSA) as the standard.

3.2.4.2 BCA assay for protein quantification

Microsomes were placed on ice all the time during the experiment. Working reagent was prepared by mixing Reagent A (bicinchonic acid and tartrate in an alkaline carbonate buffer) with Reagent B (4% copper sulfate pentahydrate solution) in the BCA protein assay kit at a ratio of 50:1 as per the manufacturer's recommendation. Triplicate 10 µL of the microsome samples were added to the working reagent (190 µL) in 1.5-mL tubes. The standards of protein concentrations were prepared from the stock of 2 mg/mL with the working reagent to get final concentrations of 0.1, 0.2, 0.4, 0.6, 0.8 and 1 mg/mL respectively. Two hundred µL of working reagent containing the samples or standards was then transferred into a clear bottom 96 well plate. The plate was covered with aluminum foil and incubated at 37 °C for 30 min. After incubation, the plate was read on a Biotek plate reader for the absorbance at 570 nm to determine the microsomal protein concentrations.

3.2.4.3 Enzyme assays

The enzyme assay procedures for measuring UGTs' activities were the same as previously published in the literature (Joseph TB et al., 2007; Liu X et al., 2007; Tang L et al., 2009). A final mixture for incubation procedures comprised of liver or placental microsomes (final concentration in range of 0.0053-0.053 mg of protein per mL as optimum for reaction), alamethicin (0.022 mg/mL), saccharolactone (4.4 mM), magnesium chloride (0.88 mM), different concentrations (1.25-50 µM) of substrate in a 50 mM potassium phosphate buffer (pH 7.4), and UDPGA (3.5 mM, added the last). The mixture (200 µL) was incubated at 37°C for predetermined periods of time and the reaction was stopped by adding acetonitrile/acetic acid (94:6) containing 100 µM testosterone (IS). Pooled human liver microsomes (pHLM) were used as the positive

control, whereas the negative control was the sample with the same amount of potassium phosphate replacing microsomes. Genistein, a typical known substrate of UGT, was used to investigate the UGT activities in pregnant ewe model.

3.2.4.4 UPLC analysis and confirmation of glucuronide structures by LC-MS/MS

Parent compounds and their generated glucuronides were analyzed using a Waters UPLC system. DEX and its glucuronide were separated and identified using the LC-MS/MS assays in Section 3.2.1 with minor modifications. The detect transition ion from a specific precursor ion to product ion $[M+H]^+$ for DEX glucuronide is m/z 377.1 → 201.5. The collision energy was set at 22 eV for the DEX glucuronide.

Genistein and its glucuronide were analyzed by UPLC with photodiode array detector and Empower software, using the following method that was described in the literature (Liu Y et al., 2002; Tang L et al., 2009). Briefly, the mobile phase A is 0.5% formic acid in water and mobile phase B is 100% acetonitrile. The elution was achieved with a BEH C18 column (1.7 μm, 2.1 × 50 mm). Mobile phase was eluted for 5 min at a flow rate of 0.5 ml/min with gradient (10% B at 0 to 0.3 min, 10–50% B at 0.3 to 2 min, 50–90% B at 2 to 3.5 min, 90% B at 3.5 to 4.0 min, 90-10% at 4.0 to 4.5 min, and 10% B at 4.5 to 5 min). Samples of 10 μL were injected into UPLC for analysis. Genistein and its glucuronide were detected and quantified at the wavelength of 254 nm. The LLOQ was 0.78 μM (Tang L et al., 2009).

3.2.4.5 Kinetic analysis

Metabolism rates in liver and placental microsomes were expressed as amounts of metabolites formed per min per mg protein (nmol/min/mg). Kinetic parameters (V_{max} and K_m) were estimated by fitting the Michaelis-Menten and/or atypical profiles equations to

the substrate concentrations and initial rates. Eadie-Hofstee plots were used to confirm the kinetic model selection. If the Eadie-Hofstee plot was linear, the standard Michaelis-Menten equation could be used to fit the glucuronides formation rates (V) at different substrate concentrations (C).

$$v = \frac{V_{max} \times C}{K_m + C}$$

If Eadie-Hofstee plots showed characteristic profiles of atypical kinetics (e.g. biphasic kinetics), atypical profiles equations, such as the Hill equation ($v = \frac{V_{\max} \times S^n}{K_m^n + S^n}$), substrate inhibition ($v = \frac{V_{\max}}{1 + (K_m/S) + (S/K_{si})}$) and biphasic two sites ($v = \frac{V_{\max 1} \times S}{K_{m1} + S} + \frac{V_{\max 2} \times S}{K_{m2} + S}$), could be used to adequately fit the data using SigmaPlot. Akaike's information criterion (AIC) and R^2 values were used to evaluate the goodness-of-fit of each model.

3.2.5. Pharmacokinetic/pharmacodynamic modeling

3.2.5.1 Phoenix NLME

Pharmacokinetic analysis was performed by a nonlinear mixed-effect modeling approach, using Phoenix NLME software (nonlinear mixed-effects, version 1.3). This NLME modeling could provide a good solution for modeling sparse datasets with deviated sampling time and/or missing samples. These models also account for both fixed effects (population parameters assumed to be constant each time when data are collected) and random effects (sample-dependent random variables).

3.2.5.2 Pharmacokinetic modeling of free and total DEX

The pharmacokinetic model was developed based on the data collected from a total of eight pregnant ewes and twelve fetuses in Section 3.2.2. Model development and simulation were performed using the first-order conditional estimation with η-σ interaction. The pharmacokinetics of free and total DEX concentrations in pregnant ewe and fetus were studied sequentially, described as follows: (1) the pharmacokinetics of DEX in pregnant ewes were investigated; (2) the fetal data were connected to the pregnant ewe model, and the corresponding parameters in fetus were estimated, but the maternal parameters were fixed; (3) protein binding model was evaluated to describe the relationship between free and total DEX plasma concentrations; and (4) all the parameters of the integrated model were estimated simultaneously for free and total DEX data from both pregnant ewe and fetus.

For the maternal data, one-, two- and three-compartment models were tested. For fetal concentrations, two models were tested: (a) an additional compartment linked to maternal compartment and (b) an effect compartment of negligible volume linked to the maternal circulation by first-order processes to the maternal circulation. Nonlinear and linear protein-binding models were considered for describing the relationship between free and total DEX concentrations.

Estimation of individual PK parameters was assumed to follow a log-normal distribution. Therefore exponential distribution models were used to describe the intersubject variability as follows:

$$P_i = P \cdot exp(\eta_i)$$

Where P_i is the individual parameter estimate for individual *i*, *P* is the typical population parameter estimate, and η_i was assumed to be distributed *N* (0, ω^2). Only significant intersubject variability in pharmacokinetic parameters was retained.

Residual unexplained variability was implemented as either a proportional or combined error model:

$$C_{observed,ij} = C_{pred,ij} \times (1 + \varepsilon_{p,ij}) + \varepsilon_{a,ij}$$

Where $C_{observed,ij}$ represents the observed concentration for individual *i* and observation *j*, $C_{pred,ij}$ represents the individual predicted concentration, and $\varepsilon_{p,ij}$ and $\varepsilon_{a,ij}$ represent the proportional and additive errors distributed following N (0, σ^2). The residual error model was selected based on the likelihood ratio tests as well as evaluation of the goodness-of-fit diagnostic plots.

3.2.5.3 Model selection and evaluation

To determine an appropriate PK model, model discrimination and identification of variability were based on evaluations of the -2 × log likelihood (-2LL) of the data, plausible parameter estimates, and adequate parameter precision, as well as evaluation of diagnostic plots. A difference in -2LL of at least 3.84 (corresponding to $p < 0.05$) was used to discriminate between competing models. The accuracy of the final model was tested with a bootstrap method in Phoenix NLME, based on the random resampling from the original data. The resampling was repeated sufficiently to meet FDA guidelines (FDA Guidance for Industry - Population Pharmacokinetics, 1999). Predicted parameters obtained from the bootstrap validation were compared to the estimates from the original data.

3.2.5.4 Pharmacodynamic modeling

Pharmacodynamic models were also analyzed by Phoenix (version 1.3). The observed pharmacodynamic effects of blood pressure and heart rate were linked to predicted maternal and fetal plasma concentrations via a sigmoidal E_{max} model:

$$E = E_0 + \frac{E_{max} \cdot C_e^n}{C_e^n + EC_{50}^n}$$

Where E_0 is the baseline effect, E_{max} is the maximal effect, EC_{50} is the effect-site concentration that could produce half of the maximum response, n is a slope factor and E is the estimated effect at effect-site concentration of C_e. The effect-site concentration is assumed to be the same as the plasma concentration at steady-state.

Chapter 4 Results

The results of this investigation are summarized in the following six subtopics: (1) Development and validation of LC-MS/MS assay for quantification of DEX in the pregnant ewe model, (2) Maternal and fetal pharmacokinetics of DEX after intravenous administration to pregnant ewes, (3) Pharmacodynamic studies of DEX in pregnant ewe and fetus; (4) *In vitro* plasma protein binding assay, (5) UGT metabolism of DEX with liver and placental microsomes, and (6) Pharmacokinetic and pharmacodynamic models of DEX in pregnant ewe model.

4.1. LC-MS/MS assay for quantification of DEX in plasma

4.1.1. LC Chromatographs

No significant interfering peaks from plasma endogenous components were present at the retention time of DEX (3.20 min) or IS (3.56 min). The LLOQ for DEX was 25 pg/mL with a 3200 QTRAP mass spectrometer. The chromatograms for blank plasma, and blank plasma samples spiked with DEX at LLOQ are shown in **Figure 9** for pregnant ewe and in **Figure 10** for fetus, respectively. A lower LLOQ of 10 pg/mL was achieved with a 5500 QTRAP mass spectrometer.

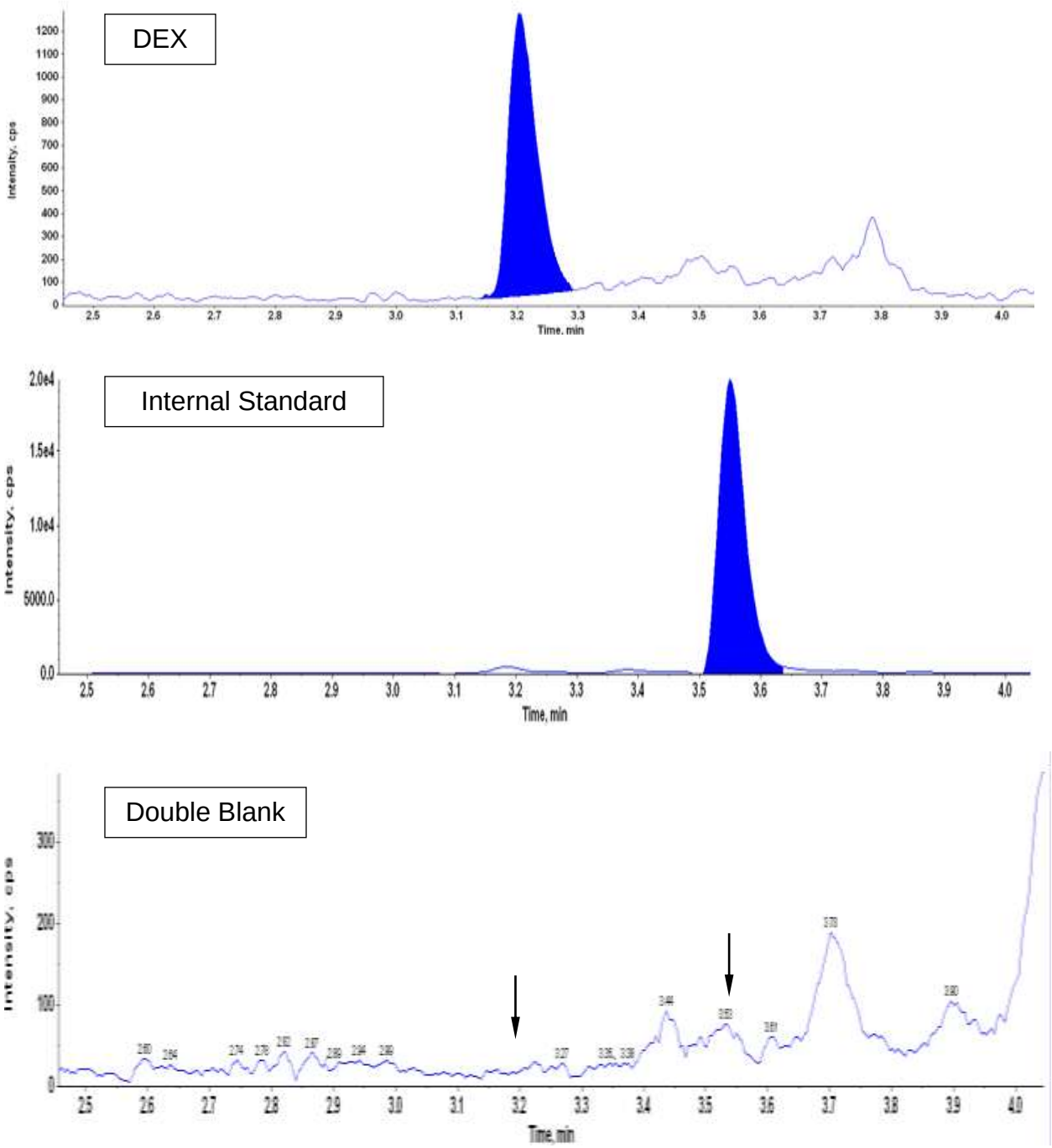

Figure 9 Chromatograms of DEX with LLOQ (25 pg/mL) in maternal plasma

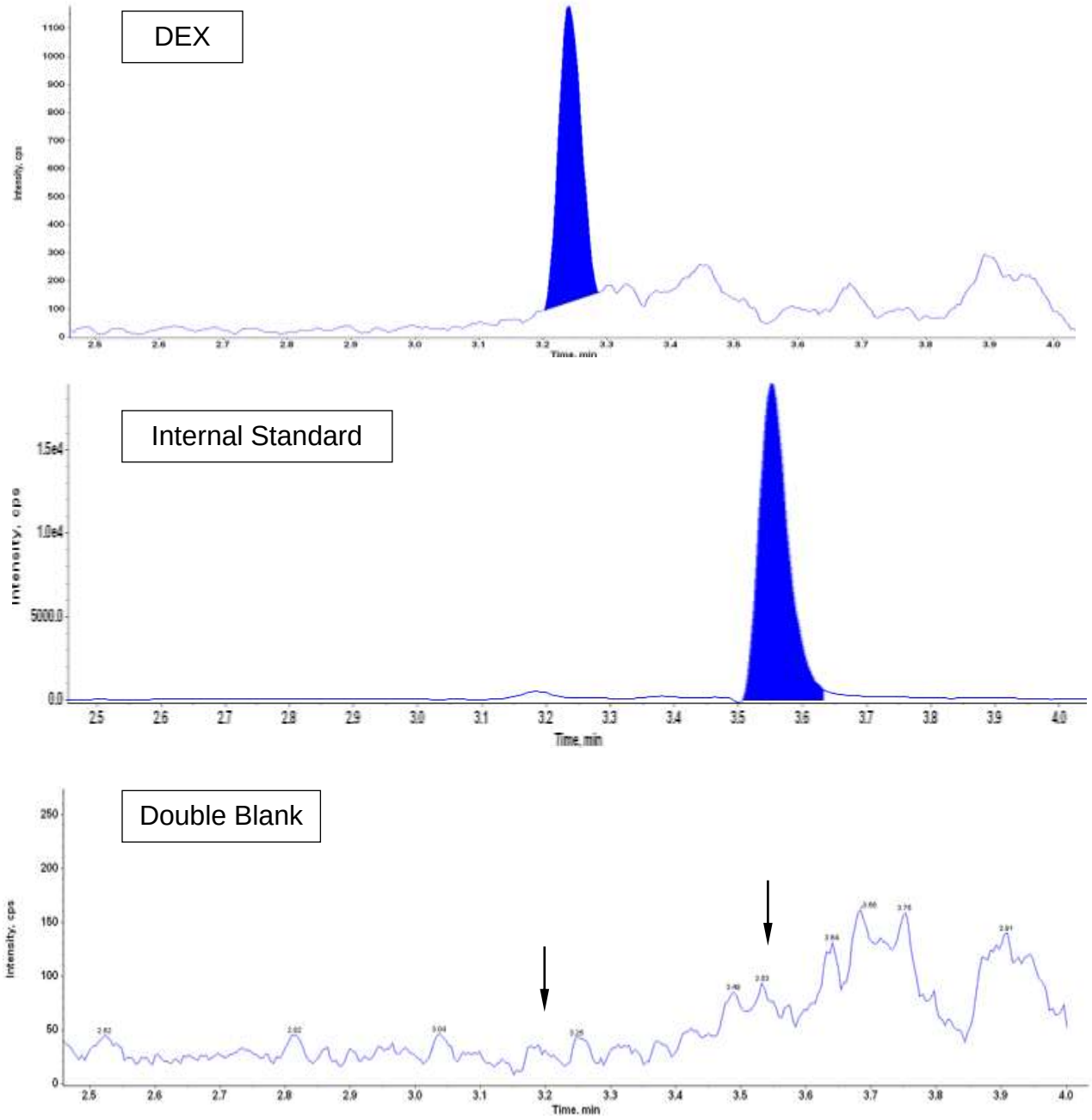

Figure 10 Chromatograms of DEX with LLOQ (25 pg/mL) in fetal plasma

4.1.2. Linearity of calibration curves

The assay exhibited excellent linear response over the selected concentration ranges (25-5000 pg/mL in plasma) by linear regression analysis (**Figure 11**). Inter-day assay variability of the calibration curves from six different sources was presented in **Table 5**. Correlation coefficients (r^2) from inter-day batches over calibration curves were greater than 0.99.

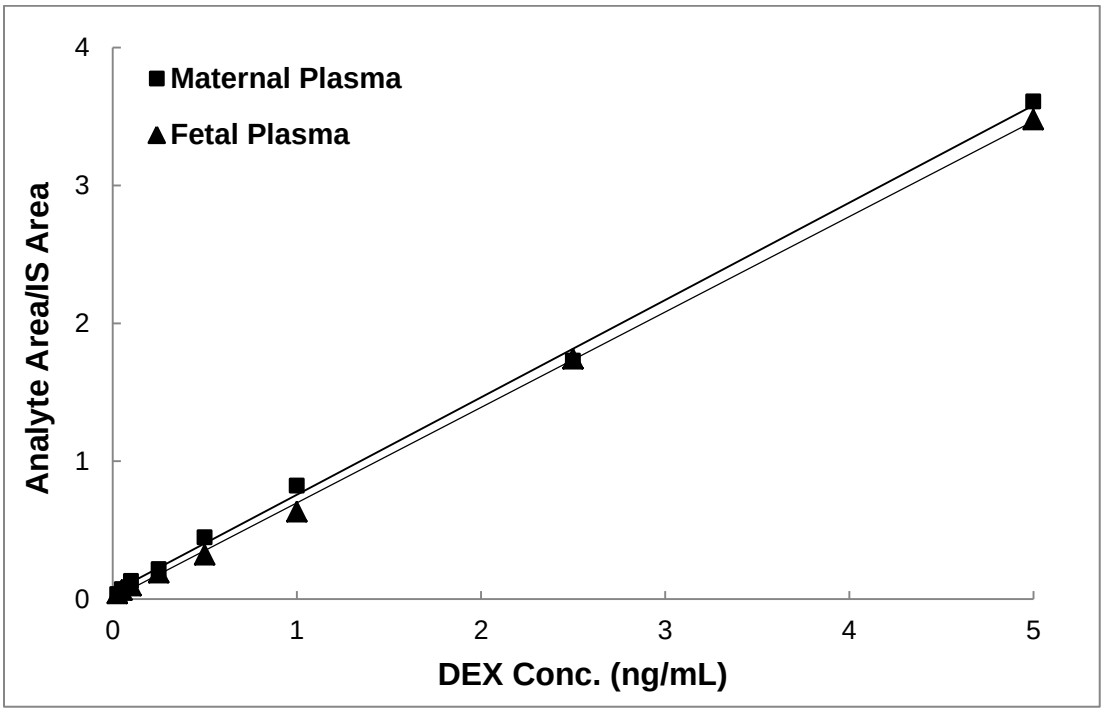

Figure 11 Calibration curves of DEX in maternal plasma (R^2 = 0.9985) and fetal plasma (R^2 = 0.9993)

Table 5 Linearity of calibration curves for DEX (n=6)

Inter-day Assays	Range (pg/ml)	Slope (ng^{-1})		R^2	
		Mean ± SD	CV (%)	Mean ± SD	CV (%)
Maternal Plasma	25-5000	0.63±0.06	9.17	0.9943±0.0136	1.38
Fetal Plasma	25-5000	0.61±0.03	5.16	0.9997±0.0002	0.02

4.1.3. Accuracy and precision

Data of intra- and inter-day accuracy and precision for DEX are summarized in **Table 6.** The intra-day accuracy and precision, based on the coefficient variation replication for QC samples, ranged from 97.7 to 100.0% and 3.3 to 5.2% in maternal plasma, respectively, and 98.2 to 102.6% and 3.1 to 5.0% in fetal plasma, respectively. The inter-day accuracy and precision ranged from 94.8 to 100.1% and 4.5 to 5.6% in maternal plasma, respectively, and 99.5 to 100.2% and 4.2 to 6.0% in fetal plasma, respectively. These data revealed that the developed assay was accurate and reproducible.

Table 6 Accuracy and precision of DEX at three levels of QC samples

Nominal Conc. (pg/mL)	Intra-day Batch (n=6)		Inter-day Batch (n=18)	
	Accuracy (%)	***Precision (%)***	***Accuracy (%)***	***Precision (%)***
Maternal Plasma				
50	98.73	5.24	94.80	5.64
500	100.02	3.27	100.07	5.37
2500	97.73	3.25	100.03	4.50
Fetal Plasma				
50	102.60	3.10	100.20	4.53
500	99.17	4.38	99.97	5.99
2500	98.21	4.97	99.52	4.19

4.1.4. Recovery and matrix effect

The mean (±SD) extraction recoveries and matrix effects on DEX are tabulated in **Table 7**. In maternal plasma samples, extraction recoveries at 50, 500 and 2500 pg/mL were 83.7±2.5%, 87.2±3.4% and 82.9±2.5%, respectively, while in fetal plasma samples, extraction recoveries at 50, 500 and 2500 pg/mL were 86.2±2.5%, 89.7±3.1% and 88.4±0.8%, respectively. The CV % for all recoveries were less than 3.9% indicating the extraction efficiency for DEX using liquid-liquid extraction was consistent and reproducible. The mean (±SD) percentage matrix factors were 110.8 ± 11.4% and 101.3 ± 7.5% in maternal and fetal plasma, respectively. No significant difference in matrix effect was observed between maternal and fetal plasma samples, and the effects were concentration-independent in the tested concentration ranges. These indicated a low ion enhancement and that the analytical method is free from significant interference from endogenous substances in plasma.

Table 7 Recovery and matrix effect of DEX in pregnant ewes and fetuses (n=6)

Nominal Conc. (pg/mL)	Recovery of Extraction (%)		Matrix Effect (%)	
	Mean ± SD (%)	CV (%)	Mean ± SD (%)	CV (%)
Maternal Plasma				
50	83.74±2.48	2.96	122.6±8.35	6.81
500	87.23±3.40	3.89	110.0±4.68	4.26
2500	82.92±2.48	2.98	99.82±7.39	7.40
Overall	**84.63±2.29**	**2.70**	**110.8±11.4**	**10.29**
Fetal Plasma				
50	86.17±2.49	2.88	107.3±7.20	6.71
500	89.67±3.07	3.42	92.86±5.46	5.88
2500	88.35±0.80	0.91	103.5±10.7	10.35
Overall	**88.06±1.77**	**2.01**	**101.3±7.51**	**7.42**

4.1.5. Stability

The stability experiments were designed based on the expected conditions during the sample storage and processing procedures. Each stability test included three replicates of three levels of QC samples. The stability data under various storage and process conditions are presented in **Table 8**. The results of freeze and thaw stability experiment indicated that DEX was stable in plasma (95.6-103.4%) for three cycles when stored at -80°C and thawed to room temperature. The results of the post-preparative stability study confirmed that DEX could be analyzed for 24 h in the autosampler tray at 20°C with 96.0-102.9% of nominal concentration. In addition, the short-term stability result ensured reliable stability (94.8-101.5%) for 3 h under the sample preparation procedures at room temperature.

Table 8 Stability of DEX under various conditions (n=3)

Nominal Conc. (pg/mL)	Mean (± SD) Percent of Nominal Conc.		
	Freeze/Thaw Stability Three Cycles, - 80°C	***Post-preparative Stability Autosampler, 20 °C, 24 h***	***Short-term Stability Sample at RT, 3 h***
Maternal Plasma			
50	95.61±4.95	100.8±3.34	101.5±2.72
500	101.3±1.56	102.9±1.68	94.79±2.08
2500	97.54±2.37	95.96±5.56	96.29±4.28
Fetal Plasma			
50	98.55±0.91	100.6±0.82	95.42±1.36
500	100.8±3.75	99.63±1.05	98.68±5.08
2500	103.4±3.90	99.88±4.27	95.19±1.52

4.2. Pharmacokinetics of DEX in pregnant ewe and fetus

Pharmacokinetic experiments were completed in all eight third-trimester ewes (mean weight 72.8 ± 11.0 kg) and their twelve fetuses. Complete paired pharmacodynamic data were obtained in four maternal-fetal units.

4.2.1. Plasma concentration-time profiles

A total of 107 DEX concentrations measured above the LLOQ were included in the PK evaluation, among which 47 and 21 concentrations were from maternal artery and vein, respectively, and 62 and 19 concentrations were from fetal arterial and vein, respectively. Maternal and fetal concentrations ranged from 29.8 to 6197.9 pg/mL, and from 8.0 to 265.0 pg/mL, respectively. The mean (± SD) plasma DEX concentration-time profiles in maternal arterial and venous blood, as well as those in fetal arterial and venous blood are depicted in **Figure 12**.

DEX concentration profiles in maternal arterial and venous blood were similar except in one ewe at early time points with three extremely high venous concentrations that resulted in large variations in the maternal concentrations during infusion with a coefficient of variation (CV%) = 141.1%, whereas the fetal concentrations during infusion were relatively constant with a CV% of 48.0%. The fetal arterial and venous DEX concentration profiles were comparable.

At the end of the loading dose (10 min), DEX concentrations in maternal artery and fetal vein were 815.1±497.2 and 104.5±40.3 pg/mL, respectively. This indicated a rapid transplacental transfer of DEX after drug administration to the pregnant ewe. At 70 min (the end of the one hour infusion), maternal DEX concentrations started declining rapidly

for 1 h (at 130 min), followed by a slower decline. On the other hand, fetal DEX levels remained relatively constant, markedly lower than those in the pregnant ewe before one hour post the end of infusion.

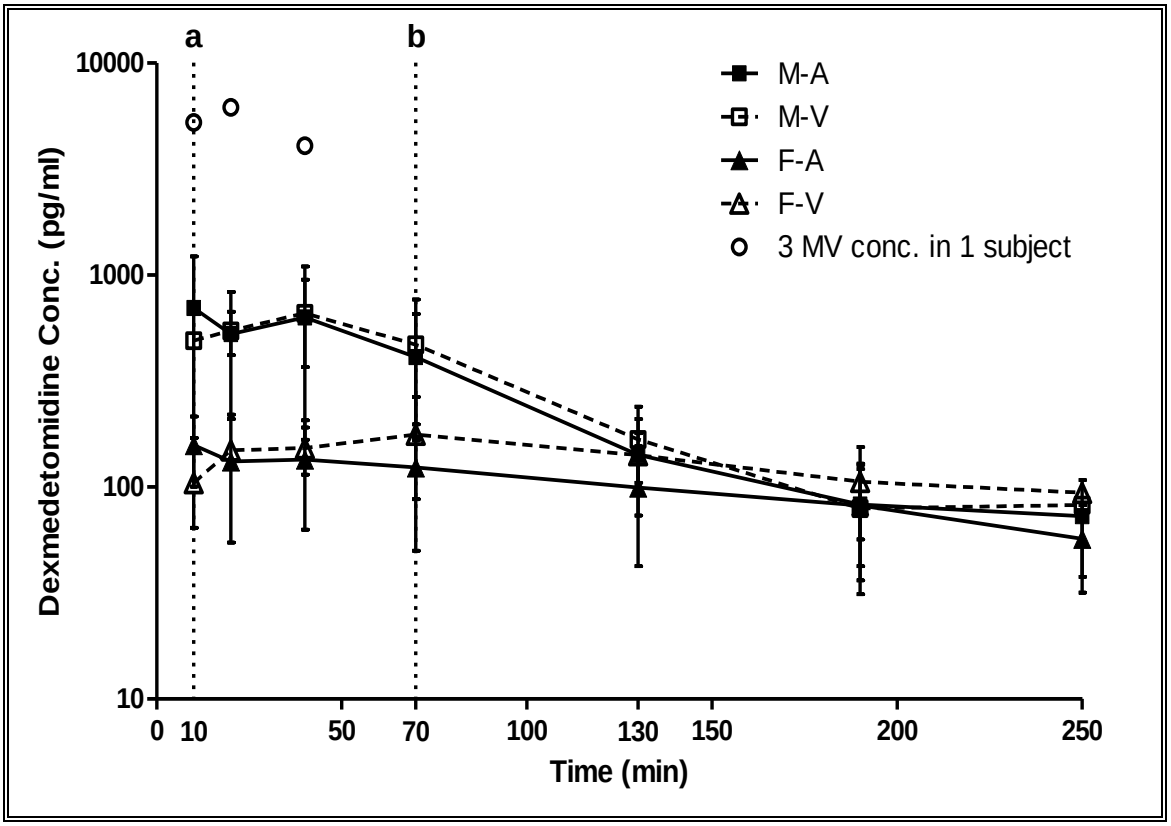

Figure 12 Mean (± SD) DEX concentration-time profiles for pregnant ewes (n=8) and fetuses (n=12). Line a: end of loading dose and Line b: end of infusion.

M-A: maternal arterial concentrations
M-V: maternal venous concentrations excluding 3 high concentrations during infusion in one ewe (3 MV conc. in 1 subject, shown as open circles)
F-A: fetal arterial concentrations
F-V: fetal venous concentrations

4.2.2. Non-compartmental pharmacokinetic analysis

Data of maternal and fetal arterial concentrations were sequentially used for non-compartmental PK analysis. The estimates of PK parameters for individual ewes and fetuses are tabulated in **Table 9**. The C_{max} of DEX was 778.1 ± 398.4 and 143.6 ± 86.6 pg/mL in pregnant ewe and fetus, respectively. The t_{max} (time to reach the C_{max}) occurred at approximately 40 and 47.5 min (70 min, at the end of infusion for four subjects and 10 min for the other four subjects) in pregnant ewe and fetus, respectively. The maternal and fetal AUC_t were 61.8 ± 22.5 and 20.5 ± 11.9 ng/(mL*min), respectively. The maternal CL and V were 38.64 ± 17.72 mL/(min*kg) and 3357.6 ± 1292.2 mL/kg, respectively. The C_{max} and AUC_t between pregnant ewes and fetuses were statistically different, whereas $t_{1/2}$ was not.

Table 9 Pharmacokinetic parameters by non-compartmental analysis of arterial concentration in pregnant ewes (n=8) and fetuses (n=12)

	Unit	Pregnant Ewe	Fetus
t_{max}	min	40.0 ± 32.1	47.5 ± 29.0
*C_{max}	pg/mL	778.1 ± 398.4	143.6 ± 86.6
*AUC_t	ng/(mL*min)	61.8 ± 22.5	20.5 ± 11.9
AUC_∞	ng/(mL*min)	69.5 ± 21.1	34.9 ± 20.7
$t_{1/2}$	min	63.62 ± 24.0	143.6 ± 86.6
CL	mL/(min*kg)	38.64 ± 17.72	--
V	L/kg	3.36 ± 1.29	--

Note:

* indicates values are significantly different between pregnant ewes and fetuses by Student's t-test at $p<0.05$.

-- indicates values that cannot be derived because the amount of DEX transferred to the fetus is unknown.

4.2.3. Placental transfer of DEX

The placental transfer partition coefficient (K_{FM}) of DEX from the pregnant ewe to the fetus is calculated by AUC ratios between fetuses and ewes, and is shown in **Table 10**. K_{FM} was 0.13 ± 0.10 and 0.13 ± 0.08 at 10 min and 70 min respectively. Distributions in mothers and fetuses reached equilibrium rapidly. At 250 min, three hours after the end of infusion, K_{FM} reached 0.23 ± 0.14. Based on the placental transfer partition ratio (K_{FM}), the fetal exposure to DEX was approximately 23% of maternal exposure. There was no statistical difference among the K_{FM} at any of the time points.

Table 10 K_{FM} from pregnant ewe (n=8) to fetus (n=12) at different time points

Time (min)	K_{FM}
10	0.13 ± 0.10
20	0.15 ± 0.11
40	0.13 ± 0.17
70	0.13 ± 0.08
130	0.16 ± 0.10
190	0.20 ± 0.15
250	0.23 ± 0.14

4.3. Pharmacodynamics of DEX in pregnant ewe and fetus

Pharmacodynamics of blood pressure and heart rate in pregnant ewe and fetus after drug administration are shown in **Figures 13** and **14**, respectively. Significant decreases were observed in maternal diastolic blood pressure and maternal heart rate. Pregnant ewes exhibited a 30% decrease in mean arterial pressure (MAP) with a clinically significant difference between the MAP at baseline and MAP at 120 min of the study (**Figure 15**). An approximately 50% decrease in heart rate upon administration of DEX was observed which continued throughout the period of drug administration. This decrease in heart rate was statistically significant between baseline and 120 min. In contrast, only a negligible decrease in the MAP (1%) and a 16% decrease in the heart rate of the fetus were observed with fetal exposure to DEX. While decreases in both parameters continued to be observed over the initial 2 h period of the study; 14% and 12% reduction in fetal MAP and heart rate, respectively, after 2 h of drug administration, both values remained within clinically normal parameters and were not statistically significant compared to the values at baseline. **Table 11** summarizes arterial blood gas values obtained at baseline and 120 min. Decreases in fetal arterial oxygen content and an increase in fetal metabolic acidosis were noted by the conclusion of the study, but these changes were not statistically significant between baseline and 120 min.

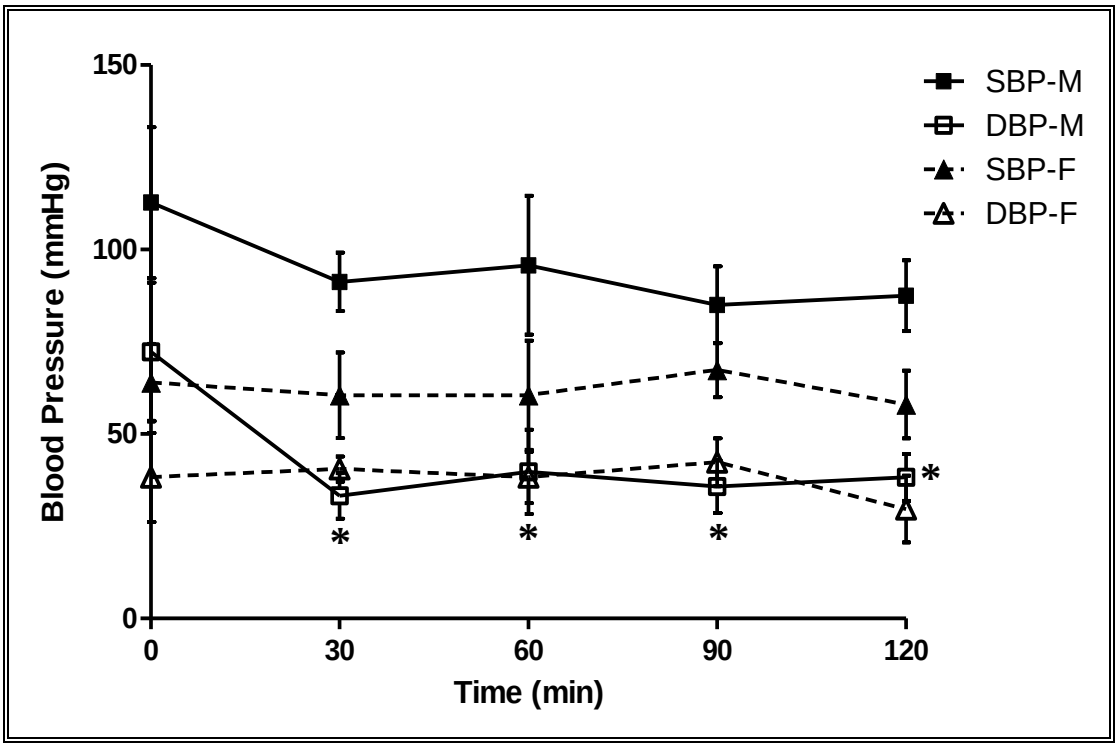

Figure 13 Mean (±SD) blood pressure profiles of pregnant ewe and fetus (n=4)

SBP-M: maternal systolic blood pressure
DBP-M: maternal diastolic blood pressure
SBP-F: fetal systolic blood pressure
DBP-F: fetal diastolic blood pressure

Note:

* indicates values are significantly different compared to values at baseline by one-way ANOVA with post hoc Tukey's test at $p<0.05$

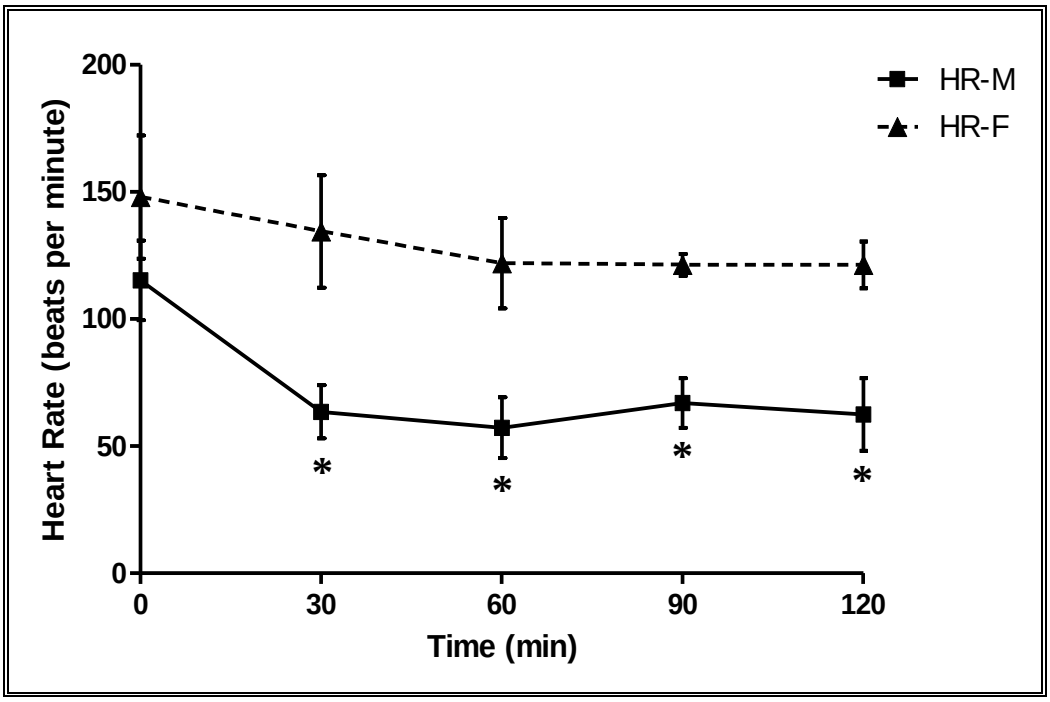

Figure 14 Mean (±SD) heart rate profiles of pregnant ewe and fetus (n=4)

HR-M: maternal heart rate
HR-F: fetal heart rate

Note:

* indicates values are significantly different compared to values at baseline by one-way ANOVA with post hoc Tukey's test at $p<0.05$

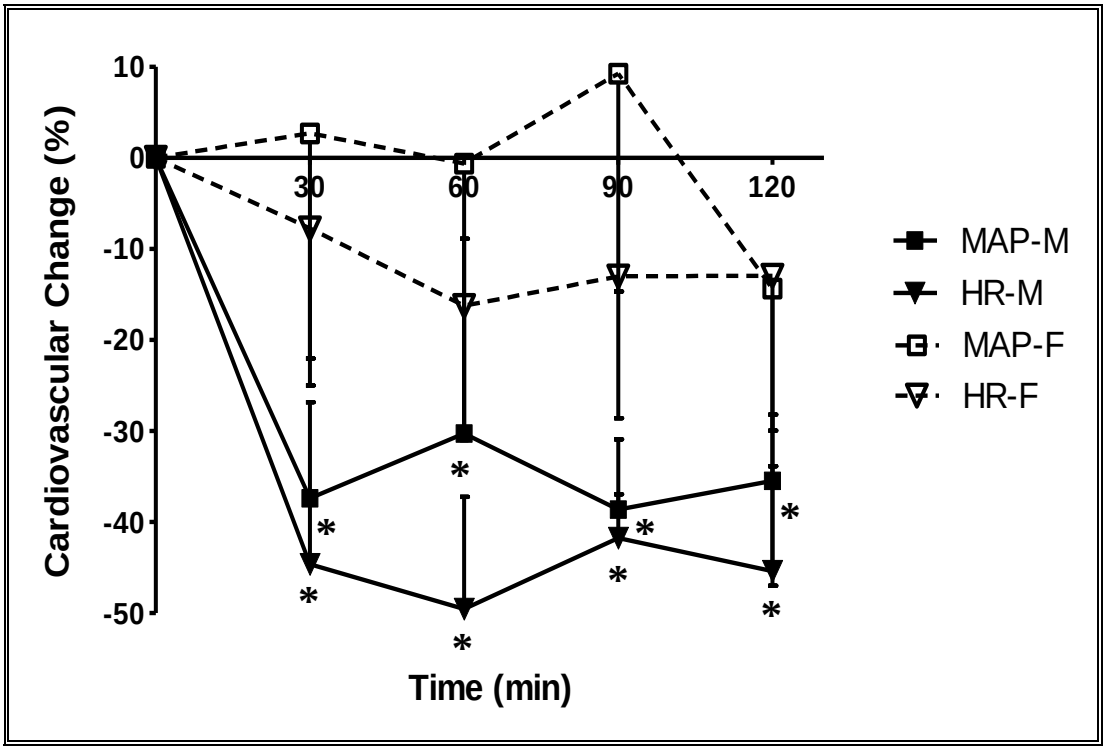

Figure 15 Mean (±SD) profiles of cardiovascular effects (percentage change)

MAP-M: maternal mean arterial pressure
MAP-F: fetal mean arterial pressure
HR-M: maternal heart rate
HR-F: fetal heart rate

Note:

* indicates values are significantly different compared to values at baseline by one-way ANOVA with post hoc Tukey's test at $p<0.05$

Table 11 Arterial blood gas at baseline and 120 min (n=4)

	Baseline		120 min	
	Pregnant Ewe	***Fetus***	***Pregnant Ewe***	***Fetus***
pH	7.42 ± 0.12	7.31 ± 0.06	7.56 ± 0.13	7.13 ± 0.12
Pa_{O2}	279 ± 139	21 ± 2	338 ± 109	13 ± 6
Pa_{CO2}	43 ± 14	59 ± 23	39 ± 14	84 ± 29
SaO_2	99.6 ± 0.5	31.3 ± 2.5	99.9 ± 0.1	12 ± 12
BE	5.8 ± 4.6	4.3 ± 5.6	6.7 ± 4.0	-1.4 ± 9.2
HCO_3	29.5 ± 5.8	30.2 ± 6.6	29.7 ± 5.1	26.0 ± 6.0

SaO_2: Oxygen Saturation

BE: Base Excess

4.4. Plasma protein binding assay

Nonspecific binding (NSB) was determined as 17.8 ± 2.1 % (n=3) at three concentration levels of 100, 500 and 2500 pg/ml in PBS (**Table 12**). The calibration curves containing 5 concentration points were constructed at the linearity range of 50-2500 pg/mL in PBS with correlation coefficients > 0.999 (**Figure 16**).

Fractions of unbound (fu) DEX in pregnant ewe and fetus were 25.1 ± 4.8 % (n=4-7) and 38.9 ± 3.2 % (n=3), respectively. Therefore, the extents of plasma protein binding (PPB) were 74.9 ± 4.8 % for pregnant ewe, significantly higher than those in fetus (61.1 ± 3.2 %) (**Table 13**), and were concentration-independent over the respectively selected concentration ranges of 50-2500 pg/mL for maternal samples and 50-200 pg/mL for fetal samples (**Figure 17**).

The fu in DEX-spiked blank plasma of pregnant ewe (27.2 ± 3.3 % for 50pg/mL and 24.2 ± 5.0 % for 100pg/mL) were significantly lower (p<0.05) than those in fetal plasma, 38.5 ± 3.5 % for 50 pg/mL and 39.6 ± 3.4 % for 100 pg/ml (**Table 13** and **Figure 18**).

The PPB in PK samples was determined in 26 maternal samples and 24 fetal samples from four pregnant ewes. The mean (± SD) fu of PK samples were 19.6 ± 3.9 % for pregnant ewe, also significantly lower than the fu in fetus, 36.9 ± 4.8 % (**Figure 19**).

Table 12 Nonspecific binding with the Centrifree® device (n=3)

Nominal Conc. (pg/ml)	Ultrafiltrate Conc. (pg/ml)	Recovery (%)	NSB (%)	Overall (%)
100	82.1 ± 4.3	82.1	17.9	17.8 ± 2.1
500	409.4 ± 5.5	81.9	18.1	
2500	2064.1 ± 76.9	82.6	17.4	

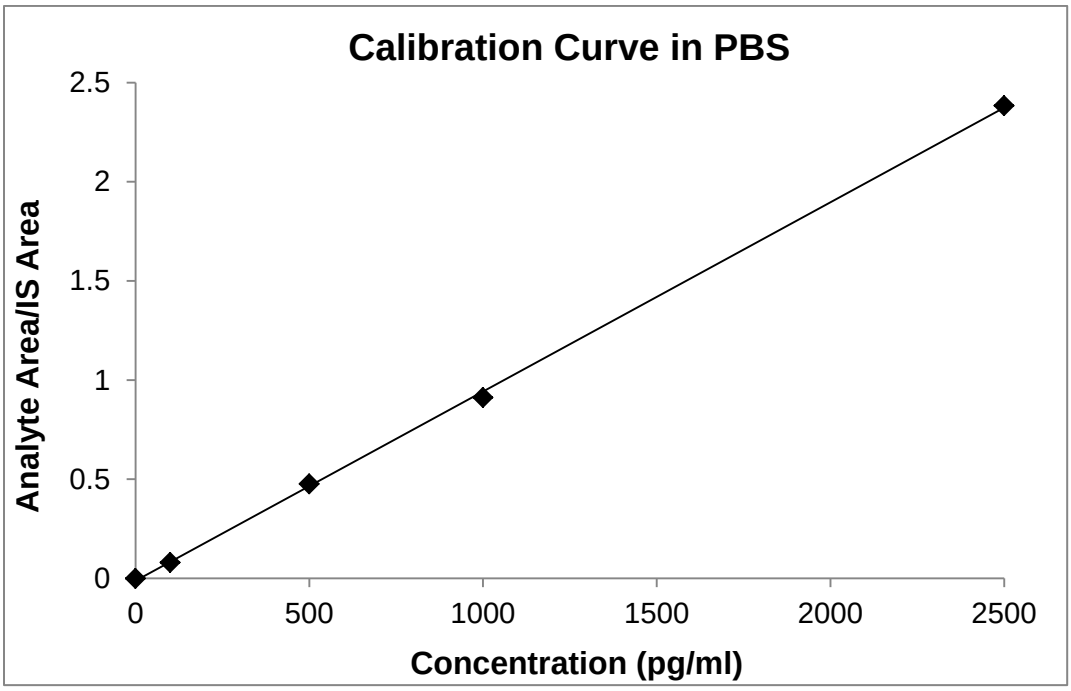

Figure 16 Calibration curve of DEX in PBS (R^2 = 0.9997) for nonspecific binding

Table 13 Plasma protein binding assay of fraction unbound DEX

C_p (pg/ml)	*Pregnant Ewe*			*Fetus*		
	Mean	**SD**	**N**	**Mean**	**SD**	**N**
50	27.2	3.3	6	38.3*	3.5	3
100	24.2	5.0	7	39.6*	3.4	3
200	--	--	--	39.1	2.7	3
250	23.5	3.4	3	--	--	--
500	28.8	6.4	4	--	--	--
1000	27.4	4.3	6	--	--	--
2500	23.9	4.2	6	--	--	--
Overall	25.1	4.8	32	38.9*	3.2	9

Note:

* indicates values are significantly different between pregnant ewes and fetuses by Student's t-test at $p<0.05$.

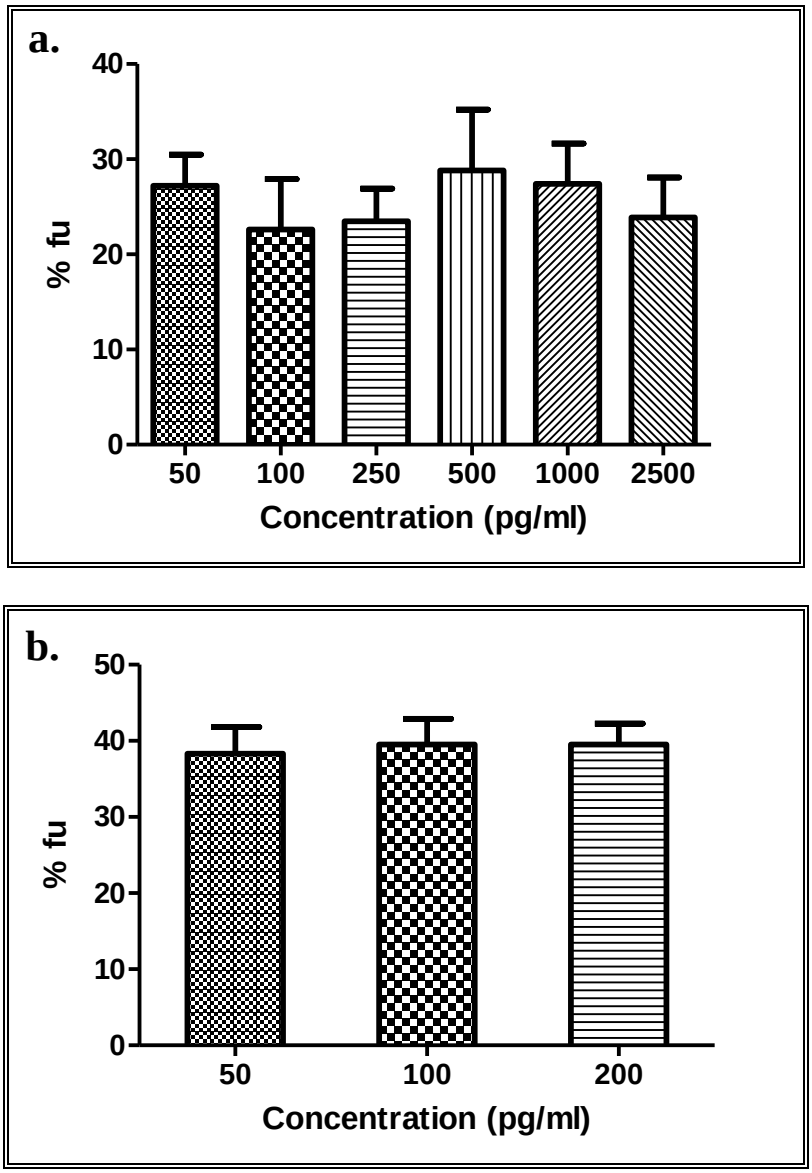

Figure 17 Fractions unbound (%) in DEX-spiked (a) maternal plasma, and (b) fetal plasma over selected ranges

Note:

No significant difference among samples within pregnant ewe and fetus groups, respectively by one-way ANOVA with Tukey's post hoc test at $p<0.05$

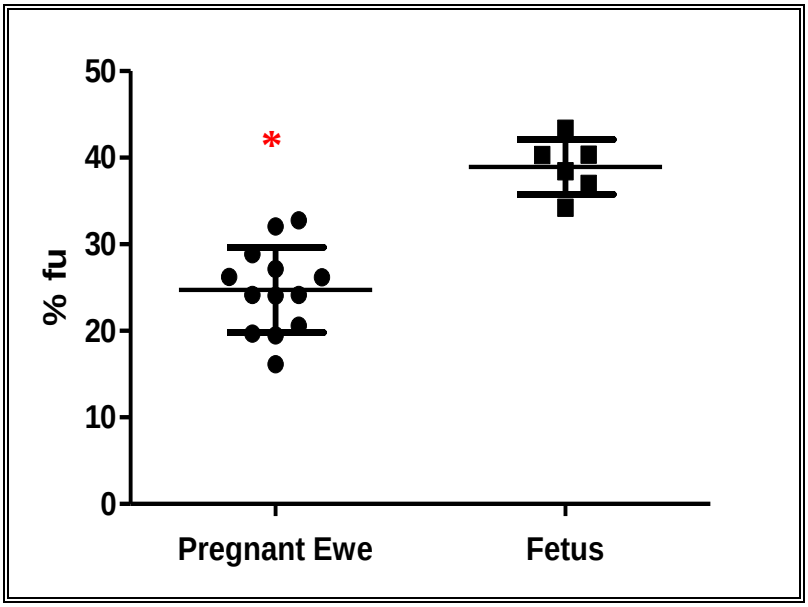

Figure 18 Fractions unbound (%) DEX at concentrations of 50 and 100 pg/ml in pregnant ewe and fetus. * Two-tailed t-test at $p<0.05$.

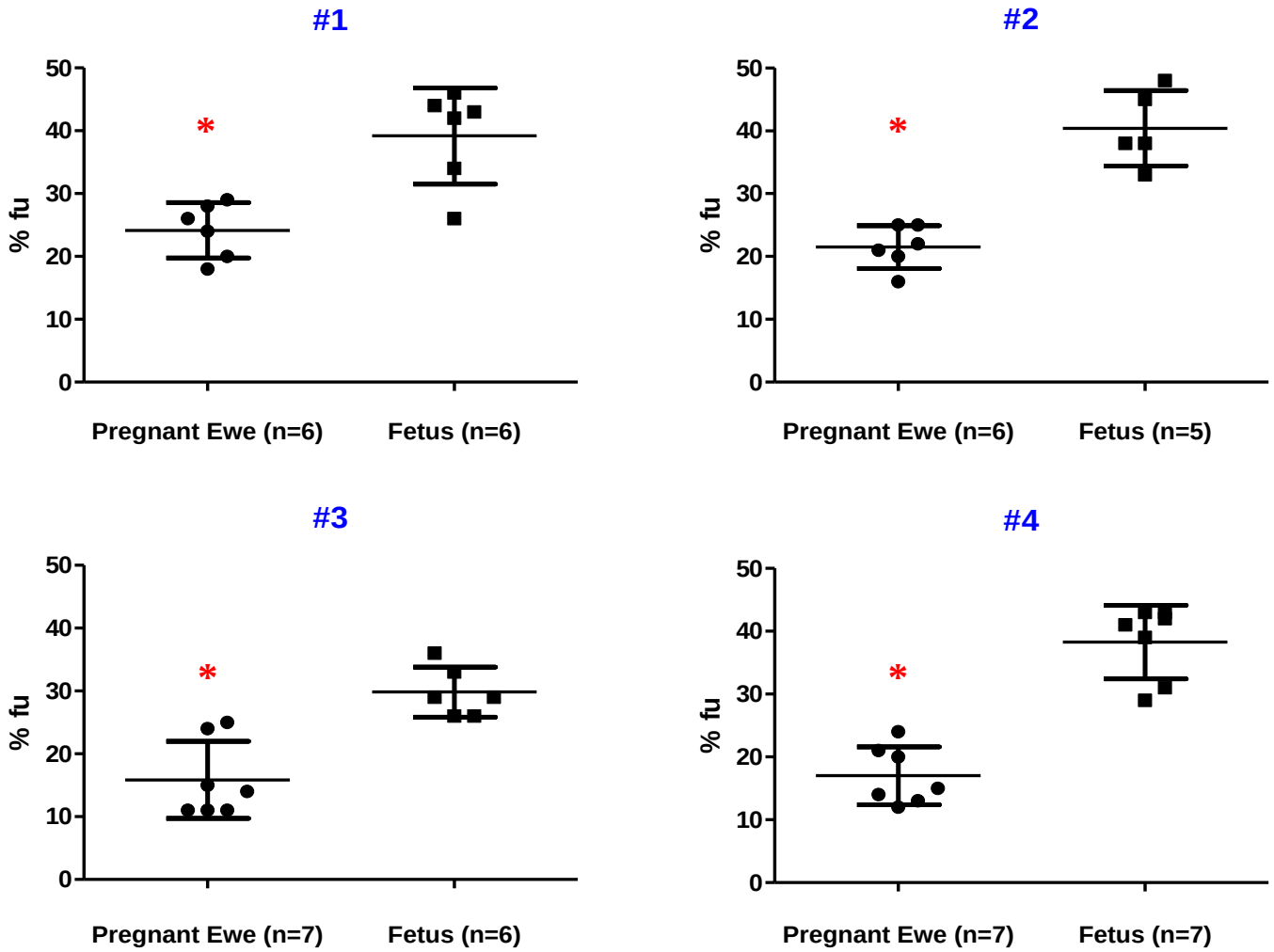

Figure 19 Fractions unbound (%) DEX in PK samples. N indicated the number of samples for each pregnant ewe and fetus. Significant differences were evaluated by Student's t-test at $p<0.01$.

4.5. UGT metabolism of DEX in pregnant ewe and fetus

4.5.1. Negligible N-glucuronidation of DEX in the pregnant ewe model

The Waters ACQUITY UPLC (Ultra performance liquid chromatography) system was used to analyze DEX and its corresponding glucuronide conjugate. Representative chromatograms and UV spectra were shown in **Figure 20**. The DEX and IS peaks were observed at the retention times of 1.86 and 2.25 min, respectively, at the wavelength of 214 nm (**Figure 21**). The calibration curve of DEX in potassium phosphate buffer (KPI) with linear range of 1.06 - 42.2 μM is shown in **Figure 22**. Correlation coefficient (R^2) of the calibration curve was greater than 0.99 indicating an excellent linear response over the selected concentration range. Very few or no DEX glucuronidation metabolites were identified after the incubation of DEX (10 μM in final mixture) with hepatic microsomes prepared from pregnant ewe and fetus, as well as that from placenta, respectively. The negligible DEX glucuronide concentrations were also confirmed by the same UPLC system coupled with a mass spectrometer. DEX glucuronide structure was not detectable (**Figures 23-25**). The DEX and IS peaks were observed at the retention times of 2.62 and 3.12 min, respectively.

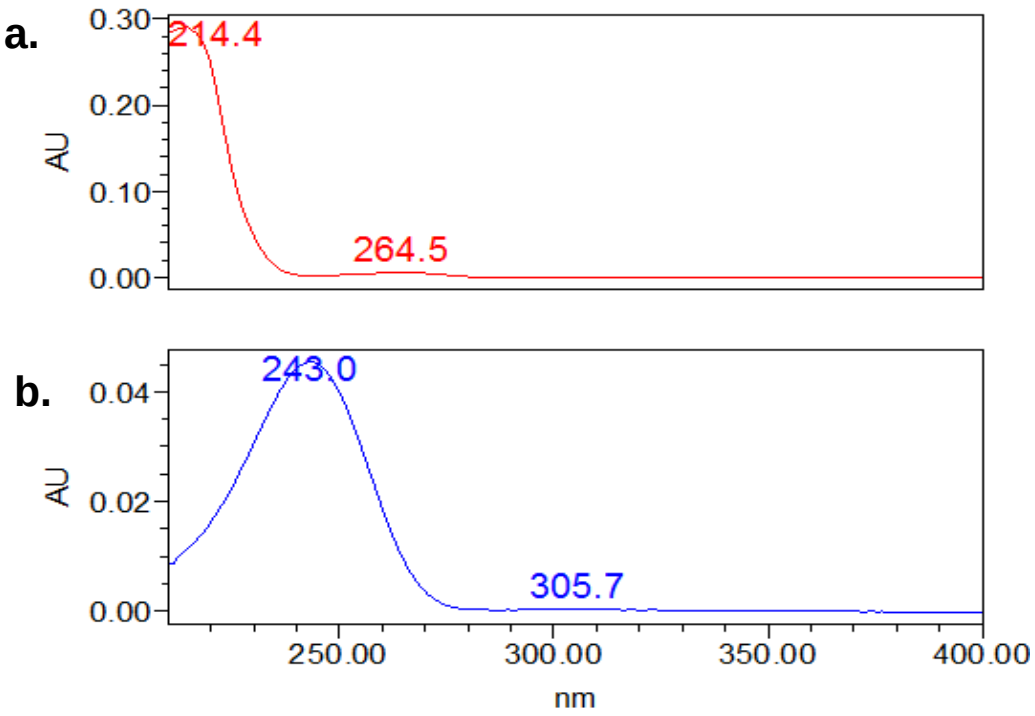

Figure 20 UV spectra of (a) DEX and (b) IS

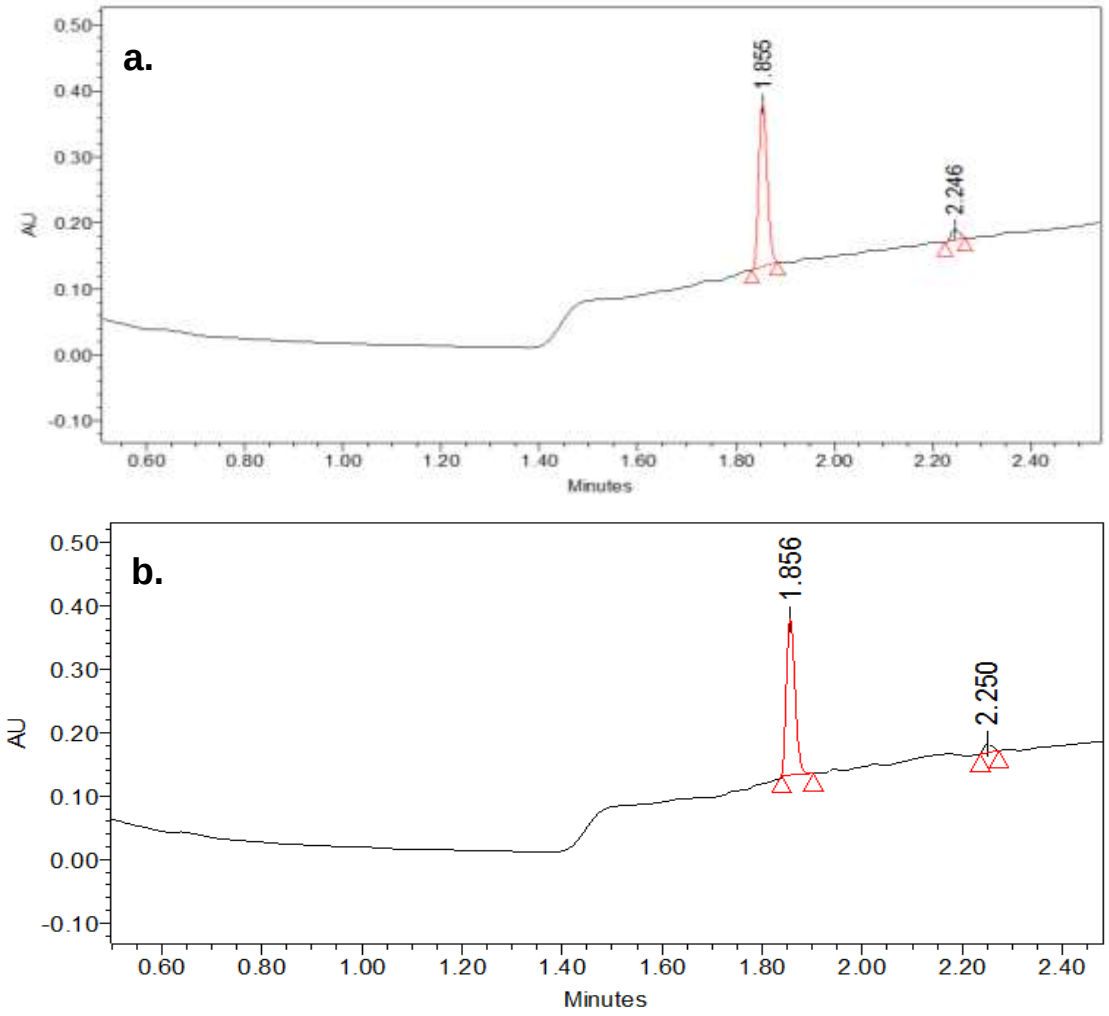

Figure 21 Chromatograms of DEX and IS (a) with and (b) without pregnant ewe liver microsomes after 12 h-incubation

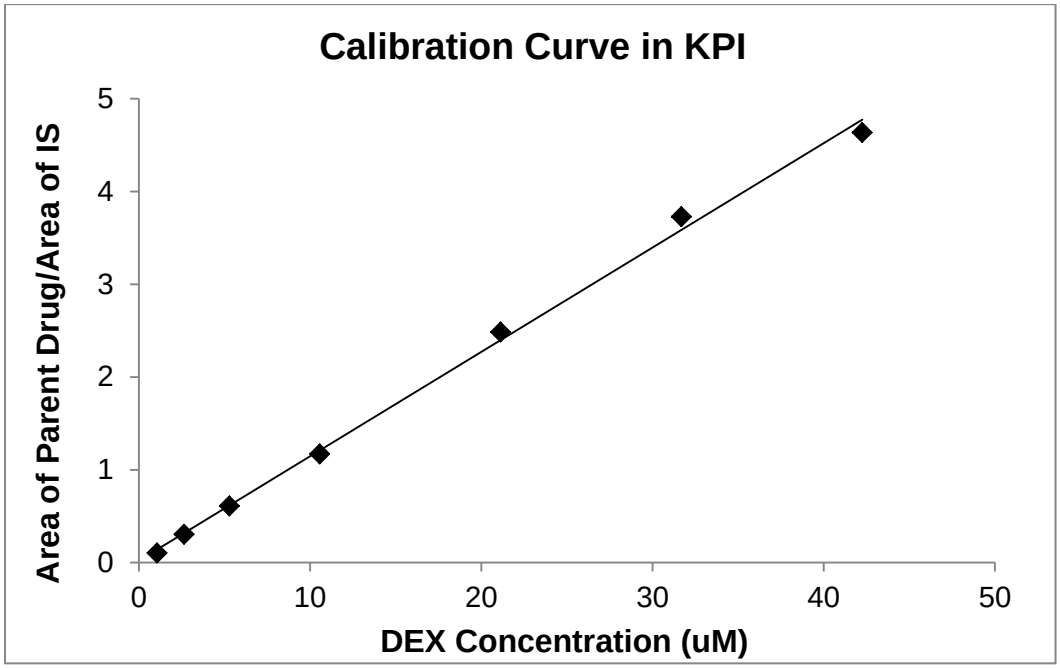

Figure 22 Calibration curve of DEX in KPI buffer (R^2 = 0.9974)

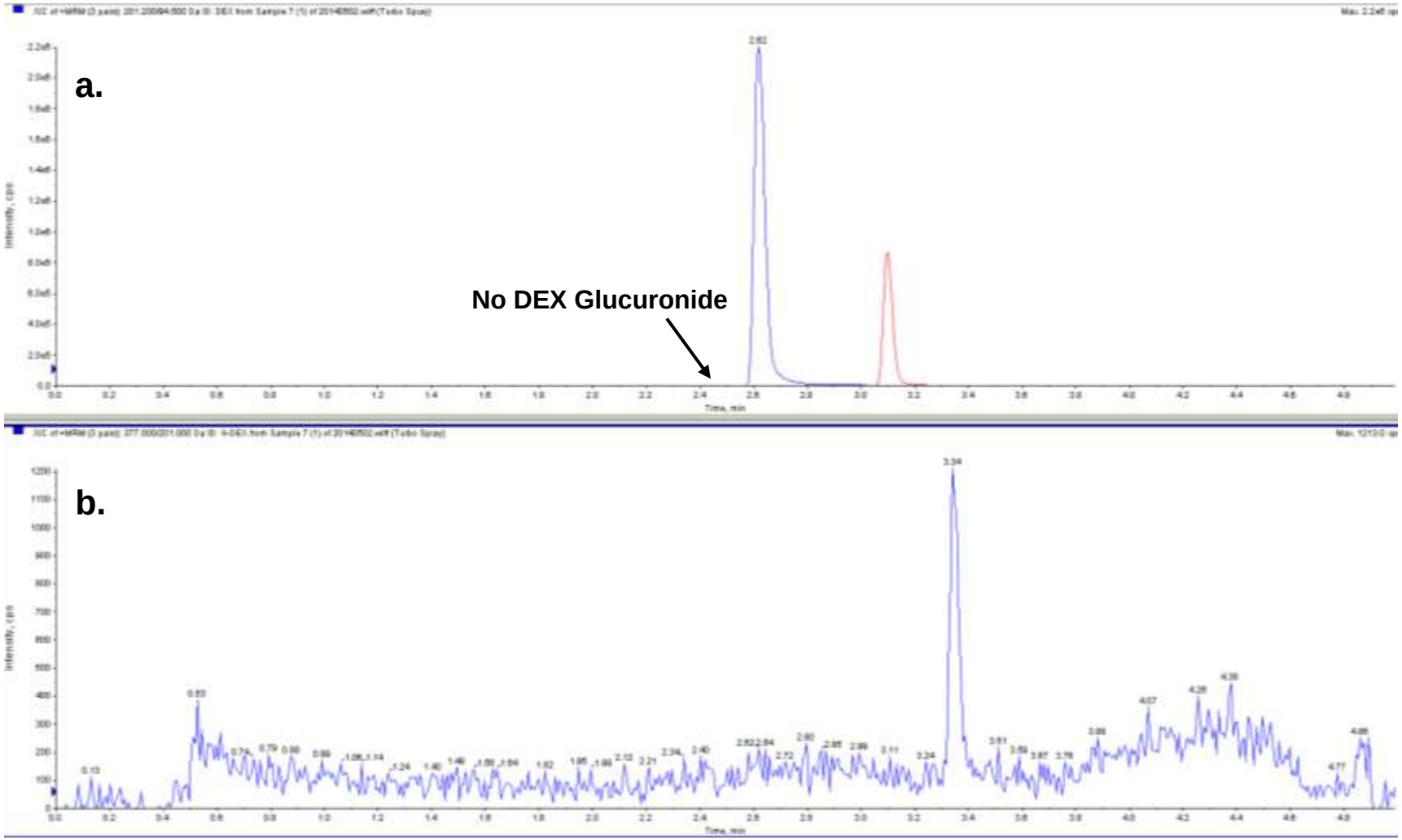

Figure 23 LC-MS/MS chromatograms of (a) DEX and IS, (b) extracted ion chromatograms (XIC) of DEX glucuronide (m/z: 377→201) in liver microsomes prepared from pregnant ewe.

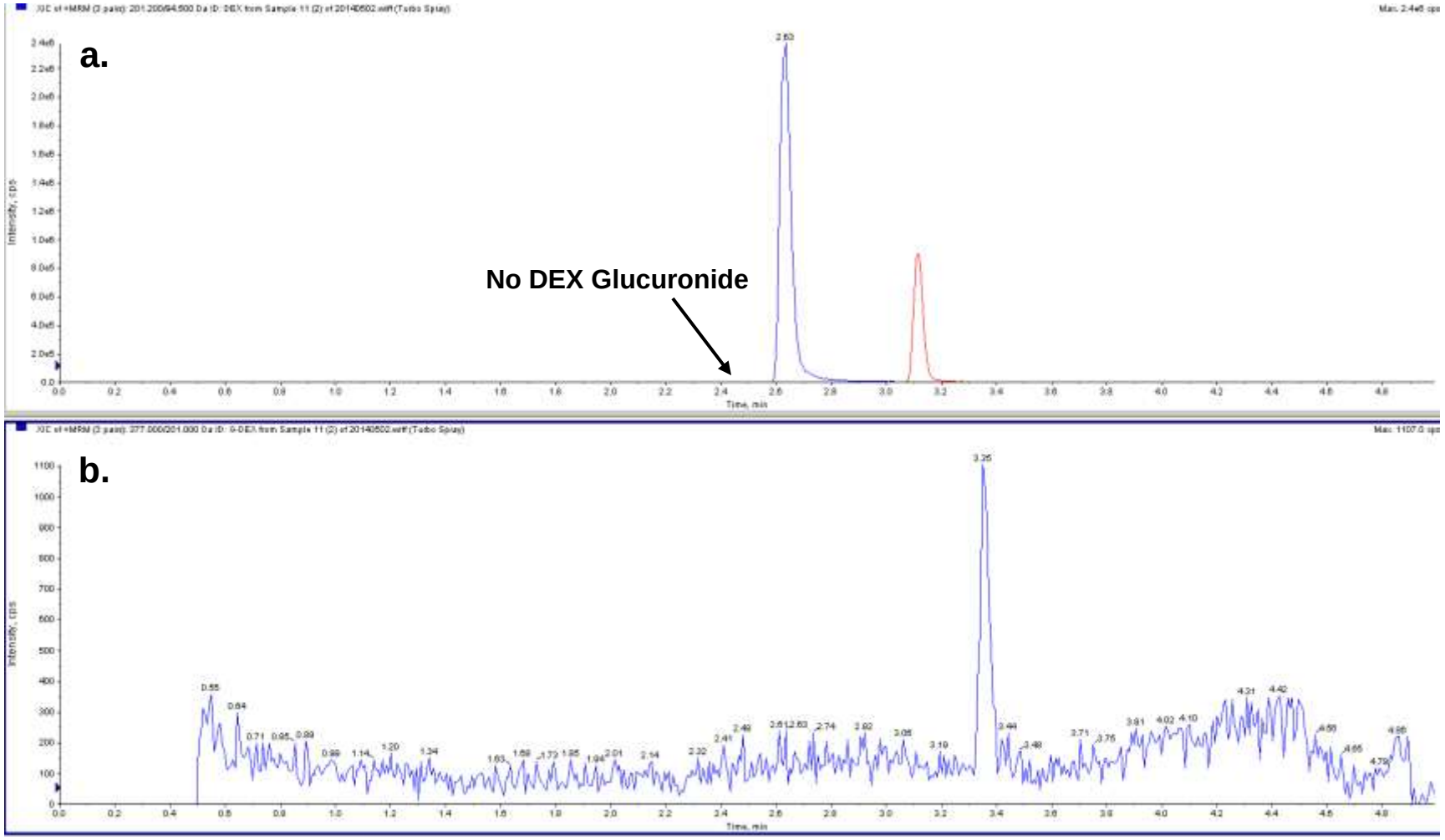

Figure 24 LC-MS/MS chromatograms of (a) DEX and IS, (b) XIC of DEX glucuronide (m/z: 377→201) in liver microsomes prepared from fetus.

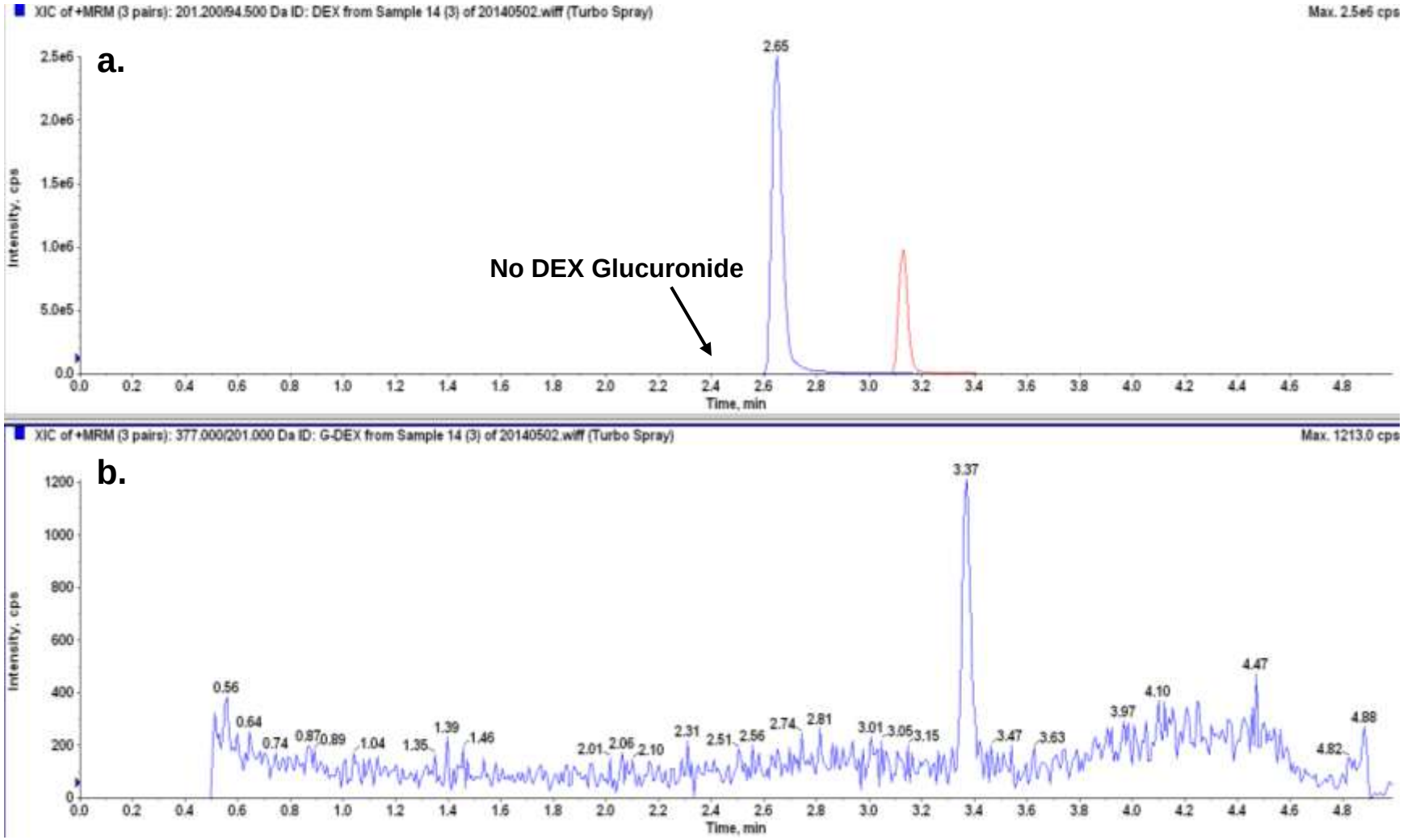

Figure 25 LC-MS/MS chromatograms of (a) DEX and IS, (b) XIC of DEX glucuronide (m/z: 377→201) in placental microsomes.

4.5.2. DEX glucuronidation by human liver microsomes

In contrast, DEX glucuronide was observed at 1 h with pHLM (pooled human liver microsomes) of the same protein concentration. **Figure 26** demonstrated the representative chromatogram of DEX and DEX glucuronide after 24 hr incubation with pHLM. The DEX, DEX-Glucuronide and IS peaks were observed at the retention times of 2.62, 2.42 and 3.12 min, respectively. This indicated that N-glucuronidation is a negligible pathway for DEX in pregnant ewe which differs from that in humans.

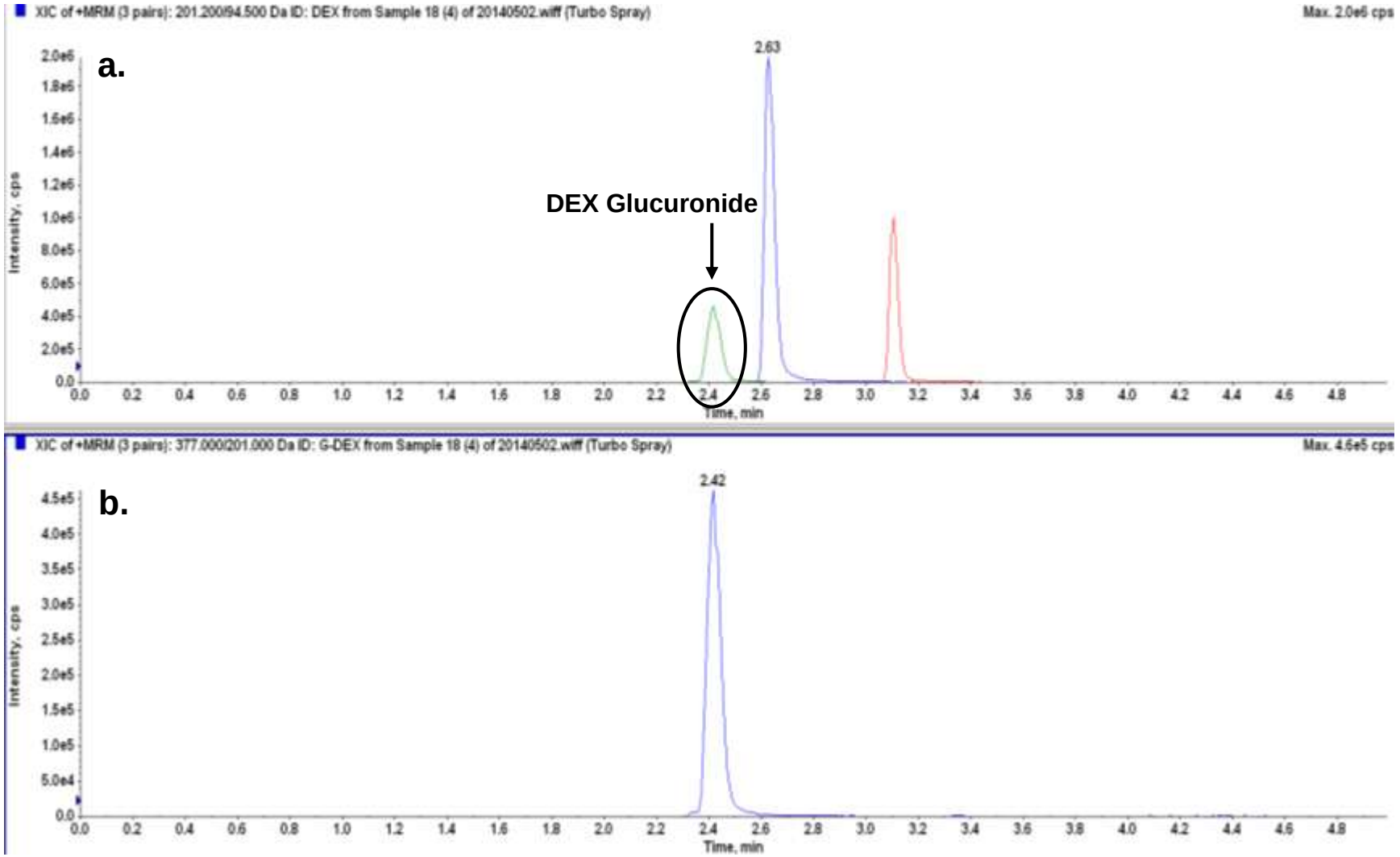

Figure 26 LC-MS/MS chromatograms of (a) DEX and IS, (b) XIC of DEX glucuronide (m/z: 377→201) in pHLM

4.5.3. Differential UGT activities in hepatic microsomes between pregnant ewe and fetus

Differential UGT activities in liver microsomes between pregnant ewe and fetus were characterized by using genistein as a reference substrate. The optimal reaction time for genistein with maternal and fetal liver micromsomes was determined to be 30 and 40 min, respectively, based on the results of a time-course study. Final genistein concentrations at 1.25, 2.5, 5, 10, 15, 20, 35 and 50 μM were investigated for evaluation of kinetic profiles.

4.5.3.1 UPLC analysis

The Waters ACQUITY UPLC (Ultra performance liquid chromatography) system was used to analyze genistein and its corresponding glucuronide. Representative chromatograms and UV spectra are shown in **Figure 27**. The genistein, genistein glucuronide and IS peaks were observed at the retention times of 2.04, 1.74 and 2.25 min, respectively, at the wavelength of 260 nm (**Figure 28** in pregnant ewe and **Figure 29** in fetus). A calibration curve for genistein in KPI buffer with a linear range of 0.5 - 50 μM is shown in **Figure 30**. The correlation coefficient (R^2) of the calibration curves was greater than 0.99 indicating an excellent linear response over the selected concentration range. Genistein and its glucuronide chemical structures were also confirmed by an LC-MS/MS assay (**Figures 31 & 32**).

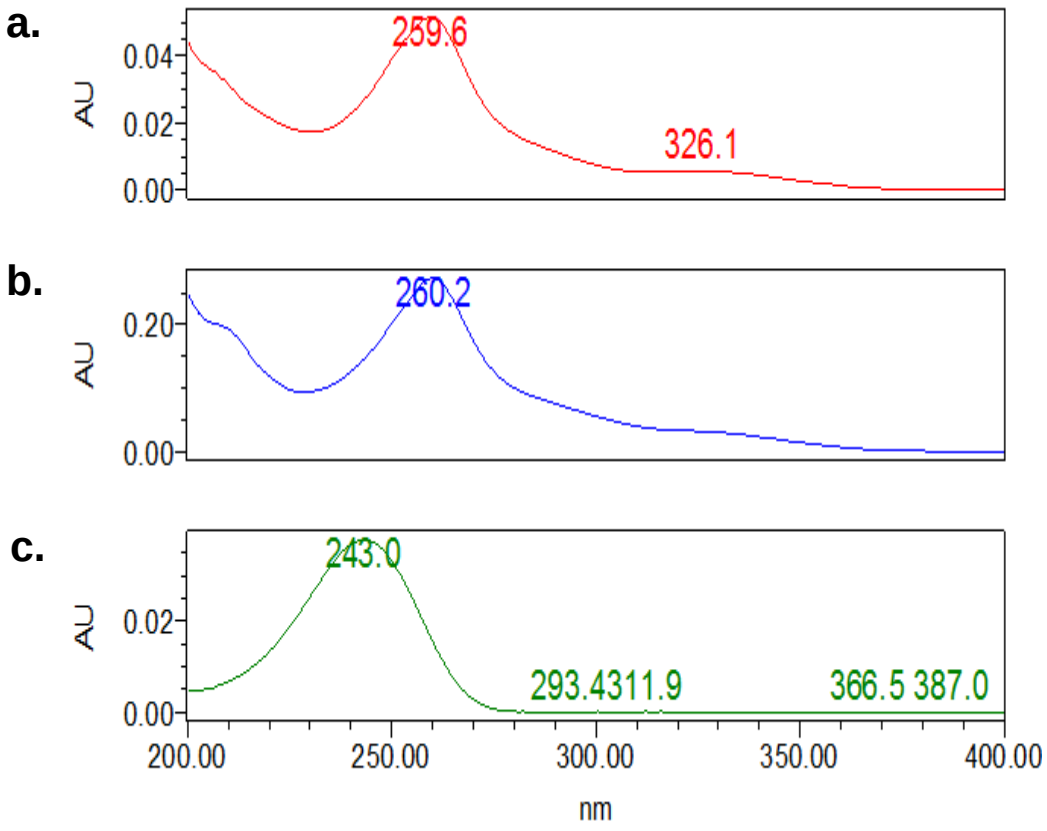

Figure 27 UV spectra of (a) genistein, (b) genistein glucuronides and (c) IS

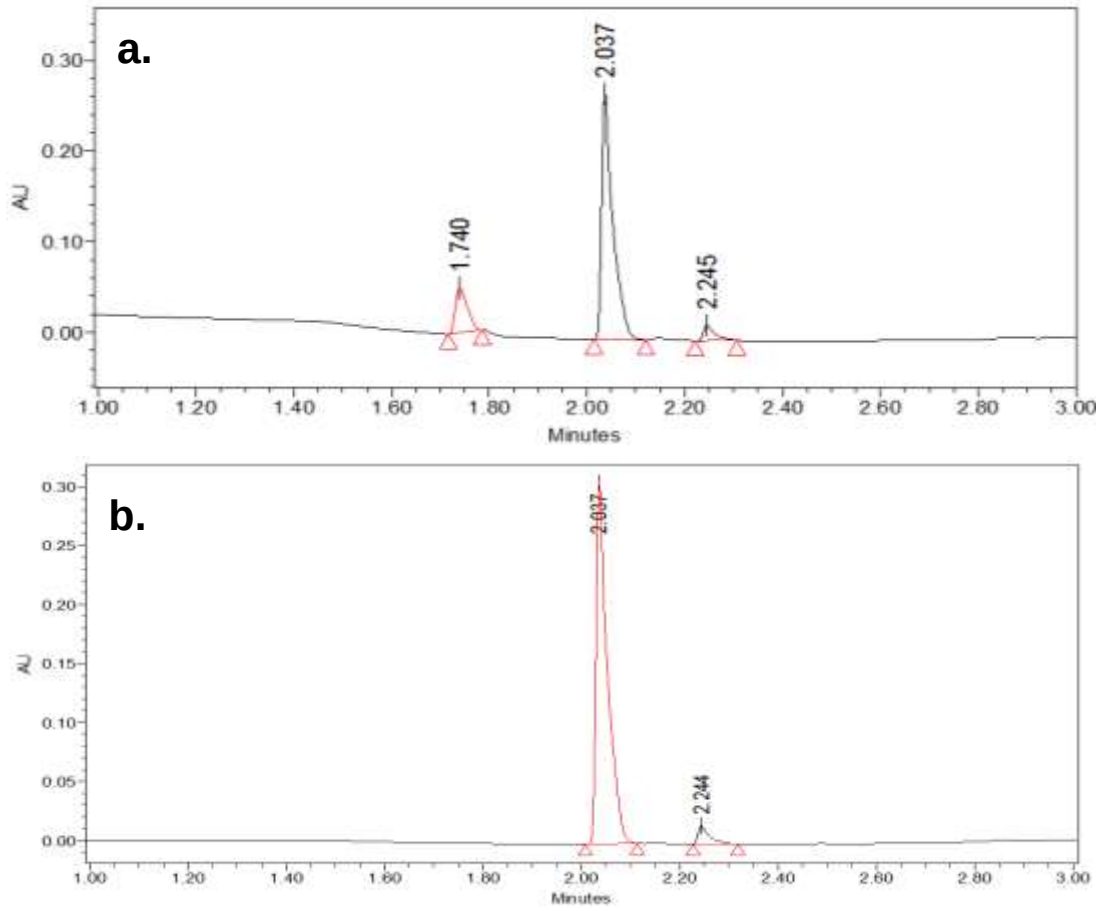

Figure 28 Chromatograms of genistein, genistein glucuronide and IS (a) with and (b) without maternal liver microsomes after 30 min-incubation.

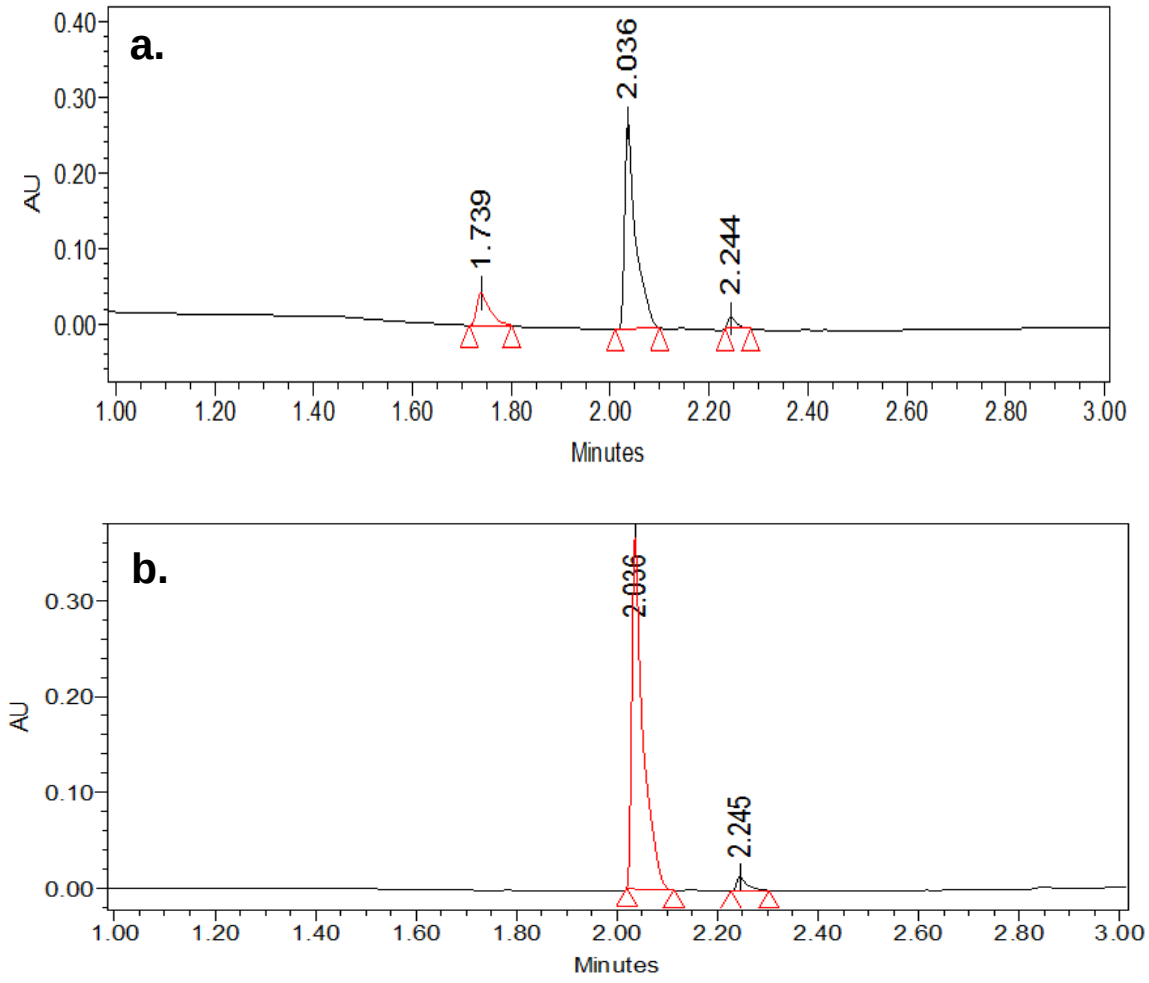

Figure 29 Chromatograms of genistein, genistein glucuronide and IS (a) with and (b) without fetal liver microsomes after 40 min-incubation.

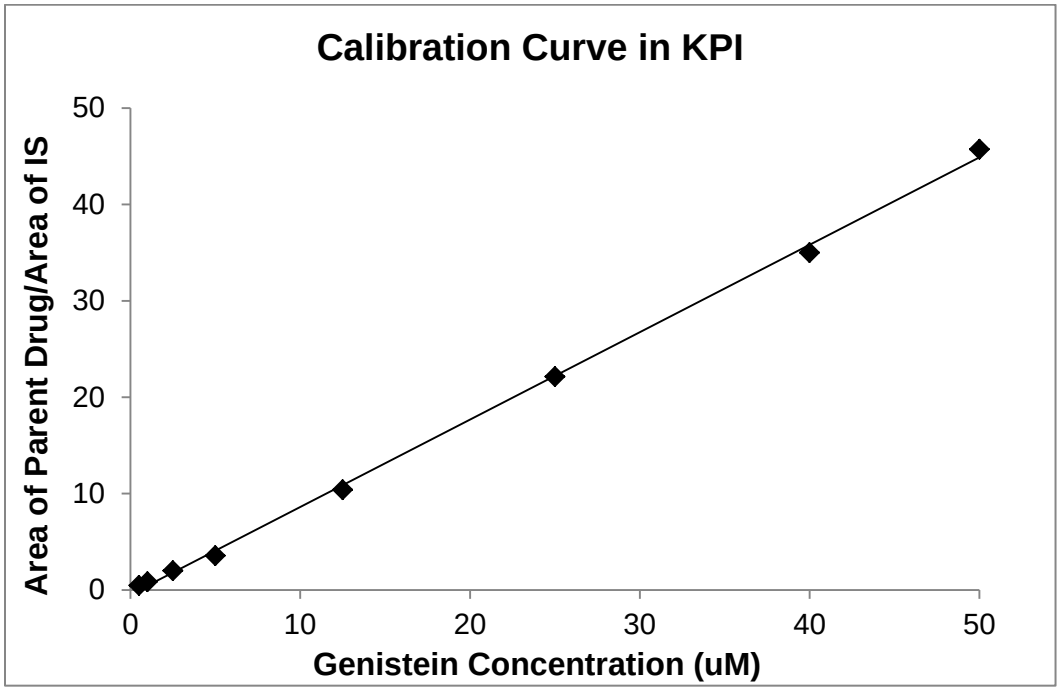

Figure 30 Calibration curve of genistein in KPI buffer (R^2 = 0.9989)

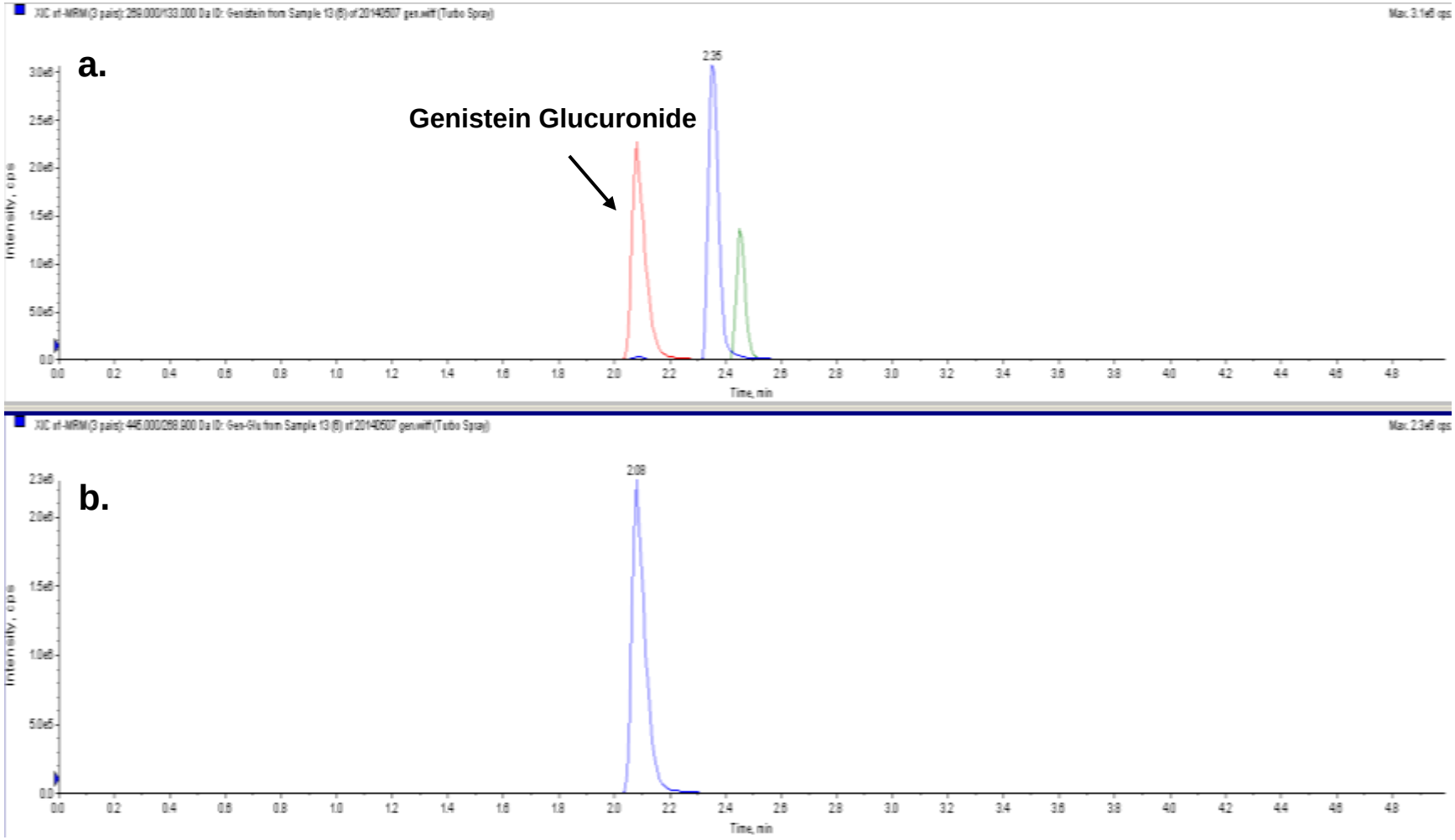

Figure 31 **LC-MS/MS chromatograms of (a) genistein, genistein glucuronide and IS, (b) XIC of genistein glucuronide (m/z: 445.0→268.9) in liver microsomes prepared from pregnant ewe.**

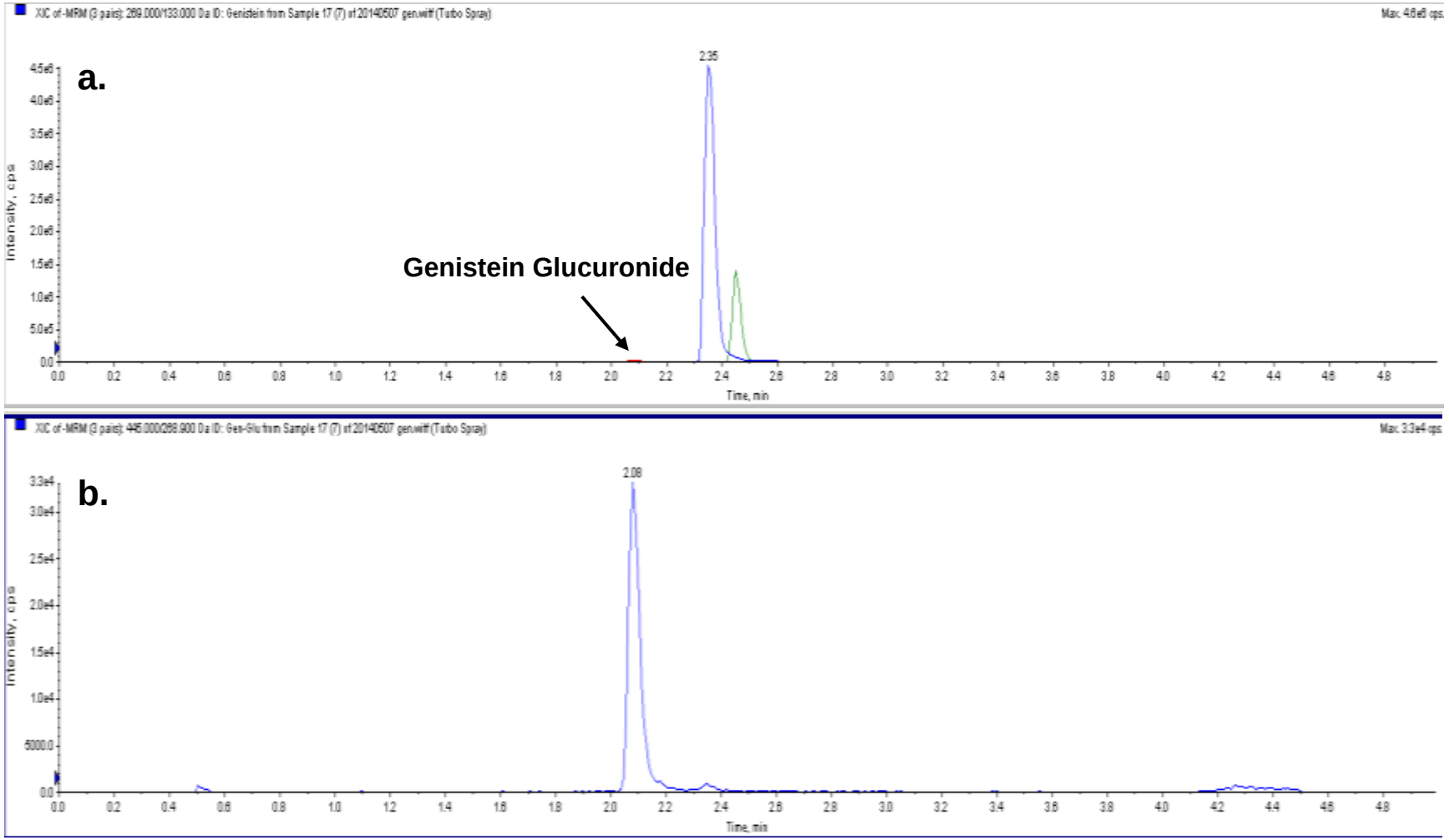

Figure 32 **LC-MS/MS chromatograms of (a) genistein, genistein glucuronide and IS, (b) XIC of genistein glucuronide (m/z: 445.0→268.9) in liver microsomes prepared from fetus.**

4.5.3.2 Kinetic study

Kinetic parameters (V_{max}, K_m) were estimated by fitting the initial rate data to Michaelis-Menten and atypical kinetic rate equations by nonlinear least-squares regression. The goodness-of-fit was evaluated on the basis of AIC and R^2 values. **Table 14** summarizes the kinetic analysis after using the Michaelis-Menten, substrate inhibition, sigmoidal Hill and biphasic two sites equations. **Figure 33** and **34** show the kinetic plots of genistein after metabolism incubation with different concentrations of genistein in maternal and fetal liver microsomes, respectively. These results indicated that genistein follows the biphasic kinetic metabolic pattern in both pregnant ewe (**Figure 33**) and fetus (**Figure 34**), with the respective apparent $K_{m,1}$ of 1.45 and 1.79 µM, and $V_{max,1}$ of 28.03 and 1.49 nmol/min/mg of protein, respectively. Eadie-Hofstee plots were used to confirm the biphasic kinetics. In human liver microsomes, genistein glucuronidation also follows the biphasic kinetics with $K_{m,1}$ of 0.026 µM and $V_{max,1}$ of 2.5 nmol/min/mg of protein **(Figure 35)**.

Table 14 Kinetic analysis of genistein glucuronidation with different models (n=3)

Kinetic Model	AIC		R^2	
	Pregnant Ewe	***Fetus***	***Pregnant Ewe***	***Fetus***
Michaelis-Menten	-32.04	-97.1	0.94	0.91
Substrate Inhibition	-34.95	-94.2	0.94	0.91
Hill Equation	-18.23	-118.1	0.97	0.97
Biphasic Two Sites	-10.56	-130.9	0.98	0.98

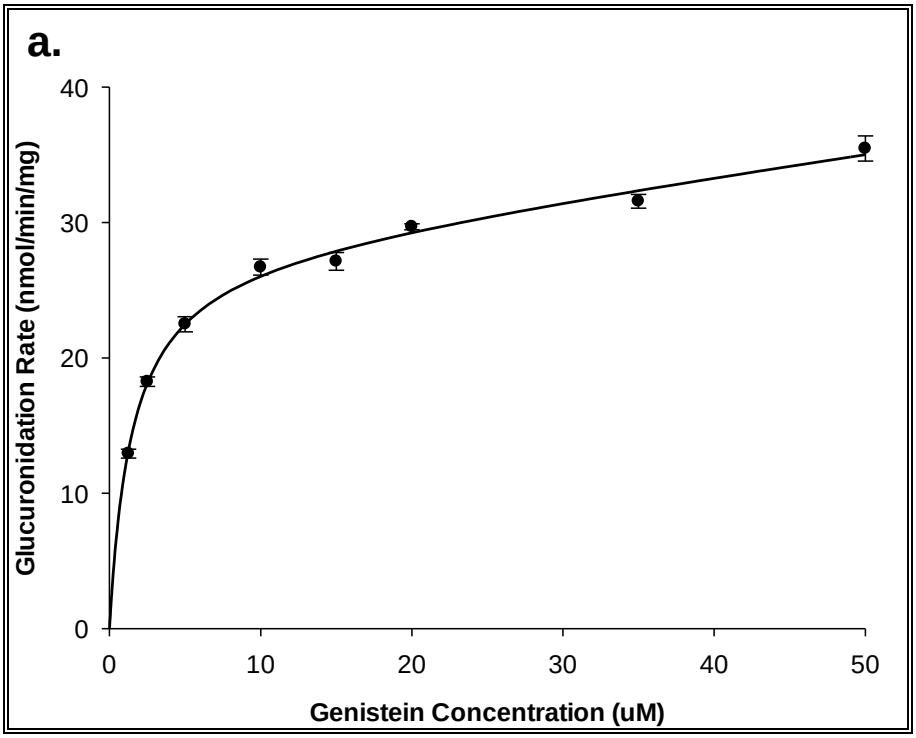

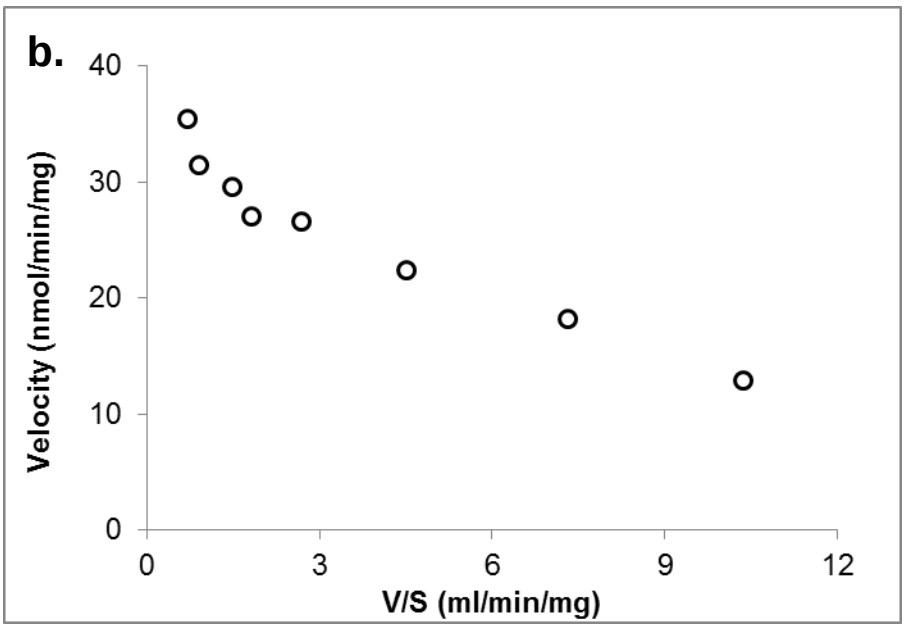

Figure 33 (a) Kinetics of genistein glucuronidation by maternal liver microsomes and (b) corresponding Eadie-Hofstee plot (n=3)

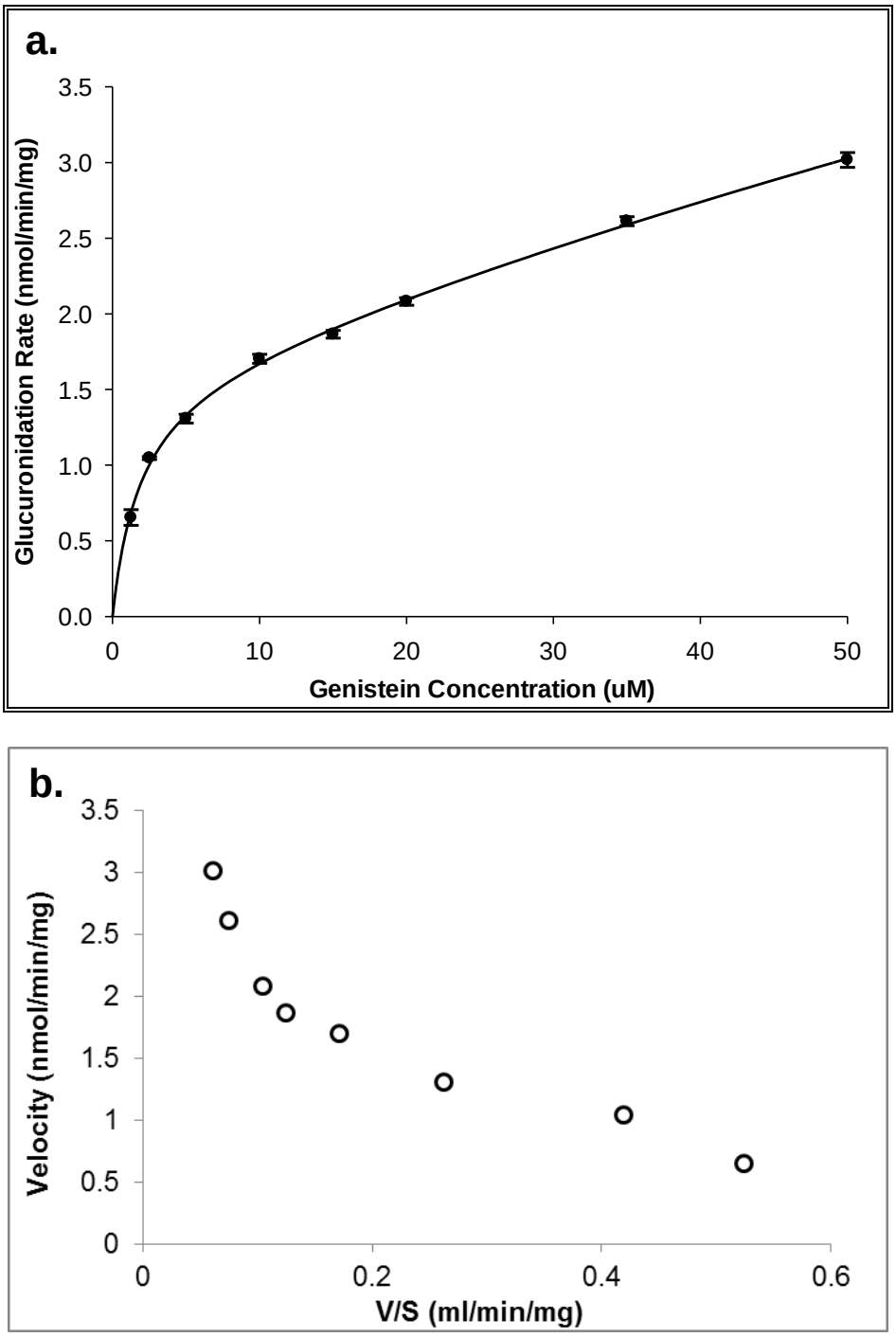

Figure 34 (a) Kinetics of genistein glucuronidation by fetal liver microsomes and (b) corresponding Eadie-Hofstee plot (n=3)

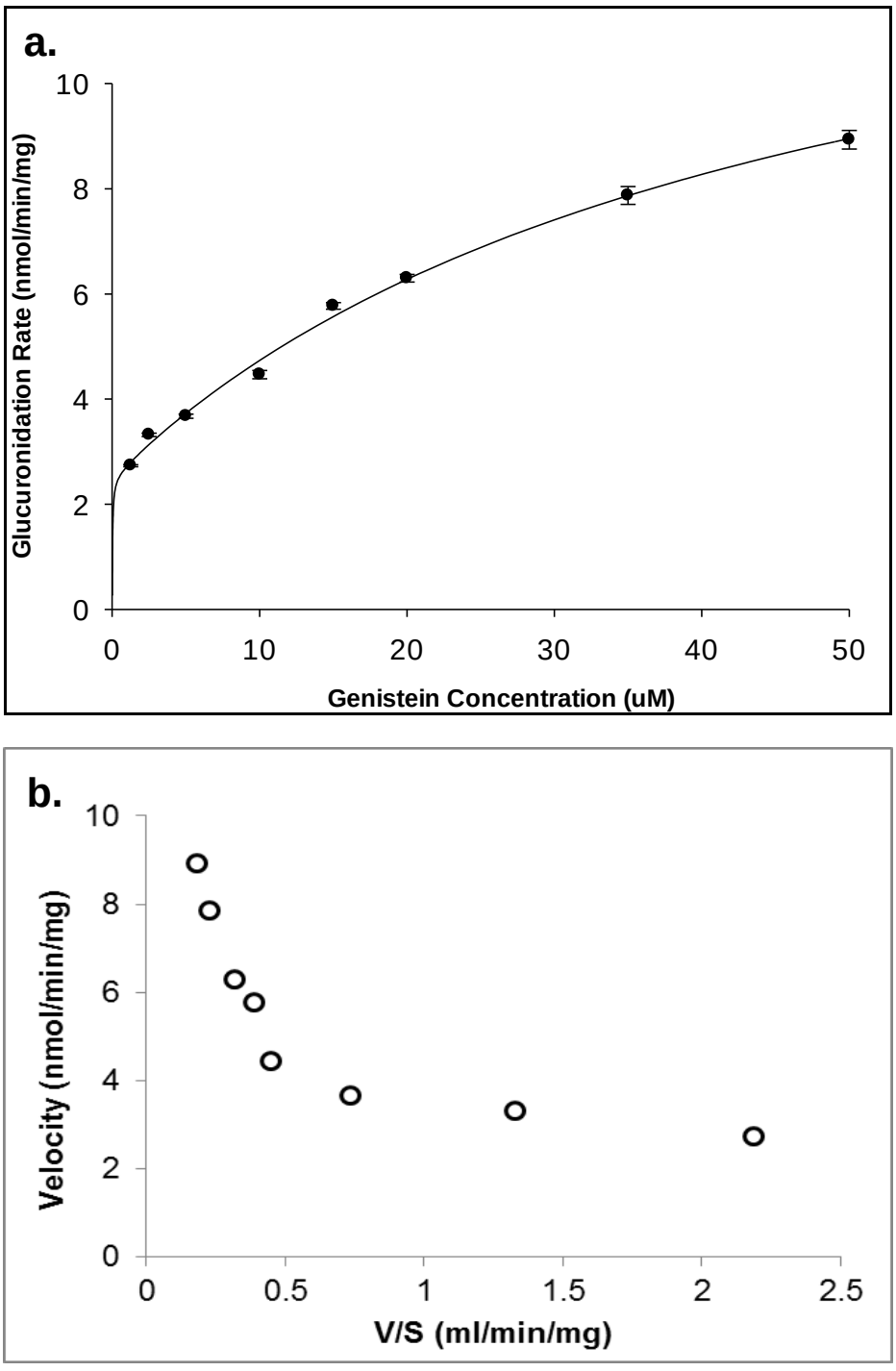

Figure 35 (a) Kinetics of genistein glucuronidation by pooled human liver microsomes and (b) corresponding Eadie-Hofstee plot (n=3)

4.6. PK and PD models of DEX in pregnant ewe model

4.6.1. PK with nonlinear mixed effect (NLME)

A total of 71 concentrations from pregnant ewe artery and 84 fetal arterial concentrations were used for the pharmacokinetic analysis of total DEX. A total of 24 maternal samples and 22 fetal samples were available to determine free DEX concentrations. Only two fetal free drug concentrations were lower than the LLOQ, so they were set to half of the LLOQ.

4.6.1.1 PK modeling with maternal data of total DEX concentrations

Of all the tested models, a two-compartment open model with first-order elimination best described the data (**Figure 36**). Compartments 1 and 2 described central and peripheral compartments. Mean (relative standard errors) parameter estimates of central volume of distribution (V), maternal peripheral volume of distribution (V_2), elimination clearance (CL), intercompartmental clearance (Q) between V and V_2 were 1.57 (27.8%) L/kg, 1.08 (54.9%) L/kg, 30.1 (11.7%) mL/(kg*min) and 12.0 (32.1%) mL/(kg*min). The available data were insufficient to estimate intersubject variability for V_2 and Q, and exclusion of these random effects had no influence on the $-2 \times \log$ likelihood (-2LL). Residual variability was best described by a log-additive model and determined to be 0.372. Mean (relative standard errors) ω_V and ω_{CL} were 0.47 (59.9%) and 0.05 (79.3%), respectively.

No apparent biases were observed by comparing population and individual predicted concentrations to observed concentrations (**Figure 37**). Diagnostic plots of population weighted residuals versus time and versus predicted concentrations did not show signs of significant bias (**Figure 38**).

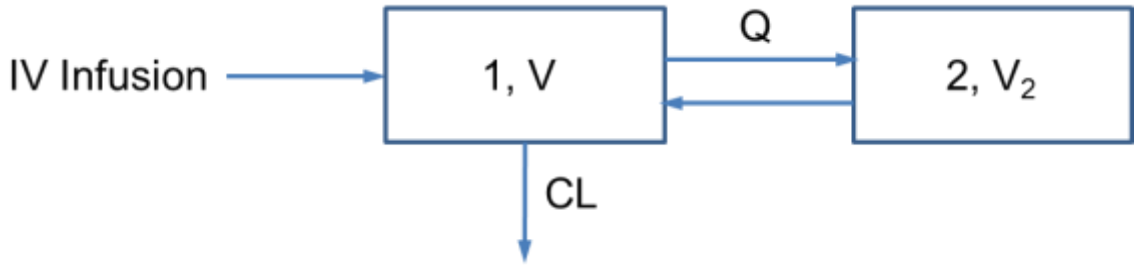

Figure 36 PK model for total DEX concentration prediction in pregnant ewes.

V: volume of the central maternal compartment
V_2 volume of the peripheral maternal compartment
CL: elimination clearance from the central compartment
Q: maternal intercompartmental clearance

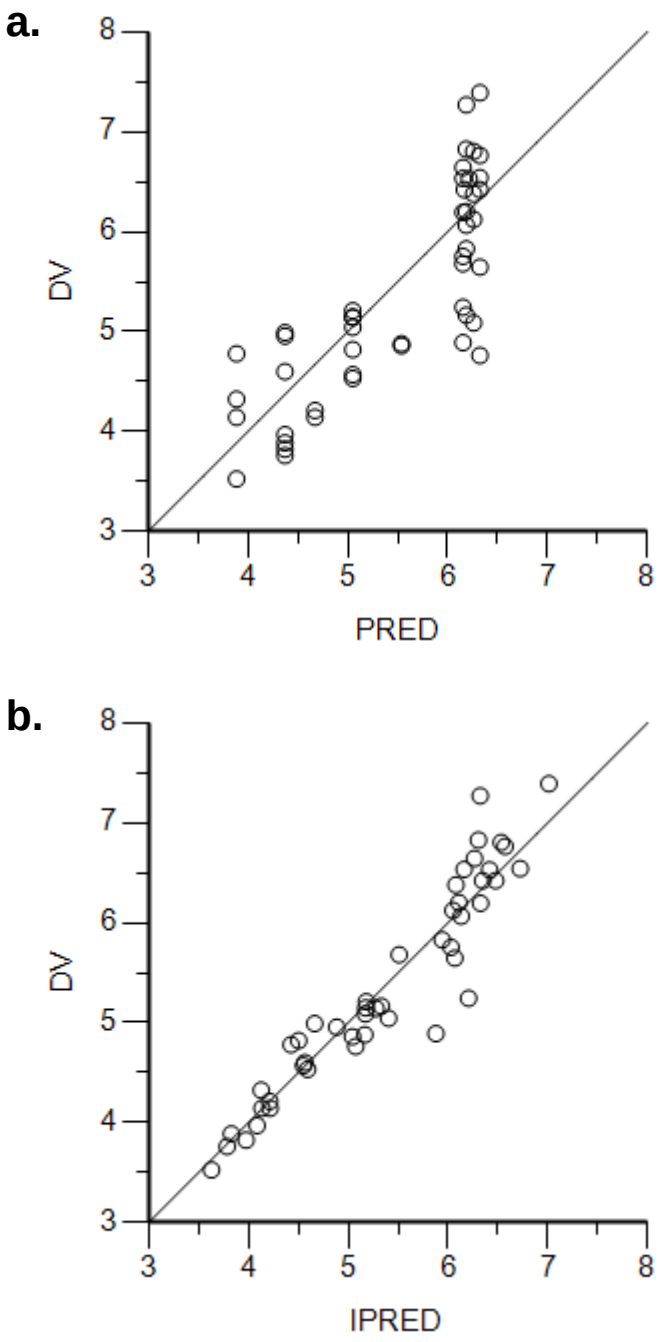

Figure 37 Observed (DV) *vs.* predicted concentrations from the (a) population (PRED) and (b) individual (IPRED) fits

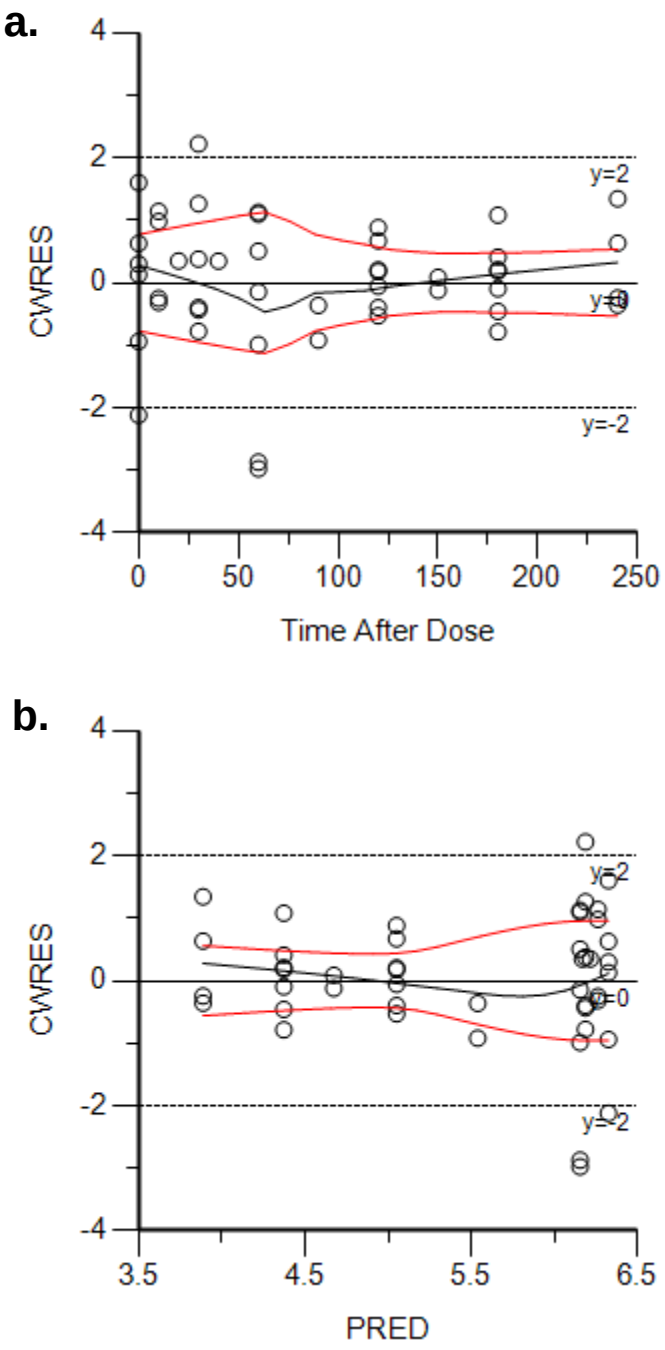

Figure 38 Population weighted residuals (CWRES) *vs*. (a) time and (b) predicted concentrations (PRED)

4.6.1.2 Protein binding model

The relationship between the free and total concentration was evaluated because of potential changes in protein binding. Nonlinear protein-binding models could not be identified based on the available data and were not visually observable. The relationship between free and total DEX concentrations was best described using a constant binding model as follows:

$$C_{total} = \frac{C_{free}}{f_u}$$

Where C_{total} represents the total drug concentration and fu represents the (estimated) fraction of free drug.

4.6.1.3 PK modeling with addition of fetal data

For fetal concentrations, several models were tested with fixed maternal parameters and then all the parameters of the integrated model were simultaneously estimated (**Figure 39**). An effect compartment of negligible volume linked to the maternal circulation by first-order processes (**Figure 39d**) adequately characterized the fetal concentrations. The differential equations used are presented in the **Appendix.**

Estimated parameters of the final model: central volume of distribution (V), maternal peripheral volume of distribution (V_2), maternal elimination clearance (CL), intercompartmental clearance (Q) between V and V_2, maternal elimination clearance (CL), maternal-to-fetal rate constant (K_{mf}), fetal-to-maternal rate constant (K_{fm}), maternal fraction of free drug (fu_1) and fetal fraction of free drug (fu_2) are summarized in **Table**

15.. The residual variability was best described by a log-additive error model. All fixed effect parameters were estimated with good precision (CV < 34%).

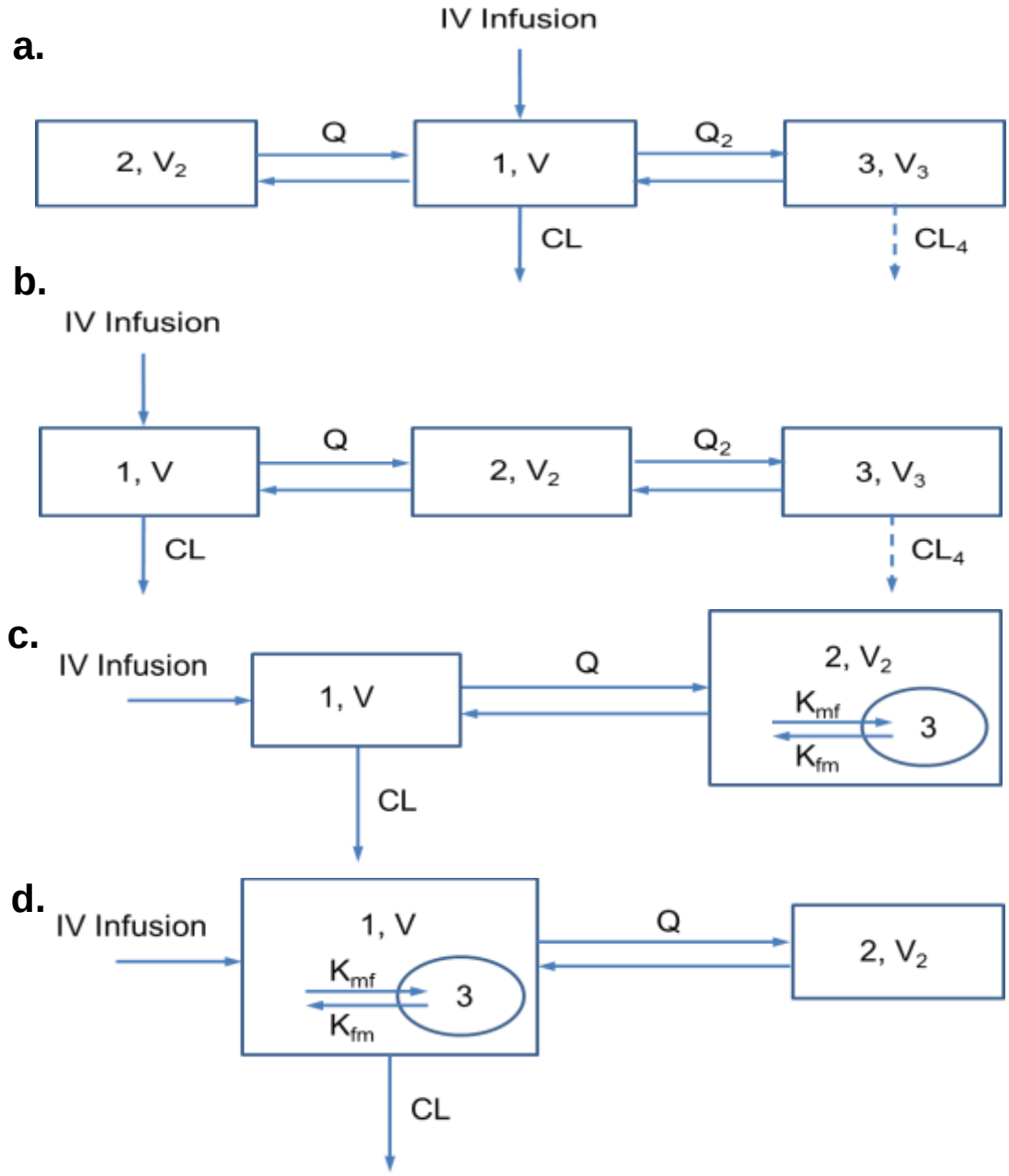

Figure 39 Schematic representations of pharmacokinetic models for the distribution of DEX to maternal central compartment, peripheral compartment and fetus after intravenous infusion administration to pregnant ewes.

1, 2 and 3 denote maternal central compartment, peripheral compartment and fetal compartment, respectively. V: volume of the maternal central compartment; V_2: volume of the maternal peripheral compartment; CL: elimination clearance from the central compartment; CL_4: elimination clearance from the fetal compartment; Q and Q_2: intercompartmental clearances; K_{mf}: maternal-to-fetal rate constant; and K_{fm}: fetal-to-maternal rate constant.

Table 15 Parameter estimates from the PK model (of Fig. 39d)

Description	Parameter	Units	Estimate	CV%
Central Volume	V	L/kg	6.66	14.5
Central Volume	CL	L/(kg*min)	0.07	20.8
Periperheral Volume	V_2	L/kg	52.63	22.8
Intercompartmental clearance	Q	L/(kg*min)	0.14	25.0
Mother-to-fetus rate constant	K_{mf}	1/min	0.06	34.0
Fetus-to-mother rate constant	K_{fm}	1/min	0.09	23.0
Free fraction, mother	fu_1		0.197	9.7
Free faction, fetus	fu_2		0.342	15.1
Log-additive, total conc., mother	σ_1		0.34	15.0
Log-additive. total conc., fetus	σ_2		0.57	22.7
Log-additive, free conc., mother	σ_3		0.41	20.1
Log-additive, free conc., fetus	σ_4		0.56	27.6

4.6.1.4 Evaluation and validation

The model performance (of **Fig. 39d**) was evaluated by comparing the logarithm of population predicted concentrations to observed free and total plasma concentrations (**Figures 40-41**) and individual predicted concentration to observed free and total plasma concentrations (**Figures 42-43**). Population weighted residuals versus time (**Figure 44**) and versus predicted concentrations (**Figure 45**) were also plotted. No significant biases were observed in any of the diagnostic plots.

Bootstrap validation was also employed to evaluate the model accuracy. The validation of the final model was performed with 100 runs and was successful for 98 runs. There was no significant difference between the estimates derived from the bootstrap and the predicted values from the Phoenix NLME PK analysis with original data. The standard errors derived from bootstrap were also comparable, except for the residual variability σ_2 and σ_4. The values differ from the standard error estimated by the model because of the small size of the investigated subjects in this study. The mean values and standard errors are represented in **Table 16**.

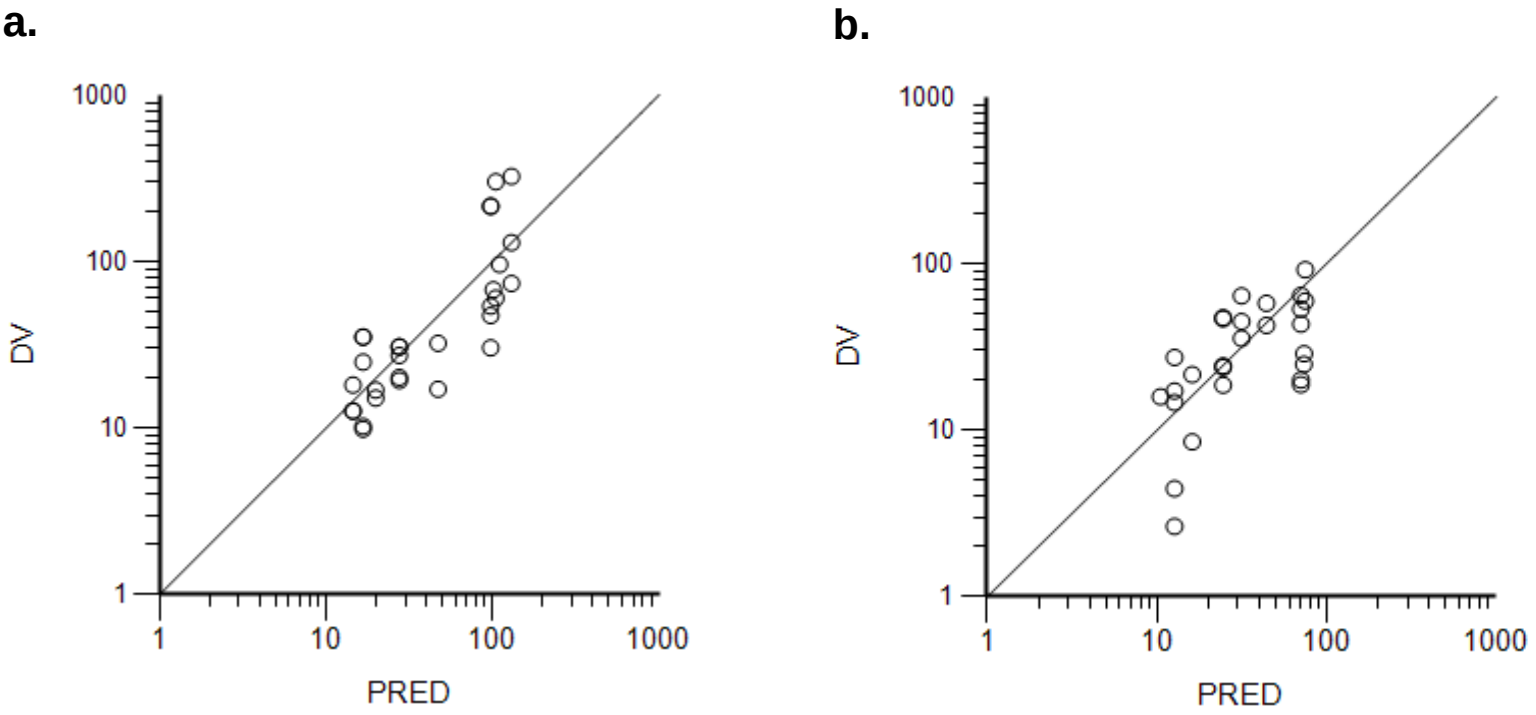

Figure 40 Observed *vs.* population predicted free DEX concentrations from Fig. 39d in (a) pregnant ewe and (b) fetus

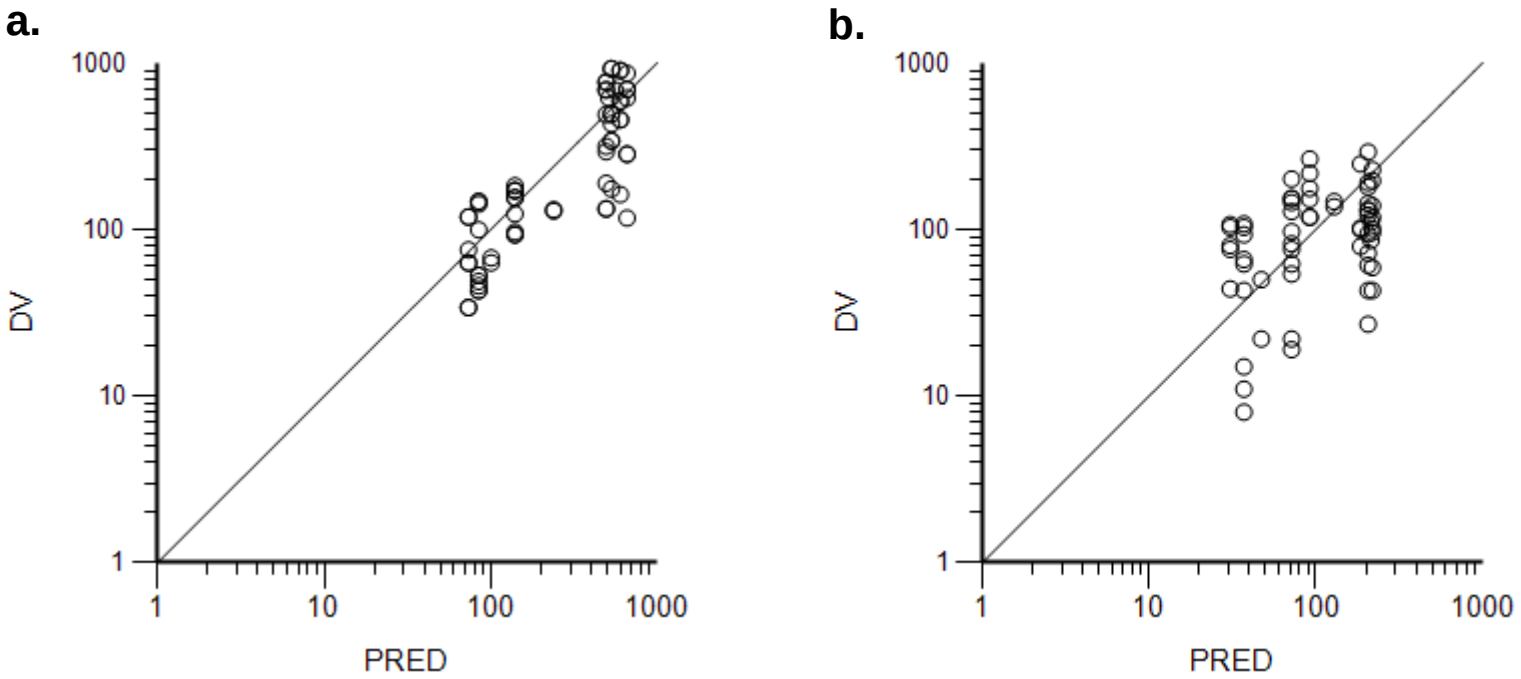

Figure 41 Observed *vs.* population predicted total DEX concentrations from Fig. 39d in (a) pregnant ewe and (b) fetus

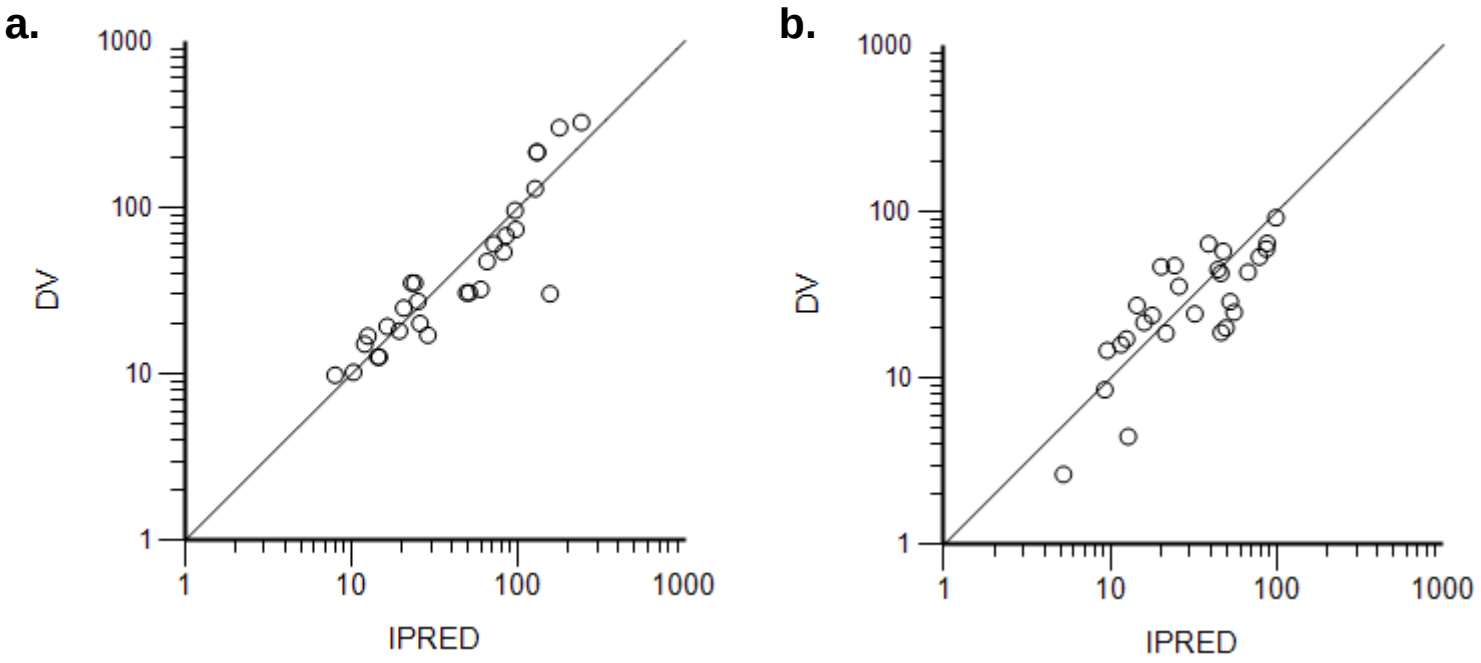

Figure 42 Observed *vs.* individual predicted free DEX concentrations from Fig. 39d in (a) pregnant ewe and (b) fetus

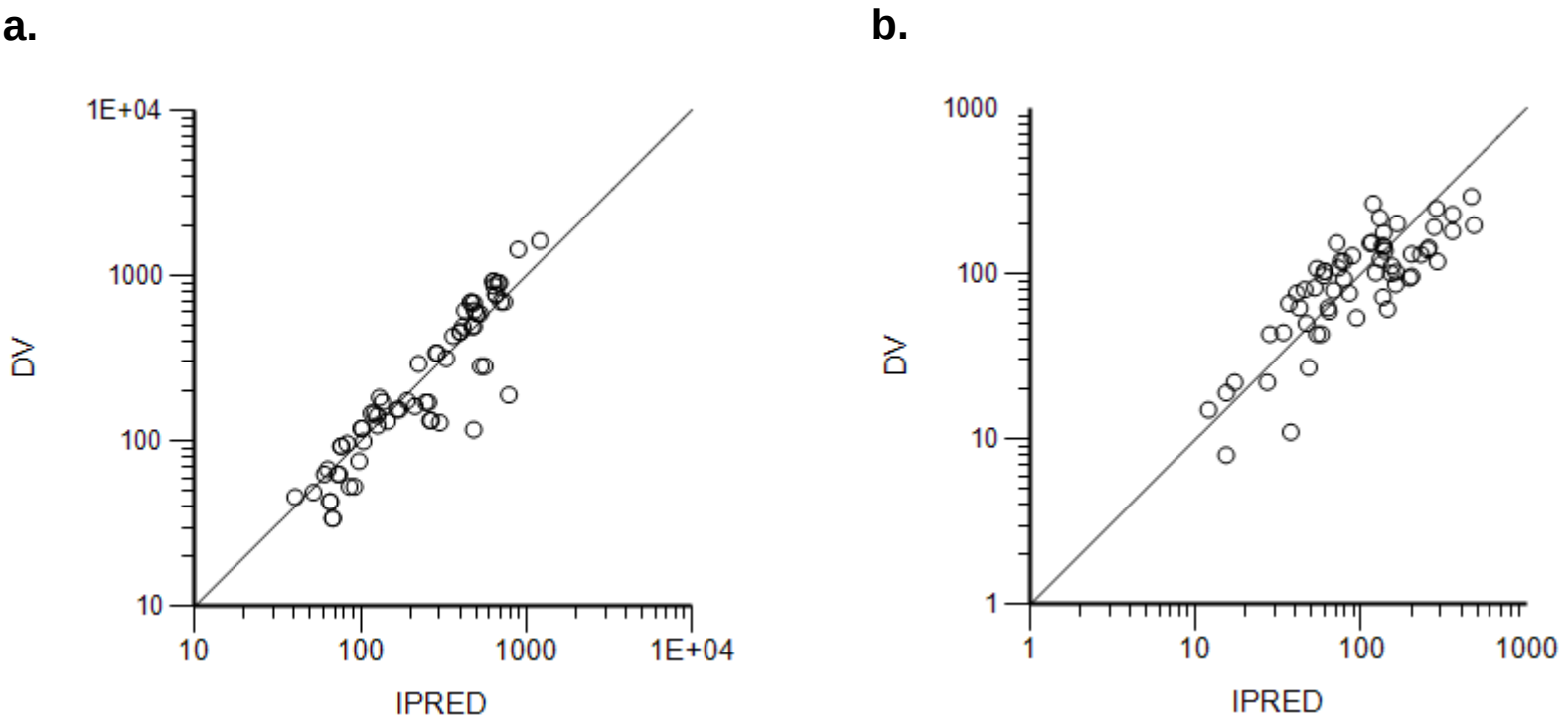

Figure 43 Observed *vs.* individual predicted total DEX concentrations from Fig. 39d in (a) pregnant ewe and (b) fetus

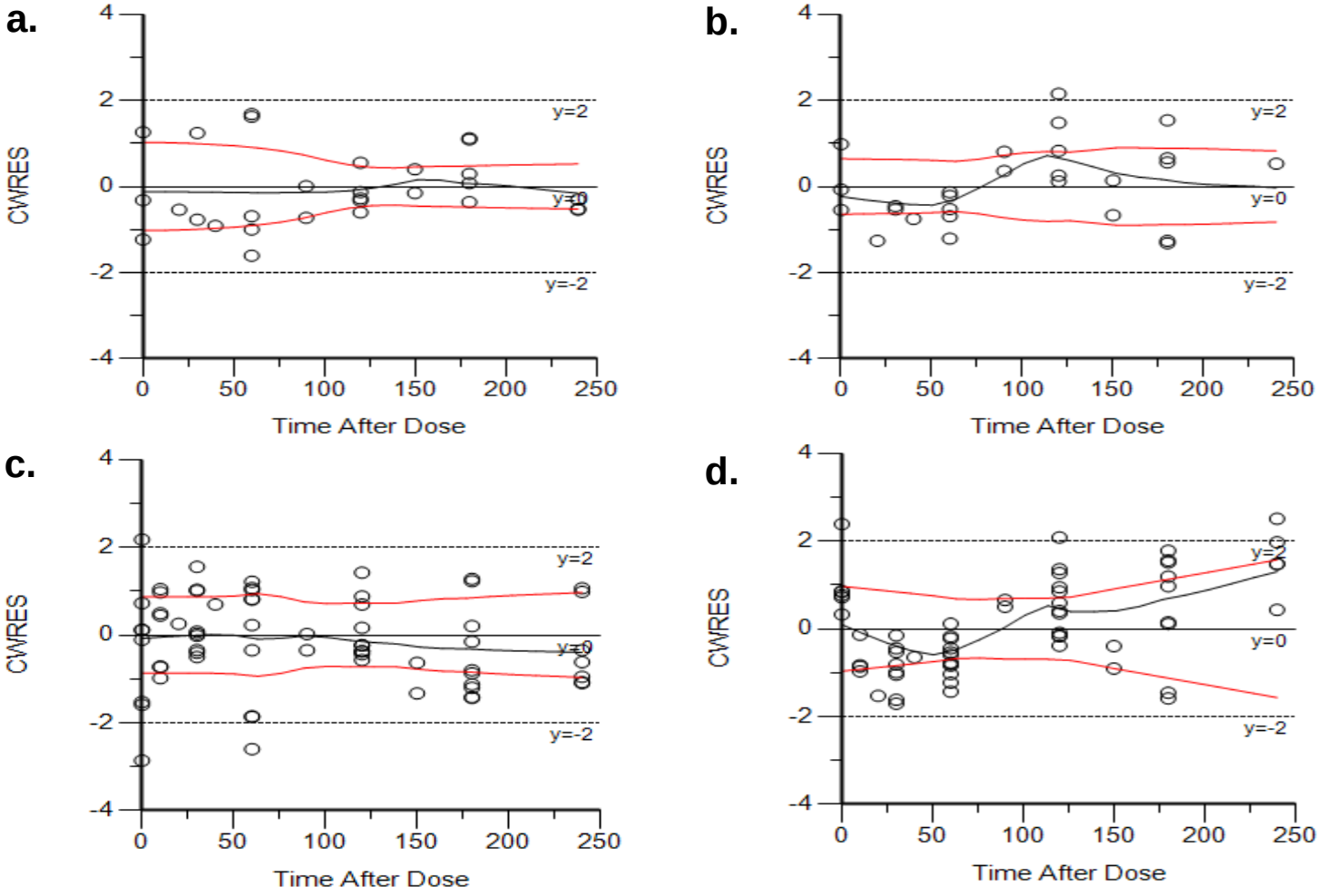

Figure 44 **Population weighted residuals *vs.* time for (a) maternal free, (b) fetal free, (c) maternal total and (d) fetal total DEX from Fig. 39d.**

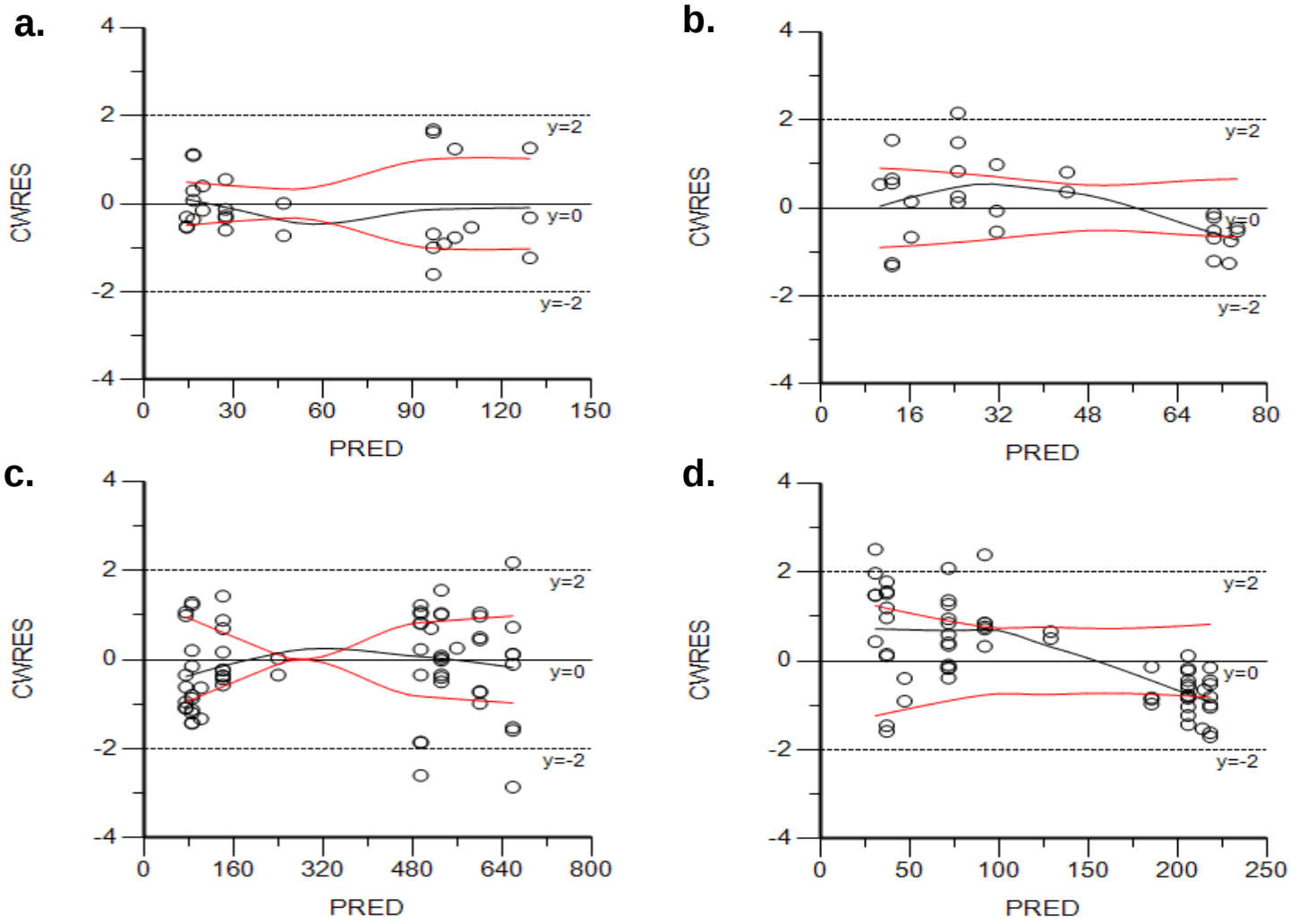

Figure 45 **Population weighted residuals *vs.* predicted concentrations for (a) maternal free, (b) fetal free, (c) maternal total and (d) fetal total DEX from Fig. 39d.**

Table 16 Pharmacokinetic parameter by bootstrap and comparison with (Fig. 39d) model parameters

Parameter	Units	Bootstrap			Model	
		Mean	CV%	95 % CI	Mean	CV%
V	L/kg	6.05	21.7	4.08, 8.55	6.66	14.5
CL	L/(kg*min)	0.08	56.1	0.02, 1.99	0.07	20.8
V_2	L/kg	53.36	70.4	8.71, 193	52.63	22.8
Q	L/(kg*min)	0.11	41.7	0.04, 2.09	0.14	25.0
K_{mf}	1/min	0.06	49.2	0.02, 0.14	0.06	34.0
K_{fm}	1/min	0.08	46.6	0.04, 0.22	0.09	23.0
fu_1		0.202	8.0	0.171, 0.241	0.197	9.7
fu_2		0.345	10.6	0.291, 0.397	0.342	15.1
σ_1		0.34	10.7	0.27, 0.43	0.34	15.0
σ_2		0.63	99.0	0.43, 0.64	0.57	22.7
σ_3		0.41	15.0	0.26, 0.48	0.41	20.1
σ_4		0.59	60.6	0.42, 0.65	0.56	27.6

4.6.2. PD modeling

Blood pressure and heart rate at baseline, 30, 60, 90 and 120 min from four pregnant ewes and their corresponding four fetuses (three of the four ewes had twin pregnancies) were recorded to develop the PD modeling. Simulated free DEX concentrations from the PK model in Section 4.6.1 were used to develop the PD model.

The relative cardiovascular changes (%) versus free DEX concentrations in pregnant ewe and fetus indicated the nonlinear relationship between PK and PD (**Figure 46**). A sigmoid E_{max} model where the effect equals to 0 at concentration 0, and the effect reaches E_{max} at infinite concentration, could be fitted to the pooled maternal heart rate and blood pressure (mean arterial pressure) response with an E_{max} of -52.6 ± 25.7%, EC_{50} of 14.5 ± 16.6 pg/mL and n of 0.67 ± 0.83 for the decrease in blood pressure in pregnant ewe. An E_{max} of -49.3 ± 4.7%, EC_{50} of 10.9 ± 6.12 pg/mL and n of 1.72 ± 1.56 were derived for the decrease in heart rate **(Table 17)**. In contrast, fetal cardiovascular response cannot be described by this model, and no apparent patterns were observed.

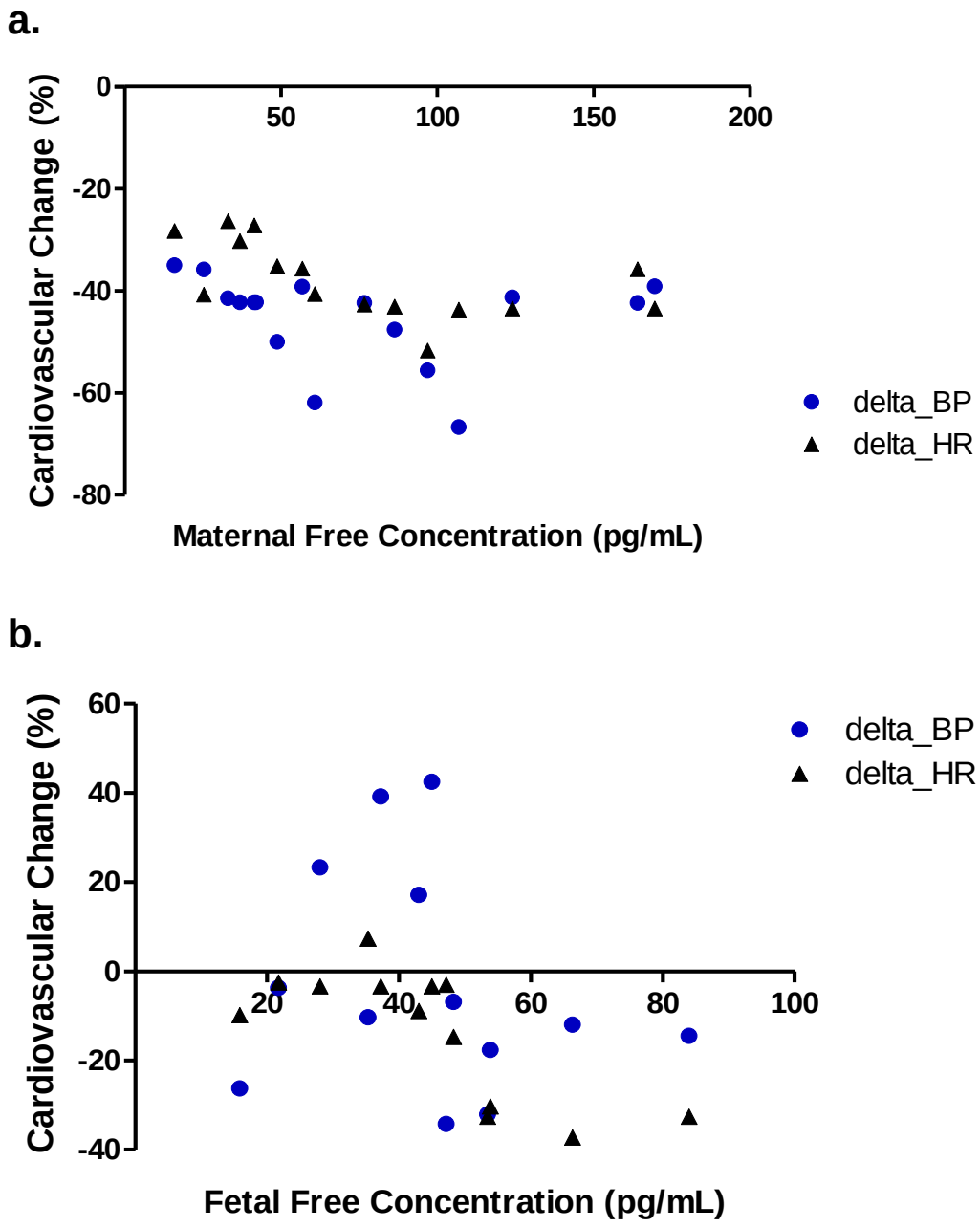

Figure 46 **Cardiovascular changes (%) *vs.* predicted free DEX concentrations in (a) pregnant ewe and (b) fetus**

Table 17 Pharmacodynamic parameter estimates in pregnant ewe

Parameters	Mean Arterial Pressure		Heart Rate	
	Mean ± SD	CV (%)	Mean ± SD	CV
Emax (%)	-52.6 ± 25.7	48.8	-49.3 ± 4.7	9.6
EC_{50} (pg/mL)	14.5 ± 16.6	113.9	10.9 ± 6.1	55.9
n	0.68 ± 0.83	124.1	1.72 ± 1.56	90.5

Chapter 5 Discussion

5.1. LC-MS/MS assay for quantification of DEX in plasma

Fetal safety is always a major concern when drugs are used in pregnant women, and the potential risk of DEX on fetuses is poorly defined. Without the knowledge of the maternal-fetal pharmacokinetics and placental transfer of DEX during pregnancy, fetuses may suffer from adverse effects when DEX is used during pregnancy. The ethical challenge of experiments on human fetuses limits fetal safety studies. In our study, the pregnant ewe model has been used for maternal-fetal pharmacokinetics studies of DEX, in which the drug concentrations in maternal plasma and fetal plasma were monitored. However, a quantification assay was not readily available for DEX in these samples when we initiated the project.

Methods for the quantification of DEX in humans have been reported, which include radioreceptor assays (Bol CJ et al., 1997), gas chromatography with tandem mass spectrometry (GC-MS) (Hui YH et al., 1997), HPLC-MS/MS (Ji QC et al., 2004; Lee JI et al., 2007; Li W et al., 2009) and UPLC-MS/MS (Inoue K et al., 2013). The radioreceptor assay was developed to quantify DEX concentration in rat plasma with an LLOQ of 24 pg/mL, but the use of radioactive materials could be hazardous and this limits its widespread application (Bol CJ et al., 1997). The GC-MS method could determine DEX over concentration ranges of 0.1-40 ng/mL with an LLOQ of 50 pg/mL, but it was for human plasma and the procedure was laborious because of the need for chemical derivatization prior to quantification (Hui YH et al., 1997). One HPLC-MS/MS method could also be used to quantify DEX in human plasma with an LLOQ of approximately 20 pg/mL, but it exhibited relatively low mean extraction recovery of 50.7-53.8% (Ji QC et

al., 2004). Recently, two more sensitive HPLC-MS/MS methods with the same LLOQ of 5 pg/mL were published, one of which was used for pediatric plasma using small volume of 200 µL. It was based on a laborious solid-phase extraction and the matrix effect on ionization alteration has not been discussed (Lee JI et al., 2007). Another HPLC-MS/MS method for human plasma used a simple liquid-liquid extraction procedure with saturated sodium carbonate solution during the sample preparation in an attempt to improve the extraction efficiency (Li W et al., 2009). However, the saturated sodium carbonate is non-volatile and may be unfriendly to mass spectrometer. Another fast and stable isotope dilution UPLC-MS/MS method has also been developed for pediatric human plasma with the use of pricy isotopic IS (Inoue K et al., 2013). Therefore, considering the influence of matrix effects of biofluid among species (Gray NP et al., 2012), as well as procedure optimization, the development of a new and single assay is necessary in order to successfully monitor DEX concentrations in pregnant ewes and fetuses.

The HPLC-MS/MS method that we developed fulfills the prerequisite for the pharmacokinetic characterization of DEX in pregnant ewe model, as it was sufficiently sensitive, specific, accurate and reliable for the determination of DEX in both pregnant ewes and fetuses. The LLOQ was 25 pg/mL for plasma using the 3200 QTRAP mass spectrometer, and a lower LLOQ of 10 pg/mL could be achieved with the 5500 QTRAP mass spectrometer.

Good linear response was demonstrated in the selected range up to 5000 pg/ml. The sample preparation and liquid-liquid extraction procedures were simple, efficient and robust. Recovery efficiency of this method from plasma was concentration-independent. The overall recoveries of DEX were 82.9-87.2% and 86.2-89.7% for maternal plasma and fetal plasma, respectively. The percentage matrix factors in maternal plasma and

fetal plasma were less than 120%, indicating that the matrix components do not significantly influence the HPLC-MS/MS ionization signal. The variation observed in matrix effect reflected the variable concentrations of endogenous components in these biological matrices. However, the evaluation of the slopes of the calibration lines from six different sources of plasma confirmed that the matrix effects were consistent and posed no significant concerns on the DEX determination in different lots of biomatrices (Matuszewski BK, 2006). In the pharmacokinetic application, the developed and validated assay enables the quantification of DEX concentrations in maternal plasma and fetal plasma with the single assay protocol. This assay can be easily modified to quantify DEX in plasma protein binding and microsome metabolism studies.

5.2. Pharmacokinetics of DEX in pregnant ewe and fetus

Ethical concerns preclude adequate study of *in vivo* pharmacokinetics and transplacental transfer of DEX in human pregnancy. Our study addresses this knowledge gap and also provides information on the pharmacokinetics of DEX in the third-trimester pregnant ewe model for the first time.

The current recommended dose of DEX in the clinical trials for sedation in the adult intensive care unit is a loading dose of 1 μg/kg over 10 min followed by a maintenance infusion of 0.2 to 0.7 μg/kg/h. However, the use of doses up to 1.5 μg/kg/h may be necessary for procedural sedation and have also been reported in various settings based on clinical requirement (Pandharipande PP et al., 2007; Riker RR et al., 2009; Pandharipande PP et al., 2010). In this work, the dose used was a loading dose of 1 μg/kg for 10 min followed by an-hour infusion dose of 1 μg/kg/h. The dose is clinically relevant, as it is equivalent to a human dose of approximately 0.97 μg/kg for pregnant

women, with a reference body weight (80 kg) based on the power equation from FDA Guidance for Industry (FDA Guidance for Industry, 2005), where the human equivalent dose (HED) = animal dose (1 μg/kg) * [animal weight (72.84 kg) ÷ human weight (80 kg)]$^{0.33}$. The recommended weight gains with normal body weight in human pregnancy are 20, and 11.3-15.9 kg for single and twin pregnancy, respectively.

The individual DEX PK in pregnant ewe and each fetus of twin pregnancy were analyzed by the non-compartmental model with maternal and fetal arterial concentrations. At 10 min-infusion after administration to pregnant ewes, DEX concentrations in fetal artery were detectable, reflecting a rapid placental transfer into the fetal circulation. The rapid decline of the maternal DEX concentration after the end of infusion of DEX, reflecting a continuous distribution, probably to a peripheral compartment, as DEX has been reported to be best described by a two-compartment PK model in the human adult (Lee S et al., 2012; Flexman AM et al., 2014), children (Petroz GC et al., 2006; Diaz SM et al., 2007; Potts AL et al., 2009), infant (Su F et al., 2010) and non-pregnant rat (Bol CJJG et al., 1997).

The following much slower decline up to 1 h post the end of infusion was related to the overall elimination of DEX. In contrast, the DEX concentrations were sustained in the fetus without further dosing.

A limitation of this work is the sparse sampling from a small number of subjects studied; 8 pregnant ewes and 12 fetuses. A large intersubject variability in DEX concentrations was noticed during infusion in pregnant ewes. One pregnant ewe with very high concentrations in maternal vein during infusion was observed. This may explain the large inter-subject variability. Half of the ewes studied had twin pregnancies; while this may be considered to be a limitation, the inclusion of twin pregnancies should not affect

the plasma concentrations of DEX, as a previous study examining medetomidine levels suggested similar plasma concentrations in both twin and singleton ewe pregnancies (Musk GC et al., 2012). While the ewes received anesthesia induced by isoflurane in addition to DEX during the entire surgery, evidence has demonstrated that the pharmacokinetics of DEX is not influenced by isoflurane anesthesia (Thornton C et al., 1999). The decreased cardiac output that may occur with increasing DEX concentrations may result in a corresponding decrease in elimination clearance, but the extent of this decrease is not significant and is unlikely to be clinically relevant (Dutta S et al., 2009).

Despite these limitations, we have established the concentration-time profiles of DEX in pregnant ewes and fetuses and derived estimates of PK parameters with non-compartmental analysis. We found that approximately 23% of systemic exposure (AUC) in the pregnant ewe crossed the placenta into fetal circulation which agrees with the transplacental transfer observed by Ala-Kokko and colleagues in the isolated human placenta model (Ala-Kokko TI et al., 1997). However, in the isolated placenta model, it remained unclear if the amount of DEX that crossed the placenta could exert hemodynamic effects on the fetus.

5.3. Pharmacodynamics of DEX in pregnant ewe and fetus

In our study, using the ewe model, we observed that the amount of DEX that crossed the placenta to the fetus did decrease the fetal heart rate, but the values remained within normal limits. This finding also lends support to El-Tahan's study in which babies delivered via cesarean section during which mothers had received DEX, were delivered with normal APGAR scores (which are used to evaluate the effects of obstetric anesthesia on newborn babies) (El-Tahan MR et al., 2012).

Prior to the administration of DEX to the pregnant ewes and fetuses, the baseline mean arterial pressures and heart rate were within normal range for sheep (Cissik JH et al., 1991; Booth LC et al., 2009). Following DEX administration in our study, significant hypotension and bradycardia was observed in the pregnant ewes with minimal change in hemodynamic parameters in the fetal lamb compared to baseline. These findings are similar to the findings by Uemura and colleagues where DEX had minimal effects on the fetal lamb (Uemura K et al., 2012). However, concurrent fetal drug levels were not obtained in their study. Our study provides conclusive evidence that while DEX administration to the pregnant ewe results in bradycardia and hypotension, the quantity that crosses the placenta into the fetal circulation is insufficient to exert similar hemodynamic effects in the fetus.

The delineation of DEX pharmacokinetics in the fetus, determination of the amount of drug that crosses the placenta and also the trend of the effect the drug has on the fetal lamb provides an aggregate of information which will be helpful to practitioners who desire to administer DEX in pregnancy.

The increase in fetal arterial oxygen tension noted between baseline and 60 min after completion of one hour infusion is consistent with previous documentation of a transient increase in fetal systemic oxygenation as a result of general anesthesia in the maternal ewe (McClaine RJ et al., 2005). The use of 2% isoflurane in oxygen in our study may also account for the observed increase in oxygenation. The worsening fetal metabolic acidosis observed after DEX infusion in our study may be related to impaired uterine perfusion following maternal hypotension. Maternal hypotension was not treated per study protocol. The possibility of fetal acidosis developing as a result of untreated

hypotension should be taken into consideration with the use of DEX, and hypotension should be treated accordingly.

Clonidine, another α_2-adrenergic agonist, when administered to the pregnant ewe, exerted bradycardia and hypoxemia in both ewe and fetus without associated hypotension (Eisenach JC et al., 1989). In contrast, in our study, DEX exerted significant bradycardia in the mother but the amount of DEX crossing the placenta was insufficient to exert a similar effect in the fetus. Similar to the clonidine study, we noted a decrease in fetal arterial pH at one hour following the end of DEX infusion. While we did not specifically measure uterine blood flow, we speculated that the observed acidosis in the fetal lamb in our study was due to potentially decreased uterine blood flow occurring as a result of hypotension in the maternal ewe.

Our studies were performed in anesthetized animals in contrast to the chronically instrumented animal models used by other groups (Eisenach JC et al., 1989; Uemura K et al., 2012). There is a theoretical concern that the hemodynamic effects noted in our study may be a summative effect of both DEX and isoflurane. However, our hemodynamic findings were similar to that in the non-anesthetized model used by Uemura et al in which isoflurane was not used (Uemura K et al., 2012). The combination of general anesthesia and DEX in our study did not result in significant hemodynamic perturbations in the fetus.

In pregnant women undergoing the ex utero intrapartum therapy (EXIT) procedure near term, high concentrations of volatile anesthetic agents are used (Garcia PJ et al., 2011). There is evidence that supplemental intravenous anesthetics decrease volatile anesthetic-induced depression of the fetal hemodynamics (Boat A et al., 2010). In our study, DEX was administered in concert with volatile anesthetic agents but with minimal

fetal hemodynamic compromise. However, volatile anesthetic agents used during the EXIT procedure may be administered at higher levels than that used in our study and in those settings, the combined hemodynamic effect with DEX may be detrimental. DEX should therefore be used with caution as a supplemental anesthetic for the EXIT procedure.

5.4. Plasma protein binding assay

Fetal exposure, which is related to fetal free drug concentrations, is affected by maternal dose and duration of exposure, maternal drug disposal, placental transfer, and fetal drug disposal. The factors affecting fetal drug exposure include molecular size and lipid solubility of the drug molecule, the plasma protein binding of the drug, and the relative pH gradients across placenta (Mihaly GW et al., 1983; Kumar S et al., 2000). The placenta is made up of lipid membranes between the maternal and fetal sides. According to the membrane permeability, compounds with lower molecular weight and higher lipid solubility can easily cross placenta, whereas the high degree of maternal plasma binding or ionization obstruct this process. In addition, phase I drug metabolites can be expected to cross the placenta, though more slowly than the parent compound, whereas phase II metabolites (conjugates) are highly polar and their placental transfer is negligible (Borrisud M et al., 1985; Wang LH et al., 1986).

As DEX is a small molecule and has high lipid solubility, it can easily cross the placenta. An *in vitro* perfusion study has shown that DEX enters the fetal circulation rapidly but with a lower transfer rate comparing to less lipophilic clonidine (Ala-Kokko TI et al., 1997). This phenomenon has also been observed for other highly lipophilic drugs using perfused human placenta, indicating the impact of protein binding on placental transfer

(Schneider H et al., 1988; Zakowski MI et al., 1994; Ala-Kokko TI et al., 1995; Johnson RF et al., 1995). In addition, high drug protein binding can contribute to the low volume of distribution and clearance for drugs. Moreover, large plasma protein bound components in the fetal compartment may retard the equilibrium by allowing less amount of drug to transfer back from fetus to mother.

DEX is highly bound to albumin and α_1-acid glycoprotein. The extents of plasma protein binding in humans, rats and dogs are 94%, 88% and 93%, respectively (Precedex injection label). However, no information is available regarding to the protein binding in the pregnant ewe model. Therefore, plasma protein binding factor should be evaluated to understand the differences in drug disposition and placental transfer between pregnant ewes and fetuses. Free drug concentration is ultimately responsible for the characterization of the placental transfer to rationalize the observed pharmacological effect.

Two of the most commonly used methods for protein binding measurements are ultrafiltration and equilibrium. Many researchers have used ultrafiltration devices for the plasma protein binding measurement as ultrafiltration is a simple and rapid method in which centrifugation forces the buffer containing free drugs through the size exclusion membrane and achieves a fast separation of free from protein-bound drug molecules. The major concern of this method is nonspecific binding of the drugs on filter membrane and plastic devices. Equilibrium is less susceptible to experimental artifacts, but it is time consuming and it requires substantial equilibration time (3-24 h) at 37 °C. The degradation of DEX due to the duration of exposure to 37 °C has not yet been evaluated. Therefore, ultrafiltration devices were employed in our study and nonspecific binding was determined to correct the plasma protein binding.

We found that the fetus has about 15% less plasma protein binding than that in the pregnant ewe, which can be explained by lower protein concentrations and lower binding affinity in the fetus comparing to those in pregnant ewes (Syme MR et al., 2004). In humans, maternal and fetal albumin and α_1-acid glycoprotein levels change continuously during pregnancy. As the gestational age increases, the maternal albumin and α_1-acid glycoprotein concentrations decrease, whereas fetal albumin and α_1-acid glycoprotein concentrations increase. The (fetal/maternal) concentration ratio of albumin increases from 0.38 at 12-15 weeks to 1.2 after 35 weeks of gestation, while the fetal/maternal concentration ratio of α_1-acid glycoprotein increase from 0.1 at 10 weeks to 0.3-0.4 at term pregnancy (Hamar C et al., 1980; Wood M et al., 1981; Krauer B et al., 1984). In addition, differential structures in albumin forms between pregnant women and fetuses have suggested that maternal albumin exhibits a higher affinity for local anesthetics (Krasner J et al., 1973; Wallace S, 1977). Moreover, competing binding between drugs and endogenous ligands may contribute to the protein binding differences between pregnant women and fetuses (Ridd MJ et al., 1983; Nau H et al., 1984). However, the differential plasma protein binding between pregnant women and fetuses are primarily due to the difference in plasma protein concentrations between pregnant women and fetuses, rather than other factors (Hill MD et al., 1988; Syme MR et al., 2004).

We have also observed a lower plasma protein binding in pregnant ewes compared to that in non-pregnant humans, rats and dogs, but the plasma protein binding of DEX in non-pregnant sheep has not been reported thus making the comparison difficult. Species difference in plasma protein binding kinetics has been demonstrated, especially for α_1-acid glycoprotein binding of basic compounds (Belpaire FM et. al., 1984; Hill MD et. al., 1989; Son DS et. al., 1998; Huang Z et. al., 2013). Additionally, it is known that

there is a decrease in protein binding during pregnancy due to the decreased albumin and α_1-acid glycoprotein concentrations (Syme MR et al., 2004).

5.5. UGT metabolism of DEX in pregnant ewe and fetus

DEX undergoes almost complete biotransformation through direct glucuronidation and CYP450 metabolism in humans. Direct N-glucuronidation at the imidazolate nitrogens is the major metabolic pathway (Precedex injection label), and UGT1A4 (for lower-affinity reaction) and UGT2B10 (for high-affinity reaction) have been suggested to be responsible for the DEX N-glucuronidation reaction (Kaivosaari S et al., 2008). In contrast, in rat liver microsomes, DEX N-glucuronidation was barely detectable. Dog liver microsomes can form N-glucuronides but at a lower efficiency than human liver microsomes. The metabolic profiles for pregnant ewe model have not been investigated.

In the present study, glucuronidation metabolites of DEX were undetectable after the incubation with placental microsomes and hepatic microsome preparations from pregnant ewe and fetus, respectively, for up to 24 hr. This indicated that direct N-glucuronidation is a negligible pathway in the pregnant ewe model which differs from that in humans. Chiu and Huskey (Chiu et al., 1998) have reported that N-glucuronidation exhibits marked differences across species. The N-glucuronidation rates of aromatic N-heterocycles in humans are typically much higher than in animals, due to the activity of two enzymes, UGT1A4 and UGT2B10 (Kaivosaari S et al., 2011). Because of the diverse structures of aromatic N-heterocycles, this difference in N-glucuronidation across species is largely compound-dependent. Moreover, to date only six UGT isoforms have been identified in adult sheep liver including UGT1A1, UGT1A3, UGT1A4, UGT1A6, UGT1A9 and UGT2B7; UGT2B10 isoform is not detectable (Pretheeban M et al., 2011),

explaining the negligible DEX N-glucuronidation observed in pregnant ewe liver microsomes. Furthermore, the critical amino acid residue of UGT1A4 in human (Pro40) is different from that in sheep (His40) (Kubota T et. al., 2007; Pretheeban M et al., 2011). Therefore, while DEX N-glucuronides are formed efficiently in humans, pregnant ewes appear to lack the ability to conjugate the aromatic N-heterocycles.

Different from UGT-mediated metabolism of DEX via N-glucuronidation, genistein primarily undergoes O-glucuronidation by UGT1As (UGT1A1, 1A8, 1A9 and 1A10). In this study, we were able to determine the differential UGT activities in hepatic microsomes between pregnant ewe and fetus by a kinetic study with genistein as a typical UGT substrate. The reaction kinetic data for genistein showed biphasic kinetics in which two isoforms with different kinetic behaviors were responsible for the glucuronidation. For the high-affinity reaction of the biphasic kinetics, the affinity in pregnant ewe and fetus is similar whereas pregnant ewe has 17 times higher capacity than that in fetus.

It is well known that the fetus has a greatly reduced metabolizing enzyme capacity compared to adults and some enzymes do not appear to be expressed at all in the fetus. Studies have indicated both phase I and phase II metabolism can occur in human fetal liver (Krauer B et al., 1991; Hines RN et al., 2002; McCarver DG et al., 2002). The markedly lower activity of UGTs in fetuses than in adults has been suggested to be caused by the low transcripts (Strassburg CP et al., 2002; Izukawa T et al., 2009; Ekström L et al., 2013). No UGT transcripts were detected in two fetal liver samples at 20 weeks' gestation in a study to analyze expression of UGT1A and UGT2B genes and hepatic glucuronidation activity in human fetal liver (Strassburg CP et al., 2002). Ontogenesis of UDP-glucuronosyltransferase enzymes (UGTs) has been determined in

sheep and showed that mRNA levels of UGT1A6, UGT1A9 and UGT2B7 genes are expressed in fetal livers, but the levels are lower in the fetus than in the pregnant ewe (Pretheeban M et al., 2011).

5.6. PK and PD modeling of DEX in pregnant ewe and fetus

Free and total DEX PK in maternal and fetal concentrations was satisfactorily described by the proposed compartmental model. Data for fetal arterial blood samples were used due to the sparse samples collected from fetal vein (only 19 concentrations versus 62 concentrations from arterial blood samples) and similar concentration profiles observed in fetal arterial and venous blood samples. The rate constants of distribution and elimination were 0.082 min^{-1} (= K_{mf} + Q/V) and 0.011 min^{-1} (= CL/V) from pregnant ewe, respectively. This reflected the rapid placental transfer into the fetal circulation. The rapid decline of the maternal DEX concentration post the end of infusion demonstrated a continuous distribution to a peripheral compartment, probably the placenta. The following much slower decline was for the overall elimination of DEX. In contrast, the DEX concentrations were sustained with a longer $t_{1/2}$ in the fetus even without further dosing. Despite the small number of subjects in this studied for PK analysis with NLME approach, all structural parameters estimated from the developed model were of adequate precision (i.e. CV < 34 %).

The changes in blood pressure and heart rate in pregnant ewes were best fitted by the sigmoid E_{max} model. In the literature, the sigmoid E_{max} model was also used to describe the PK/PD relationships of DEX concentrations with blood pressure and heart rate effects in adult rats (Bol CJJG et al., 1997). The CV% in EC_{50} and n derived from the PD model is relatively large mainly due to the few datum points available at the low DEX

concentrations. This could be considered as one of the limitations to develop the PD model with the current data. Usually, the PK concentrations selected should cover the range of 3-fold EC_{50} in order to adequately describe the PK/PD relationship in the slope phase. Another limitation of this study is the lack of control experiments, and evaluation of PD response with dose escalation. Therefore, further investigation of PK/PD correlation is warranted.

5.7. Data extrapolation from pregnant ewe to pregnant women

Extrapolation of data from pregnant ewes to pregnant women should be interpreted with extreme caution. Although the pregnant ewe has been a popular animal model for placental transfer studies, the nature of its placental structure differs from that of human placenta and the pregnant ewe placenta is less permeable for drug transfer. In our study, this effect should be less pronounced for DEX as it is a highly lipid soluble compound with a low molecular weight (Vertommen et al., 1995). In addition, placental blood flows are known to be similar between pregnant ewes and pregnant women.

The developed PK and PD models in our study contribute to the current state of knowledge of DEX exposure and maternal-fetal cardiovascular response to DEX. Unfortunately, direct comparison of estimates from PK and PD models between pregnant ewe and pregnant women is not yet possible. To the best of our knowledge, data on PK/PD parameters of DEX in pregnant women are still unavailable as a reference for comparison. A previous case study reported the placental transfer of DEX in pregnant women who underwent caesarean delivery (Neumann MM et al., 2009). A total dose of 1.84 µg/kg was administered intravenously over approximately 40 min. In that study, the concentrations in maternal vein, umbilical artery and umbilical vein were

710, 540 and 543 pg/mL, respectively, at the time of delivery (110 min). No bradycardia and hemodynamic changes were detected in the fetus. The finding of the fetal/maternal concentration ratio (0.76) is consistent with the fetal/maternal concentration ratio (0.77) reported by Ala-Kokko et al. using the isolated perfused human placenta with the same amount of albumin on both maternal and fetal sides (Ala-Kokko TI et al., 1997). In our study, the fetal/maternal concentration ratios were 0.59 and 0.69 at 130 and 250 min, respectively. The comparison between the case study in pregnant women and our study is still complicated and difficult as DEX doses, blood sampling times and metabolism pathways are different between the two models. Nevertheless, no significant fetal adverse effects were observed in either situation. The fetal arterial and venous concentrations were similar in the two species. The slightly lower fetal/maternal concentration ratio in pregnant ewe compared to that in pregnant women might be explained by the lower permeability of pregnant ewe placenta compared to that of human placenta.

Chapter 6 Summary

The contribution of our study is the quantitative characterization of fetal exposure and cardiovascular response to maternal administration of DEX in the pregnant ewe model. We have demonstrated that

- Our developed and validated LC-MS/MS method can be applied to quantify DEX concentrations in the pregnant ewe model.
- DEX rapidly crossed the pregnant ewe placenta with a partition coefficient (K_{fm}) of 23% after pregnant ewe was given DEX at a clinically relevant dose.
- The pregnant ewe has a rapid distribution and a relatively slow elimination after DEX administration.
- Total drug concentrations ranged from 29.8 to 6197.9 pg/mL in pregnant ewes, and from 8 to 265 pg/mL in fetuses.
- Plasma protein binding of DEX was concentration-independent over the PK relevant concentrations in the pregnant ewe model.
- Fractions of unbound DEX (fu) in pregnant ewe and fetus were 19.6 ± 3.9 % and 36.9 ± 4.8 % for PK samples, respectively, and 25.1 ± 4.8 % and 38.9 ± 3.2 % for DEX-spiked blank plasma samples. The fu is significantly lower in pregnant ewe (19.7 ± 1.9 %) than those in the fetus (34.2 ± 5.2 %) in the PK model predictions. The fetus has significantly less plasma protein binding.
- The amount of DEX transferred from the pregnant ewe to the fetus did not result in fetal hypotension or significant bradycardia.

- Direct N-glucuronidation is a negligible pathway for DEX in pregnant ewes, which differs from that in humans. Therefore, the pregnant ewe model may not be a representative model for humans in DEX phase II metabolism.
- Differential UGT enzyme capacity between pregnant ewe and fetus has been characterized.
- Findings from this study support further studies to determine if DEX can be used clinically during pregnancy.

Appendix

The differential equations connected with the model depicted in Figure 39d were as follows:

$A_1 = - CL * C - Q * C + Q * C_2$

$A_2 = Q * C - Q * C_2$

$C_3 = K_{mf} * C - K_{fm} * C_3$

$C = A_1/V$

$C_2 = A_2/V_2$

$C_{t1} = C/f_{u1}$

$C_{t3} = C_3/f_{u2}$

$C_{Obs} = C_{t1} * \exp(C_{Eps1})$

$C_{Obs2} = C_{t3} * \exp(C_{Eps2})$

$C_{Obs3} = C * \exp(C_{Eps3})$

$C_{Obs4} = C_3 * \exp(C_{Eps4})$

$V = tvV * \exp(nV)$

$CL = tvCL * \exp(nCL)$

$V_2 = tvV_2 * \exp(nV_2)$

$Q = tvQ * \exp(nQ)$

$K_{mf} = tvK_{mf} * \exp(nK_{mf})$

$K_{fm} = tvK_{fm} * \exp(nK_{fm})$

$f_{u1} = tvf_{u1} * \exp(nf_{u1})$

$f_{u2} = tvf_{u2} * \exp(nf_{u2})$

References

Afonso J, Reis F. Dexmedetomidine: current role in anesthesia and intensive care. Rev Bras Anestesiol. 2012 Jan-Feb; 62(1):118-33.

Ala-Kokko TI, Pienimäki P, Herva R, Hollmén AI, Pelkonen O, Vähäkangas K. Transfer of lidocaine and bupivacaine across the isolated perfused human placenta. Pharmacol Toxicol. 1995 Aug; 77(2):142-8.

Ala-Kokko TI, Pienimaki P, Lampela E, Hollmen AI, Pelkonen O, Vahakangas K. Transfer of clonidine and dexmedetomidine across the isolated perfused human placenta. Acta Anaesthesiol Scand 1997; 41:313-9.

Andaluz A, Tusell J, Trasserres O, Cristòfol C, Capece BP, Arboix M, Garcia F. Transplacental transfer of propofol in pregnant ewes. Vet J. 2003 Sep;166(2):198-204.

Angel I, Langer SZ. Adrenergic-induced hyperglycemia in anaesthetized rats: involvement of peripheral alpha 2-adrenoceptors. Eur J Pharmacol 1988 Sep 13; 154(2):191-6.

Arcangeli A, D'Alò C, Gaspari R. Dexmedetomidine use in general anaesthesia. Curr Drug Targets. 2009 Aug; 10(8):687-95.

Barry JS, Anthony RV. The pregnant sheep as a model for human pregnancy. Theriogenology. 2008 Jan 1; 69(1):55-67.

Belpaire FM, Braeckman RA, Bogaert MG. Binding of oxprenolol and propranolol to serum, albumin and alpha 1-acid glycoprotein in man and other species. Biochem Pharmacol. 1984 Jul 1;33(13):2065-9.

Boat A, Mahmoud M, Michelfelder EC, Lin E, Ngamprasertwong P, Schnell B, Kurth CD, Crombleholme TM, Sadhasivam S. Supplementing desflurane with intravenous anesthesia reduces fetal cardiac dysfunction during open fetal surgery. Paediatr Anaesth 2010; 20:748-56.

Bol CJ, IJzerman AP, Danhof M, Mandema JW. Determination of dexmedetomidine in rat plasma by a sensitive [3H]clonidine radioreceptor assay. J Pharm Sci. 1997 Jul; 86(7):822-6.

Bol CJ, Danhof M, Stanski DR, Mandema JW. Pharmacokineticpharmacodynamic characterization of the cardiovascular, hypnotic, EEG and ventilatory responses to dexmedetomidine in the rat. J Pharmacol Exp Ther 1997; 283:1051-8.

Booth LC, Malpas SC, Barrett CJ, Guild SJ, Gunn AJ, Bennet L. Is baroreflex control of sympathetic activity and heart rate active in the preterm fetal sheep? Am J Physiol Regul Integr Comp Physiol 2009; 296:R603-9.

Borrisud M, O'Shaughnessy R, Alexander MS, Andresen BD. Metabolism and disposition of ritodrine in a pregnant baboon. Am J Obstet Gynecol. 1985 Aug 15; 152(8):1067-72.

Bucklin A, Fuller A. Physiologic Changes In Pregnancy. In: Suresh M, Segal B, Preston R, Fernando R, Mason C, editors. Shnider and Levinson's Anesthesia for Obstetrics. Fifth ed. China: Lippincott Williams and Wilkins; 2012. p6.

Capeless EL, Clapp JF. Cardiovascular changes in early phase of pregnancy. Am J Obstet Gynecol. 1989 Dec; 161(6 Pt 1):1449-53.

Carter AM. Animal models in fetal growth and development. In: Hau J, Van Hoosier Jr GL, eds. Handbook of laboratory animal science. Animal models. 2nd edition, Vol. II. Boca Raton: CRC Press; 2003. p41-54.

Carter AM. Animal models of human placentation-a review. Placenta. 2007 Apr;28 Suppl A:S41-7.

Cheek TG, Baird E. Anesthesia for nonobstetric surgery: maternal and fetal considerations. Clin Obstet Gynecol. 2009 Dec; 52(4):535-45.

Chen J, Lin H, Hu M. Metabolism of flavonoids via enteric recycling: role of intestinal disposition. J Pharmacol Exp Ther. 2003 Mar; 304(3):1228-35.

Cissik JH, Ehler WJ, Hankins GD, Snyder RR. Cardiopulmonary reference standards in the pregnant sheep (Ovis aries): a comparative study of ovine and human physiology in obstetrics. Comp Biochem Physiol A Comp Physiol 1991;100:877-80.

Clark SL, Cotton DB, Lee W, Bishop C, Hill T, Southwick J, Pivarnik J, Spillman T, DeVore GR, Phelan J, et al. Central hemodynamic assessment of normal term pregnancy. Am J Obstet Gynecol. 1989 Dec; 161(6 Pt 1):1439-42.

Cohen SE. Nonobstetric surgery during pregnancy. In: Chestnut DH, editor. Obstetric anesthesia: principles and practice. 2nd ed. St. Louis (Mo) 7 Mosby; 1999. p. 279.

Coonen JB, Marcus MA, Joosten EA, van Kleef M, Neef C, van Aken H, Gogarten W. Transplacental transfer of remifentanil in the pregnant ewe. Br J Pharmacol. 2010 Dec;161(7):1472-6.

Costantine MM. Physiologic and pharmacokinetic changes in pregnancy. Front Pharmacol. 2014 Apr 3; 5:65.

Craft JB Jr, Coaldrake LA, Bolan JC, Mondino M, Mazel P, Gilman RM, Shokes LK, Woolf WA. Placental passage and uterine effects of fentanyl. Anesth Analg. 1983 Oct;62(10):894-8.

Davison JM, Dunlop W. Renal hemodynamics and tubular function normal human pregnancy. Kidney Int. 1980 Aug;18(2):152-61.

de Haan GJ, Edelbroek P, Segers J, Engelsman M, Lindhout D, Dévilé-Notschaele M, Augustijn P. Gestation-induced changes in lamotrigine pharmacokinetics: a monotherapy study. Neurology. 2004 Aug 10; 63(3):571-3.

Diaz SM, Rodarte A, Foley J, Capparelli EV. Pharmacokinetics of dexmedetomidine in postsurgical pediatric intensive care unit patients: preliminary study. Pediatr Crit Care Med 2007;8:419-24.

Dutta S, Lal R, Karol MD, Cohen T, Ebert T. Influence of cardiac output on dexmedetomidine pharmacokinetics. J Pharm Sci 2000; 89:519-27.

Dyck JB, Maze M, Haack C, Vuorilehto L, Shafer SL. The pharmacokinetics and hemodynamic effects of intravenous and intramuscular dexmedetomidine hydrochloride in adult human volunteers. Anesthesiology. 1993 May; 78(5):813-20.

Eisenach JC, Castro MI, Dewan DM, Rose JC, Grice SC. Intravenous clonidine hydrochloride toxicity in pregnant ewes. Am J Obstet Gynecol 1989; 160:471-6.

El-Tahan MR, Mowafi HA, Al Sheikh IH, Khidr AM, Al-Juhaiman RA. Efficacy of dexmedetomidine in suppressing cardiovascular and hormonal responses to general anaesthesia for caesarean delivery: a dose-response study. Int J Obstet Anesth 2012; 21:222-9.

Ekström L, Johansson M, Rane A. Tissue distribution and relative gene expression of UDP-glucuronosyltransferases (2B7, 2B15, 2B17) in the human fetus. Drug Metab Dispos. 2013 Feb; 41(2):291-5.

Eshkoli T, Sheiner E, Ben-Zvi Z, Holcberg G. Drug transport across the placenta. Curr Pharm Biotechnol. 2011 May; 12(5):707-14.

Farag E, Argalious M, Abd-Elsayed A, Ebrahim Z, Doyle DJ. The use of dexmedetomidine in anesthesia and intensive care: a review. Curr Pharm Des. 2012; 18(38):6257-65.

FDA Guidance for Industry Population Pharmacokinetics (1999).

FDA Guidance for Industry Bioanalytical Method Validation (2001)

FDA Guidance for Industry Estimating the Maximum Safe Starting Dose in Initial Clinical Trials for Therapeutics in Adult Healthy Volunteers (2005)

Flexman AM, Wong H, Riggs KW, Shih T, Garcia PA, Vacas S, Talke PO. Enzyme-inducing anticonvulsants increase plasma clearance of dexmedetomidine: a pharmacokinetic and pharmacodynamic study. Anesthesiology 2014;120:1118-25.

Fresno L, Andaluz A, Moll X, Cristofol C, Arboix M, García F. Placental transfer of etomidate in pregnant ewes after an intravenous bolus dose and continuous infusion. Vet J. 2008 Mar;175(3):395-402. Epub 2007 Apr 10.

Furukawa S, Kuroda Y, Sugiyama A. A comparison of the histological structure of the placenta in experimental animals. J Toxicol Pathol. 2014 Apr; 27(1):11-8.

Gabrielsson J, Weiner D. Non-compartmental analysis. Methods Mol Biol 2012;929:377-89.

Garcia PJ, Olutoye OO, Ivey RT, Olutoye OA. Case Scenario: Anesthesia for Maternal-Fetal Surgery: The Ex Utero Intrapartum Therapy (EXIT) Procedure. Anesthesiology 2011 Jun; 114(6):1446-52.

Gertler R, Brown HC, Mitchell DH, Silvius EN. Dexmedetomidine: a novel sedative-analgesic agent. Proc (Bayl Univ Med Cent). 2001 Jan; 14(1):13-21.

Gin T, Chan MT. Decreased minimum alveolar concentration of isoflurane in pregnant humans. Anesthesiology 1994; 81: 829-32.

Gin T, Mainland P, Chan MT, Short TG. Decreased thiopental requirements in early pregnancy. Anesthesiology. 1997 Jan; 86(1):73-8.

Goodman S. Anesthesia for nonobstetric surgery in the pregnant patient. Semin Perinatol. 2002; 26: 136-45

Gray NP, McDougall SA, Dean JR. Analytical bias between species caused by matrix effects in quantitative analysis of a small-molecule pharmaceutical candidate in plasma. Bioanalysis. 2012 Mar; 4(6):675-84.

Hall JE, Uhrich TD, Barney JA, Arain SR, Ebert TJ. Sedative, amnestic, and analgesic properties of small-dose dexmedetomidine infusions. Anesth Analg. 2000 Mar; 90(3):699-705.

Hamar C, Levy G. Serum protein binding of drugs and bilirubin in newborn infants and their mothers. Clin Pharmacol Ther. 1980 Jul; 28(1):58-63.

Hegewald MJ, Crapo RO. Respiratory physiology in pregnancy. Clin Chest Med. 2011 Mar; 32(1):1-13, vii.

Hellgren M. Hemostasis during pregnancy and puerperium. Haemostasis. 1996 Oct;26 Suppl 4:244-7.

Hill MD, Abramson FP. The significance of plasma protein binding on the fetal/maternal distribution of drugs at steady-state. Clin Pharmacokinet. 1988 Mar; 14(3):156-70.

Hill MD, Briscoe PR, Abramson FP. Comparison of propranolol-binding plasma proteins in sheep with those in humans, dogs and rats. Biochem Pharmacol. 1989 Dec 1;38(23):4199-205.

Hines RN, McCarver DG. The ontogeny of human drug-metabolizing enzymes: phase I oxidative enzymes. J Pharmacol Exp Ther. 2002 Feb; 300(2):355-60.

Huang Z, Ung T. Effect of alpha-1-acid glycoprotein binding on pharmacokinetics and pharmacodynamics. Curr Drug Metab. 2013 Feb;14(2):226-38.

Hui YH, Marsh KC, Menacherry S. Analytical method development for the simultaneous quantitation of dexmedetomidine and three potential metabolites in plasma. J Chromatogr A. 1997 Feb 21; 762(1-2):281-91.

Inoue K, Sakamoto T, Fujita Y, Yoshizawa S, Tomita M, Min JZ, Todoroki K, Sobue K, Toyo'oka T. Development of a stable isotope dilution UPLC-MS/MS method for quantification of dexmedetomidine in a small amount of human plasma. Biomed Chromatogr. 2013 Jul; 27(7):853-8.

Izukawa T, Nakajima M, Fujiwara R, Yamanaka H, Fukami T, Takamiya M, Aoki Y, Ikushiro S, Sakaki T, Yokoi T. Quantitative analysis of UDP-glucuronosyltransferase (UGT) 1A and UGT2B expression levels in human livers. Drug Metab Dispos. 2009 Aug; 37(8):1759-68.

Jeyabalan A, Conrad KP. Renal function during normal pregnancy and preeclampsia. Front Biosci. 2007 Jan 1; 12:2425-37.

Ji QC, Zhou JY, Gonzales RJ, Gage EM, El-Shourbagy TA. Simultaneous quantitation of dexmedetomidine and glucuronide metabolites (G-Dex-1 and G-Dex-2) in human plasma utilizing liquid chromatography with tandem mass spectrometric detection. Rapid Commun Mass Spectrom. 2004; 18(15):1753-60.

Johnson RF, Herman N, Arney TL, Gonzalez H, Johnson HV, Downing JW. Bupivacaine transfer across the human term placenta. A study using the dual perfused human placental model. Anesthesiology. 1995 Feb; 82(2):459-68.

Joseph TB, Wang SW, Liu X, Kulkarni KH, Wang J, Xu H, Hu M. Disposition of flavonoids via enteric recycling: enzyme stability affects characterization of prunetin glucuronidation across species, organs, and UGT isoforms. Mol Pharm 2007; 4:883–94.

Kaivosaari S, Finel M, Koskinen M. N-glucuronidation of drugs and other xenobiotics by human and animal UDP-glucuronosyltransferases. Xenobiotica. 2011 Aug; 41(8):652-69.

Kaivosaari S, Toivonen P, Aitio O, Sipilä J, Koskinen M, Salonen JS, Finel M. Regio- and stereospecific N-glucuronidation of medetomidine: the differences between UDP glucuronosyltransferase (UGT) 1A4 and UGT2B10 account for the complex kinetics of human liver microsomes Drug Metab Dispos. 2008 Aug; 36(8):1529-37.

Kamibayashi T, Maze M. Clinical uses of alpha2-adrenergic agonists. Anesthesiology. 2000 Nov; 93(5):1345-9.

Ke AB, Rostami-Hodjegan A, Zhao P, Unadkat JD. Pharmacometrics in Pregnancy: An Unmet Need. Annu Rev Pharmacol Toxicol. 2014; 54:53-69.

Khan ZP, Ferguson CN, Jones RM. alpha-2 and imidazoline receptor agonists. Their pharmacology and therapeutic role. Anaesthesia. 1999 Feb; 54(2):146-65.

Krasner J, Giacoia GP, Yaffe SJ. Drug-protein binding in the newborn infant. Ann N Y Acad Sci. 1973 Nov 26; 226:101-14.

Krauer B, Dayer P, Anner R. Changes in serum albumin and alpha 1-acid glycoprotein concentrations during pregnancy: an analysis of fetal-maternal pairs. Br J Obstet Gynaecol. 1984 Sep; 91(9):875-81.

Krauer B, Dayer P. Fetal drug metabolism and its possible clinical implications. Clin Pharmacokinet. 1991 Jul; 21(1):70-80.

Kubota T, Lewis BC, Elliot DJ, Mackenzie PI, Miners JO. Critical roles of residues 36 and 40 in the phenol and tertiary amine aglycone substrate selectivities of UGT 1A3 and 1A4. Mol Pharmacol. 2007 Oct;72(4):1054-62.

Kuczkowski KM, Reisner LS, Benumof JL. Airway problems and new solutions for the obstetric patient. J Clin Anesth 2003; 15: 552-63.

Kumar S, Tonn GR, Riggs KW, Rurak DW. Diphenhydramine disposition in the sheep maternal-placental-fetal unit: determinants of plasma drug concentrations in the mother and the fetus. J Pharm Sci. 1999 Dec;88(12):1259-65.

Kumar S, Wong H, Yeung SA, Riggs KW, Abbott FS, Rurak DW. Disposition of valproic acid in maternal, fetal, and newborn sheep. I: placental transfer, plasma protein binding, and clearance. Drug Metab Dispos. 2000 Jul;28(7):845-56.

Kumar S, Tonn GR, Riggs KW, Rurak DW. Diphenhydramine disposition in the sheep maternal-placental-fetal unit: gestational age, plasma drug protein binding, and umbilical blood flow effects on clearance. Drug Metab Dispos. 2000 Mar; 28(3):279-85.

Kuo CD, Chen GY, Yang MJ, Lo HM, Tsai YS. Biphasic changes in autonomic nervous activity during pregnancy. Br J Anaesth 2000;84: 323-9.

Lee JI, Su F, Shi H, Zuppa AF. Sensitive and specific liquid chromatography-tandem mass spectrometric method for the quantitation of dexmedetomidine in pediatric plasma. J Chromatogr B Analyt Technol Biomed Life Sci. 2007 Jun 1; 852(1-2):195-201.

Lee S, Kim BH, Lim K, Stalker D, Wisemandle W, Shin SG, Jang IJ, Yu KS. Pharmacokinetics and pharmacodynamics of intravenous dexmedetomidine in healthy Korean subjects. J Clin Pharm Ther 2012; 37:698-703.

Li W, Zhang Z, Wu L, Tian Y, Feng S, Chen Y. Determination of dexmedetomidine in human plasma using high performance liquid chromatography coupled with tandem mass spectrometric detection: application to a pharmacokinetic study. J Pharm Biomed Anal. 2009 Dec 5; 50(5):897-904.

Little BB. Pharmacokinetics during pregnancy: evidence-based maternal dose formulation. Obstet Gynecol. 1999 May; 93(5 Pt 2):858-68.

Liu X, Tam VH, Hu M. Disposition of flavonoids via enteric recycling: determination of the UDPglucuronosyltransferase isoforms responsible for the metabolism of flavonoids in intact Caco-2 TC7 cells using siRNA. Mol Pharm 2007; 4:873–82.

Liu Y, Hu M. Absorption and metabolism of flavonoids in the caco-2 cell culture model and a perused rat intestinal model. Drug Metab Dispos 2002; 30:370–7.

Macfie AG, Magides AD, Richmond MN, Reilly CS Gastric emptying in pregnancy. Br J Anaesth. 1991 Jul; 67(1):54-7.

Mahli A, Izdes S, Coskun D. Cardiac operations during pregnancy: review of factors influencing fetal outcome. Ann Thorac Surg 2000; 69: 1622-6.

Matuszewski BK. Standard line slopes as a measure of a relative matrix effect in quantitative HPLC-MS bioanalysis. J Chromatogr B Analyt Technol Biomed Life Sci. 2006 Jan 18; 830(2):293-300.

Mazze RI, Källén B. Reproductive outcome after anesthesia and operation during pregnancy: a registry study of 5405 cases. Am J Obstet Gynecol 1989; 161: 1178-85.

McCarver DG, Hines RN. The ontogeny of human drug-metabolizing enzymes: phase II conjugation enzymes and regulatory mechanisms. J Pharmacol Exp Ther. 2002 Feb; 300(2):361-6.

McClaine RJ, Uemura K, de la Fuente SG, Manson RJ, Booth JV, White WD, Campbell KA, McClaine DJ, Benni PB, Eubanks WS, Reynolds JD. General anesthesia improves fetal cerebral oxygenation without evidence of subsequent neuronal injury. J Cereb Blood Flow Metab 2005; 25:1060-9.

Mihaly GW, Morgan DJ. Placental drug transfer: effects of gestational age and species. Pharmacol Ther. 1983; 23(2):253-66.

Musk GC, Netto JD, Maker GL, Trengove RD. Transplacental transfer of medetomidine and ketamine in pregnant ewes. Lab Anim 2012; 46:46-50.

Nau H, Luck W, Kuhnz W. Decreased serum protein binding of diazepam and its major metabolite in the neonate during the first postnatal week relate to increased free fatty acid levels. Br J Clin Pharmacol. 1984 Jan; 17(1):92-8.

Neumann MM, Davio MB, Macknet MR, Applegate RL 2nd. Dexmedetomidine for awake fiberoptic intubation in a parturient with spinal muscular atrophy type III for cesarean delivery. Int J Obstet Anesth. 2009 Oct; 18(4):403-7.

Ní Mhuireachtaigh R, O'Gorman DA. Anesthesia in pregnant patients for nonobstetric surgery. J Clin Anesth. 2006 Feb; 18(1):60-6.

Olutoye OA, Lazar D, Igboagi C, Ruano R, Nguyen K, Johnson A, Chow DSL, Olutoye OO, Pediatric Anesthesiology 2011 Abstract (2011)

Pacheco L, Costantine MM, Hankins GDV. “Physiologic changes during pregnancy,” in Clincal Pharmacology During Pregnancy ed. Mattison DR, editor. (San Diego: Academic Press) 2013: 5-14

Pandharipande PP, Pun BT, Herr DL, Maze M, Girard TD, Miller RR, Shintani AK, Thompson JL, Jackson JC, Deppen SA, Stiles RA, Dittus RS, Bernard GR, Ely EW. Effect of sedation with dexmedetomidine vs lorazepam on acute brain dysfunction in mechanically ventilated patients: the MENDS randomized controlled trial. Jama 2007; 298:2644-53.

Pandharipande PP, Sanders RD, Girard TD, McGrane S, Thompson JL, Shintani AK, Herr DL, Maze M, Ely EW, MENDS investigators. Effect of dexmedetomidine versus lorazepam on outcome in patients with sepsis: an a prioridesigned analysis of the MENDS randomized controlled trial. Crit Care 2010; 14(2):R38.

Pardi G, Cetin I. Human fetal growth and organ development: 50 years of discoveries. Am J Obstet Gynecol. 2006 Apr; 194(4):1088-99

Petroz GC, Sikich N, James M, van Dyk H, Shafer SL, Schily M, Lerman J. A phase I, two-center study of the pharmacokinetics and pharmacodynamics of dexmedetomidine in children. Anesthesiology 2006; 105:1098-110.

Potts AL, Anderson BJ, Warman GR, Lerman J, Diaz SM, Vilo S. Dexmedetomidine pharmacokinetics in pediatric intensive care--a pooled analysis. Paediatr Anaesth 2009;19:1119-29.

Precedex injection label. http://www.fda.gov/Drugs/default.htm

Pretheeban M, Hammond G, Bandiera S, Riggs W, Rurak D. Ontogenesis of UDP-glucuronosyltransferase enzymes in sheep. Comp Biochem Physiol A Mol Integr Physiol. 2011 Jun; 159(2):159-66.

Reitman E, Flood P. Anaesthetic considerations for non-obstetric surgery during pregnancy. Br J Anaesth. 2011 Dec; 107 Suppl 1:i72-8.

Reynolds F, Knott C. Pharmacokinetics in pregnancy and placental drug transfer. Oxf Rev Reprod Biol. 1989; 11:389-449.

Ridd MJ, Brown KF, Nation RL, Collier CB. Differential transplacental binding of diazepam: causes and implications. Eur J Clin Pharmacol. 1983; 24(5):595-601.

Riggs KW, Rurak DW, Taylor SM, McErlane BA, McMorland GH, Axelson JE Fetal and maternal placental and nonplacental clearances of metoclopramide in chronically instrumented pregnant sheep. J Pharm Sci. 1990 Dec;79(12):1056-61.

Riker RR, Shehabi Y, Bokesch PM, Ceraso D, Wisemandle W, Koura F, Whitten P, Margolis BD, Byrne DW, Ely EW, Rocha MG, SEDCOM (Safety and Efficacy of Dexmedetomidine Compared With Midazolam) Study Group. Dexmedetomidine vs midazolam for sedation of critically ill patients: a randomized trial. Jama 2009; 301:489-99.

Rurak DW. Development and function of the placenta. In: Harding R and Bocking AD, editor. Fetal growth and development. 1st ed. Cambridge University Press; May 24, 2001. p. 18.

Sanders RD, Xu J, Shu Y, Januszewski A, Halder S, Fidalgo A, Sun P, Hossain M, Ma D, Maze M. Dexmedetomidine attenuates isoflurane-induced neurocognitive impairment in neonatal rats. Anesthesiology. 2009 May; 110(5):1077-85.

Sanders RD, Sun P, Patel S, Li M, Maze M, Ma D. Dexmedetomidine provides cortical neuroprotection: impact on anaesthetic-induced neuroapoptosis in the rat developing brain. Acta Anaesthesiol Scand. 2010 Jul; 54(6):710-6.

Sanson BJ, Lensing AWA, Prins MH. Safety of low molecular weight heparin in pregnancy: a systematic review. Thromb Haemost 1999; 81: 668-72

Schneider H, Proegler M. Placental transfer of beta-adrenergic antagonists studied in an in vitro perfusion system of human placental tissue. Am J Obstet Gynecol. 1988 Jul; 159(1):42-7.

Son DS, Osabe M, Shimoda M, Kokue E. Contribution of alpha 1-acid glycoprotein to species difference in lincosamides-plasma protein binding kinetics J Vet Pharmacol Ther. 1998 Feb;21(1):34-40.

Strassburg CP, Strassburg A, Kneip S, Barut A, Tukey RH, Rodeck B, Manns MP. Developmental aspects of human hepatic drug glucuronidation in young children and adults. Gut. 2002 Feb; 50(2):259-65.

Su F, Nicolson SC, Gastonguay MR, Barrett JS, Adamson PC, Kang DS, Godinez RI, Zuppa AF. Population pharmacokinetics of dexmedetomidine in infants after open heart surgery. Anesth Analg 2010; 110:1383-92.

Syme MR, Paxton JW, Keelan JA. Drug transfer and metabolism by the human placenta. Clin Pharmacokinet. 2004; 43(8):487-514

Tang L, Singh R, Liu Z, Hu M. Structure and concentration changes affect characterization of UGT isoform-specific metabolism of isoflavones. Mol Pharm. 2009 Sep-Oct; 6(5):1466-82.

Taylor PJ. Matrix effects: the Achilles heel of quantitative high-performance liquid chromatography-electrospray-tandem mass spectrometry. Clin Biochem. 2005 Apr; 38(4):328-34.

Thornton C, Lucas MA, Newton DE, Dore CJ, Jones RM. Effects of dexmedetomidine on isoflurane requirements in healthy volunteers. 2: Auditory and somatosensory evoked responses. Br J Anaesth 1999; 83:381-6.

Trufelli H, Palma P, Famiglini G, Cappiello A. An overview of matrix effects in liquid chromatography-mass spectrometry. Mass Spectrom Rev. 2011 May-Jun; 30(3):491-509.

Uemura K, Shimazutsu K, McClaine RJ, McClaine DJ, Manson RJ, White WD, Benni PB, Reynolds JD. Maternal and preterm fetal sheep responses to dexmedetomidine. Int J Obstet Anesth 2012; 21:339-47.

Van Eeckhaut A, Lanckmans K, Sarre S, Smolders I, Michotte Y. Validation of bioanalytical LC-MS/MS assays: evaluation of matrix effects. J Chromatogr B Analyt Technol Biomed Life Sci. 2009 Aug 1; 877(23):2198-207

Venn RM, Bryant A, Hall GM, Grounds RM. Effects of dexmedetomidine on adrenocortical function, and the cardiovascular, endocrine and inflammatory responses in post-operative patients needing sedation in the intensive care unit. Br J Anaesth. 2001 May; 86(5):650-6.

Vertommen JD, Marcus MA, Van Aken H. The effects of intravenous and epidural sufentanil in the chronic maternal-fetal sheep preparation. Anesth Analg. 1995 Jan;80(1):71-5.

Villela NR, do Nascimento Júnior P, de Carvalho LR, Teixeira A. Effects of dexmedetomidine on renal system and on vasopressin plasma levels. Experimental study in dogs. Rev Bras Anestesiol. 2005 Aug; 55(4):429-40.

Wallace S. Altered plasma albumin in the newborn infant. Br J Clin Pharmacol. 1977 Feb; 4(1):82-5.

Wang LH, Rudolph AM, Benet LZ. Pharmacokinetic studies of the disposition of acetaminophen in the sheep maternal-placental-fetal unit. J Pharmacol Exp Ther. 1986 Jul; 238(1):198-205.

Whitehead EM, Smith M, Dean Y, O'Sullivan G. An evaluation of gastric emptying times in pregnancy and the puerperium. Anaesthesia. 1993 Jan; 48(1):53-7.

Wikipedia Pregnancy category; http://en.wikipedia.org/wiki/Pregnancy_category

Wong CA, Loffredi M, Ganchiff JN, Zhao J, Wang Z, Avram MJ. Gastric emptying of water in term pregnancy. Anesthesiology. 2002 Jun; 96(6):1395-400.

Wood M, Wood AJ Changes in plasma drug binding and α1-acid glycoprotein in mother and newborn infant. Clin Pharmacol Ther. 1981 Apr; 29(4):522-6.

Włoch S, Pałasz A, Kamiński M. Active and passive transport of drugs in the human placenta. Ginekol Pol. 2009 Oct; 80(10):772-7.

Yoo SD, Rurak DW, Taylor SM, Axelson JE. Placental transfer of diphenhydramine in chronically instrumented pregnant sheep. J Pharm Sci. 1986 Jul;75(7):685-7.

Yoo SD, Rurak DW, Taylor SM, Axelson JE. Transplacental and nonplacental clearances of diphenhydramine in the chronically instrumented pregnant sheep. J Pharm Sci. 1993 Feb;82(2):145-9.

Zakowski MI, Ham AA, Grant GJ. Transfer and uptake of alfentanil in the human placenta during in vitro perfusion. Anesth Analg. 1994 Dec; 79(6):1089-93.

Zhang Y, Huo M, Zhou J, Xie S. PKSolver: An add-in program for pharmacokinetic and pharmacodynamic data analysis in Microsoft Excel. Comput Methods Programs Biomed 2010; 99:306-14.